

Discovery of AZD4573, a Potent and Selective Inhibitor of CDK9 That Enables Short Duration of Target Engagement for the Treatment of Hematological Malignancies

Bernard Barlaam,* Robert Casella, Justin Cidado, Calum Cook, Chris De Savi, Allan Dishington, Craig S. Donald, Lisa Drew, Andrew D. Ferguson, Douglas Ferguson, Steve Glossop, Tyler Grebe, Chungang Gu, Sudhir Hande, Janet Hawkins, Alexander W. Hird, Jane Holmes, James Horstick, Yun Jiang, Michelle L. Lamb, Thomas M. McGuire, Jane E. Moore, Nichole O'Connell, Andy Pike, Kurt G. Pike, Theresa Proia, Bryan Roberts, Maryann San Martin, Ujjal Sarkar, Wenlin Shao, Darren Stead, Neil Sumner, Kumar Thakur, Melissa M. Vasbinder, Jeffrey G. Varnes, Jianyan Wang, Lei Wang, Dedong Wu, Liangwei Wu, Bin Yang, and Tieguang Yao



Cite This: <https://dx.doi.org/10.1021/acs.jmedchem.0c01754>



Read Online

ACCESS |



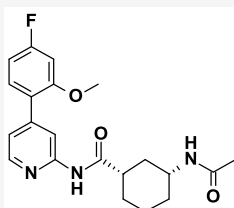
Metrics & More



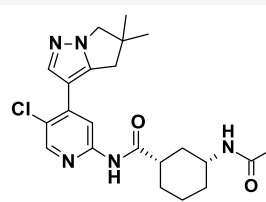
Article Recommendations



Supporting Information



2
CDK9 cell IC₅₀ 0.13 μM
in vivo probe compound
Poor solubility



24 (AZD4573)
CDK9 cell IC₅₀ 0.013 μM
Short half-life in preclinical species
Predicted short half-life (humans)
Suitable solubility (i.v. administration)

ABSTRACT: A CDK9 inhibitor having short target engagement would enable a reduction of Mcl-1 activity, resulting in apoptosis in cancer cells dependent on Mcl-1 for survival. We report the optimization of a series of amidopyridines (from compound **2**), focusing on properties suitable for achieving short target engagement after intravenous administration. By increasing potency and human metabolic clearance, we identified compound **24**, a potent and selective CDK9 inhibitor with suitable predicted human pharmacokinetic properties to deliver transient inhibition of CDK9. Furthermore, the solubility of **24** was considered adequate to allow i.v. formulation at the anticipated effective dose. Short-term treatment with compound **24** led to a rapid dose- and time-dependent decrease of pSer2-RNAP2 and Mcl-1, resulting in cell apoptosis in multiple hematological cancer cell lines. Intermittent dosing of compound **24** demonstrated efficacy in xenograft models derived from multiple hematological tumors. Compound **24** is currently in clinical trials for the treatment of hematological malignancies.

INTRODUCTION

Evasion of programmed cell death (apoptosis) is one of the hallmarks of cancer.¹ Apoptosis is a critical process for normal development and tissue homeostasis and is therefore tightly controlled by the balance of proteins that promote cell survival and cell death. In many cancers, this balance is disrupted in favor of cell survival, conferring a growth advantage. Myeloid cell leukemia 1 (Mcl-1) is an antiapoptotic member of the Bcl2 family and a key survival factor in a wide range of human cancers.^{2–4} Mcl-1 binds and sequesters pro-apoptotic proteins Bak and Bax at the mitochondrial outer membrane, thereby preventing activation of intrinsic apoptosis. Mcl-1 also binds and

neutralizes a subset of BH3-only proteins, such as Bim, Noxa and Puma, preventing the activation of pro-apoptotic proteins.^{3,5} Furthermore, overexpression of Mcl-1 has been linked to chemotherapy resistance and relapse in cancer patients.^{6–9} Given the pivotal role in tumor cell survival played by Mcl-1, it is

Received: October 6, 2020

unsurprising that depletion of Mcl-1 leads to rapid cell death in cancer cells and tumor regression in several models of hematological cancers.^{10,11} As a result, many medicinal chemistry programs have attempted to develop Mcl-1 inhibitors. However, Mcl-1 has been proven difficult to target pharmacologically, due to the long, shallow hydrophobic protein–protein interaction interface.^{12–15} Only very recently have small molecule Mcl-1 inhibitors (e.g., AZD5991,¹⁶ AMG176,¹⁷ MIK665¹⁸) entered early clinical development.

An alternative approach would be to target Mcl-1 activity indirectly by inhibiting the cyclin-dependent-kinase 9. Cyclin-dependent-kinases (CDKs) are members of the serine/threonine kinase family and are highly regulated by cyclins, a family of regulatory subunits that bind to CDKs. The human genome encodes for more than 20 CDKs and over 30 cyclins.¹⁹ CDKs are classified into two groups: CDKs involved in cell cycle control,²⁰ such as CDK1, 2, 4, and 6 and their associated cyclins A, B, D, and E; and CDKs involved in transcription regulation/RNA processing, such as CDK7, 8, and 9 and their associated cyclins C, H and T.²¹ Dinaciclib, one of multiple nonselective CDK small molecule inhibitors with potent CDK9 activity has been shown to reduce expression of Mcl-1 and ultimately lead to cancer cell death.^{22,23} The underlying hypothesis for this observation was that transient inhibition of transcription driven by CDK9 inhibition would result in the selective reduction of protein levels for genes that have short-lived transcripts and proteins, such as Mcl-1. However, because of the lack of selectivity of dinaciclib, it was unclear whether the observed effects are related to CDK9 inhibition alone.

Regulation of transcription is a complex process governed in part through the activity of CDK9.²⁴ Following successful transcription initiation, RNA polymerase II (RNAP2) pauses just downstream of the transcription start site, serving as a checkpoint.^{25,26} To release RNAP2 from this pause, multiple CDK9-mediated phosphorylation events are required, which include phosphorylation of the serine 2 (Ser2) position in the 52 heptapeptide repeats (YSPTSPS) comprising the carboxyl-terminal domain (CTD) of RNAP2.²⁷ As an integral node of the transcription regulatory network, CDK9 is the most studied transcriptional CDK and has garnered considerable interest as a potential target for cancer therapy,^{28,29} one working hypothesis being that transient inhibition of transcription by CDK9 inhibition may provide a therapeutic opportunity to target Mcl-1 activity indirectly.

Pan-CDK inhibitors, which have activity against CDK9 (e.g., 1, also known as AZD5438,³⁰ see Figure 1), have been known for some time and have been previously evaluated in clinical trials but with mixed outcomes, many of them showing complex and challenging tolerability profiles.³¹ More selective CDK9 inhibitors have since emerged. We³² and others³³ reported the characterization of the in vitro and in vivo CDK9 pharmacology using a preclinical tool 2 (AZ5576) identified as a reasonably potent and highly selective CDK9 inhibitor from a series of amidopyridines.³⁴ In vitro treatment of the acute myeloid leukemia (AML) cell line MV-4-11 with 2 resulted in a dose- and time-dependent decrease in pSer2-RNAP2 and Mcl-1 expression with subsequent activation of caspase 3/7, leading to rapid induction of cell death. This result was extended to additional hematological cancer cell lines. In vivo, a similar pharmacodynamic response was observed in MV-4-11 tumor xenografts following a single oral dose of 2 (60 mg/kg), which translated to significant antitumor efficacy after intermittent oral administration.³² Other groups also have reported that

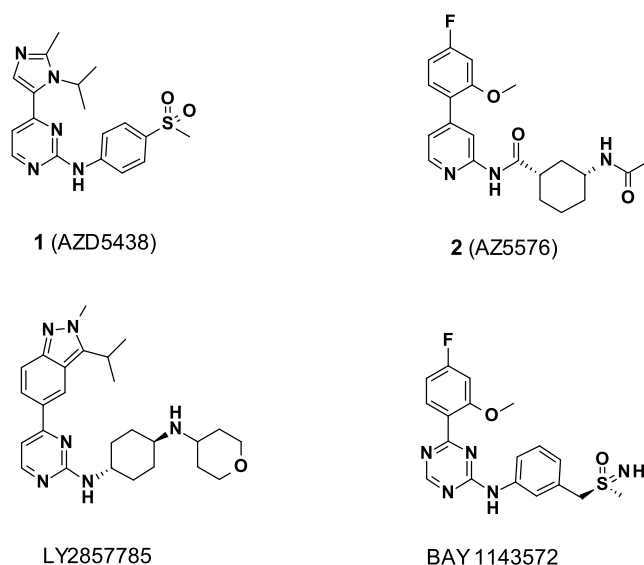


Figure 1. Structures of selected CDK9 inhibitors.

identification of more selective CDK9 inhibitors (e.g., LDC000067,³⁵ LY2857785³⁶) and characterized the pharmacology of these compounds in vitro and/or in in vivo preclinical hematological tumor models. However, at the start of this project, no selective CDK9 inhibitor had entered clinical trials.²⁸ More recently, two selective CDK9 inhibitors (BAY 1143572^{37,38} and BAY 1251152³⁹) have been reported as entering clinical trials.

On the basis of our understanding of the pharmacology of 2, we set our objective to identify a highly potent and selective CDK9 inhibitor having a predicted short half-life in humans ($t_{1/2} < 2$ h), and suitable physical properties (e.g., aqueous solubility) for intravenous (i.v.) administration, to enable controlled duration of target engagement in the clinic through modulation of the infusion duration. This profile would allow maximal flexibility in the dosing schedule to maximize the efficacy/toxicity balance of such an agent. Compound 2 is a potent CDK9 inhibitor (CDK9 enzyme assay 5 mM [ATP], IC_{50} 0.029 μ M; inhibition of pSer2-RNAP2 in MCF-7 cell line, IC_{50} 0.13 μ M; induction of caspase in MV-4-11 cell line, EC_{50} 0.22 μ M) with excellent kinase selectivity and a short half-life in rodents, making it a suitable probe compound for characterizing short target engagement of CDK9 in vitro and in vivo.³² However, its low solubility (7.5 μ M in 1 \times PBS buffer pH 7.4 (phosphate buffered saline, phosphate final concentration of 0.01 M, pH 7.4); 24 μ M in 0.1 M acetate buffer pH 4; both solubilities from crystalline material) was seen as a significant limitation for i.v. formulation, especially when considering the likely requirement of a high therapeutic dose. Furthermore, it was thought that the relatively low rate of metabolism, observed in human microsomes and hepatocytes in vitro, could result in the human $t_{1/2}$ being too long to provide an optimal duration of target engagement in the clinical setting. Details of the methodology for predicting human pharmacokinetic parameters and clinical dose are available in the section entitled “Protocol for human PK predictions and clinical dose projections” in Supporting Information. Predictions of human pharmacokinetic parameters from in vitro scaled clearance and scaled volume from preclinical species suggested a mean half-life of 4.3 h for compound 2 (Cl 2.3 mL/min/kg, V_{ss} 0.88 L/kg, mean $t_{1/2}$ 4.3 h, see Table 1).

Those two risks were considered significant, which drove our decision not to progress **2** to the clinic.

Table 1. Pharmacokinetic Properties of Compound **2 in Preclinical Species and Predicted Human Parameters**

	mouse	rat	dog	human
hepatocytes Cl_{int} ($\mu\text{L}/\text{min}/10^6$ cells) ^a	52	58	5.9	1.4
plasma Cl ($\text{mL}/\text{min}/\text{kg}$) ^b	40	77	7.5	2.3 ^c
V_{ss} (L/kg) ^b	1.1	1.3	0.62	0.88 ^c
$t_{1/2}$ (h)	0.26	0.22	1.0	4.3 ^c

^aIntrinsic clearance measured from hepatocytes, Cl_{int} . ^bFor mouse and Han Wistar rat studies ($n \geq 2$), the compound was administered respectively at a dose of 5.2 $\mu\text{mol}/\text{kg}$ and 1.3 $\mu\text{mol}/\text{kg}$ i.v. as a solution formulation. For Beagle dogs ($n = 2$), the compound was administered by intravenous infusion over 0.25 h at a dose of 5.2 $\mu\text{mol}/\text{kg}$ as a solution in 15% captisol (w/v) solution adjusted to pH 4.0. ^cItalicized text indicates human PK predictions (see Supporting Information for methods).

Here we report further optimization of this amidopyridine series as highly selective CDK9 inhibitors, with a focus on potency, pharmacokinetic, and physicochemical properties suitable for an intravenous agent with a short duration of target engagement. This work led to the discovery of the clinical candidate compound **24** (also known as AZD4573) for the treatment of hematological malignancies.

RESULTS AND DISCUSSION

Synthetic Chemistry. The synthesis of compounds **3**–**34** is outlined in Schemes 1–6 of the text and Schemes 7 and 8 of the Supporting Information. In general terms, the C-4 headgroup on the pyridine central core was introduced, in most cases, by a Suzuki coupling reaction. Alternatively, the C-4 headgroup was introduced by a Heck reaction. The C-2 amido group on the pyridine central core was installed by a palladium-catalyzed reaction between the 2-halopyridine and the corresponding primary amide side chain. Alternatively, still starting from the 2-halopyridine, the C-2 amido group on the pyridine central core was installed in two steps: nucleophilic substitution of the 2-halo substituent by ammonia, followed by amide coupling with the corresponding carboxylic acid side chain. Depending on the specific compound, the C-4 headgroup was introduced first on the pyridine core, followed by the C-2 amido group, or vice versa.

Compound **3** was made as follows: Suzuki reaction of boronic ester **35** with **36** gave **37**, which was then coupled with carboxylic acid **38**. Amine deprotection and subsequent acetylation afforded compound **3** (Scheme 1).

Intermediate **40** was obtained by amide coupling of **39** with carboxylic acid **38**. Suzuki coupling of **40** with boronic ester **41**, followed by a two-step sequence of amine deprotection and acetylation, gave compound **4**. Alternatively, **40** was converted to boronic ester **43**. Suzuki coupling of **43** with the corresponding halo-heterocycles followed by deprotection and acetylation afforded compounds **20** and **22** (Scheme 2).

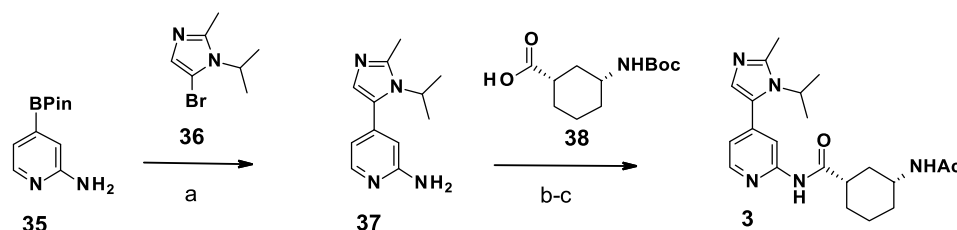
The synthesis of compounds **5**, **8**, **10**, and **21** is described in Scheme 3. Compounds **5** and **21** were synthesized from compound **45**. Suzuki coupling of **45** with boronic esters **41** and **49** gave chloro-pyridines **46** and **50** respectively. Palladium-mediated coupling of **46** and **50** with amide **47** gave **48** and **51** respectively, which were converted to **5** and **21** after amine deprotection and acetylation. Similarly starting from **52**, Suzuki coupling with the corresponding boronic ester (for **53a**) or Heck reaction with the corresponding imidazole (for **53b**) gave respectively **53a** and **53b**. The same three-step sequence of palladium-mediated coupling with amide **47** followed by amine deprotection and acetylation afforded compounds **8** and **10**.

Compound **6** was made starting from **55** (Scheme 4). Conversion of 2-fluoropyridine **55** to corresponding 2-aminopyridine **56**, followed by Suzuki coupling with **41** gave intermediate **57**. Amide coupling of **57** with carboxylic acid **38**, followed by amine deprotection and acetylation gave **6**.

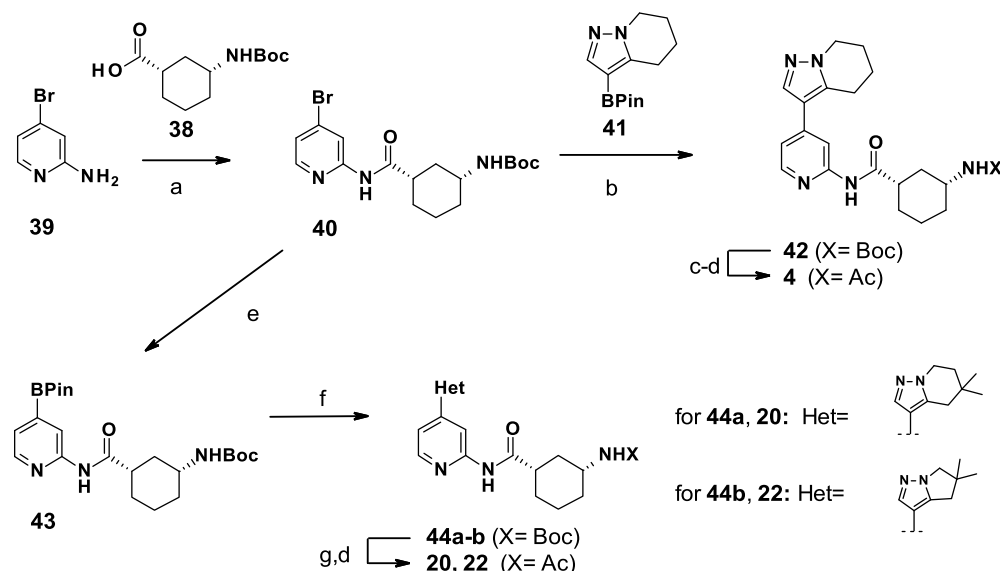
The route used for compounds **7**, **9**, **11**–**19**, and **27**–**29** where the C-2 amido group was installed first, is described in Scheme 5. 2-Amino-5-chloro-pyridine **59**, obtained by chlorination of compound **39**, was coupled with carboxylic acid **38** to give key intermediate **61** after an amine deprotection/acetylation sequence. Suzuki coupling of **61** with the corresponding boronic esters or Heck coupling of **61** with the corresponding imidazoles respectively gave compounds **7**, **19** and **9**, **11**. Compounds **12**–**18** and **27**–**29** were made starting from **56** using a similar sequence (all using a Suzuki coupling, except for **29** where a Heck reaction between **63** and the corresponding imidazole was used).

Compounds **23** and **24** were made according to Scheme 6. Key boronic ester intermediate **69** in the synthesis of **23** and **24** was made as follows: intermediate **65** made by alkylation of pyrazole was cyclized using the procedure developed by Larsen⁴⁰ to afford **66**. Reduction of ketone **66** under Wolff–Kishner conditions afforded previously described **67**,⁴¹ which was submitted to bromination conditions followed by palladium-catalyzed borylation to afford **69**. Compound **70**, which was obtained by Suzuki coupling of **45** with **69**, was subjected to palladium-catalyzed amidation with **47** to afford **71**. Final amine deprotection/acetylation sequence of **71** gave **23**. Suzuki coupling of **62** with **69**, followed by a final amine deprotection/acetylation sequence, gave **24**.

Scheme 1^a



^aReagents: (a) **36**, second generation XPhos precatalyst, K_3PO_4 , dioxane–water, 110 °C; (b) **38**, 1-chloro-*N,N*,2-trimethylprop-1-en-1-amine, DCM, 0 °C to rt, then **37**, pyridine, THF, rt; (c) HCl, dioxane–MeOH, rt then AcCl, DIPEA, DCM, rt.

Scheme 2^a

^aReagents: (a) 38, 1-chloro-*N,N,N*-trimethylprop-1-en-1-amine, DCM, 0 °C, then 39, pyridine, DCM, THF, 0 °C to rt; (b) 41, second generation XPPhos precatalyst, K₃PO₄, dioxane–water, 100 °C; (c) HCl, dioxane–DCM, rt; (d) Ac₂O, NEt₃, DCM, DMAP (optional), rt; (e) (BPin)₂, PdCl₂(dppf), KOAc, dioxane, 90 °C; (f) Het-Br or Het-I, PdCl₂(dppf), K₃PO₄, dioxane–water, 90 °C; (g) TFA, DCM, rt or HCl, dioxane–DCM, rt.

The synthesis of compounds 25, 26, and 30–34 are described in Scheme 7 and 8 (Supporting Information).

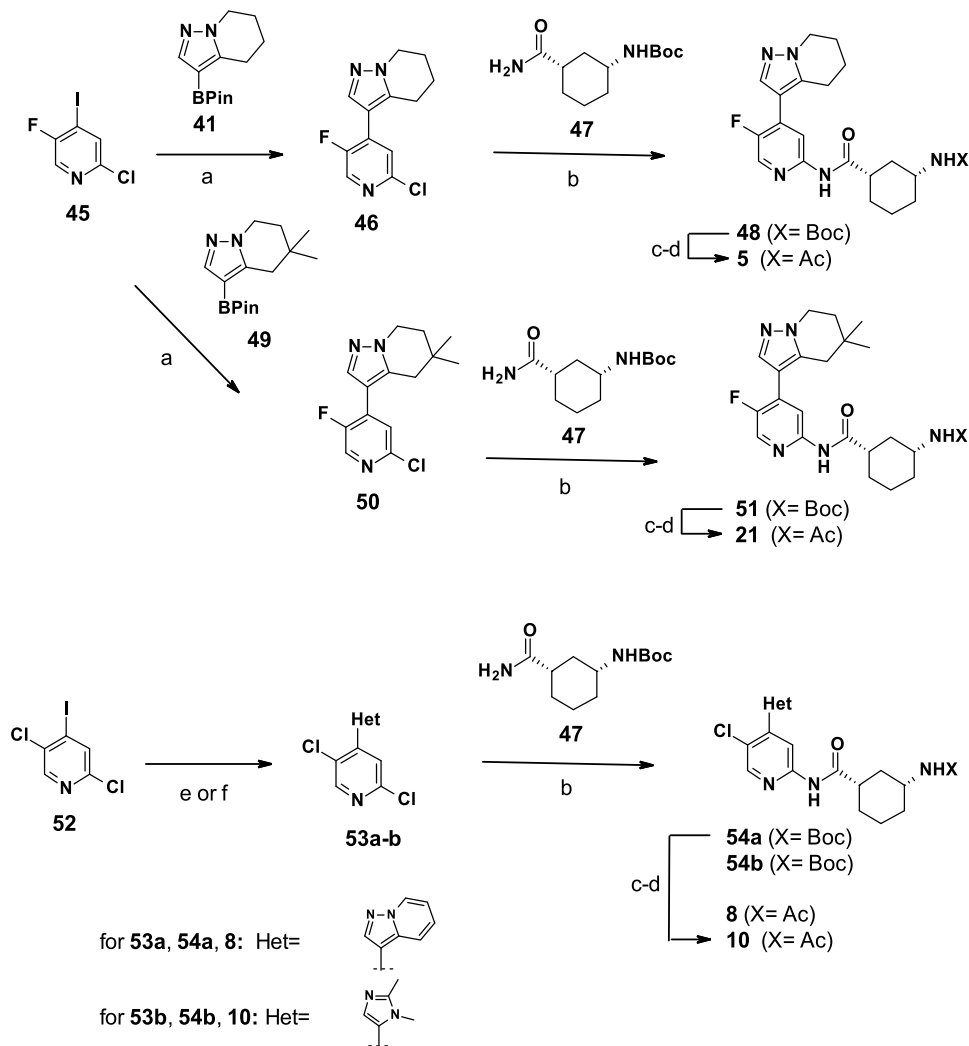
Discovery of Clinical Candidate 24. Docking of 2 into a published structure of CDK9 in complex with cyclin T1 (PDB: 4BCF)⁴² provided some understanding of the key interactions leading to the potency and selectivity achieved with this compound. According to this model, compound 2 interacts with the kinase hinge via a bidentate interaction through the pyridine and the amidic NH with the backbone atoms of Cys106 (Figure 2). The cyclohexyl amide gives access to the solvent channel. The 2-methoxy-4-fluoro phenyl motif is twisted with respect to the pyridine ring (positioned 24° out of plane), bringing the methoxy group in closer proximity to Ala153 and Leu156, which follow the catalytic HRD-motif. From our understanding of the SAR from published literature around 2³⁴ and our docking model, our initial hypothesis was that the 4-fluoro-2-methoxyphenyl at the C-4 position of the pyridine was a key element for the potency and selectivity against CDK9.

Conversely, the lipophilic nature of this group was considered as a key contributor to the poor solubility of 2. We decided to investigate alternative groups at the C-4 position of the pyridine, in particular, five-membered heterocycles which are present in some CDK inhibitors (e.g., imidazole in 1) with the thought that they might improve the physical properties of this series. Indeed, compound 3, a hybrid of compounds 1 and 2, retained some activity against CDK9. It is worth noting that compound 3 has a similar ligand-lipophilicity efficiency (LLE) compared to 2, its potency being reduced ca. 10-fold compared to 2, while its lipophilicity is reduced by 1.1 units (see Table 3). In addition, 3 showed increased solubility compared to 2. With this encouraging result in hand, we explored other five-membered heterocycles (e.g., pyrazoles, imidazoles) and other [5,6] bicyclic heterocycles from available boronic acids or esters. Among the compounds from this initial exploration, compound 4 caught our attention, having slightly improved potency against CDK9 (CDK9 enzyme assay 5 mM [ATP], IC₅₀: 0.23 μM; CDK9 cellular assay using pSer2-RNAP2 end-point, IC₅₀: 0.52

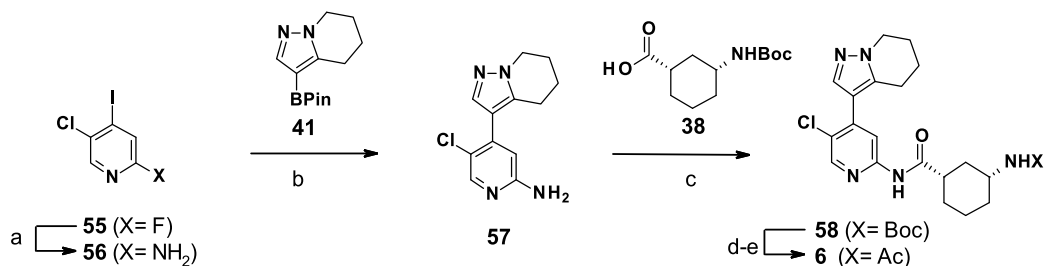
μM) while keeping high solubility. Previous work at AstraZeneca had shown that halogen substitution, such as fluorine or chlorine, at the C-5 position of the pyrimidine core of compound 1 increased potency against some CDKs (e.g., CDK2⁴³). From 4, substitution of the 5-position of the pyridine with a fluorine (compound 5) or a chlorine (compound 6) significantly increased potency against CDK9. Compound 6 was especially interesting in that it had similar potency against CDK9 and higher solubility when compared to 2. Therefore, compound 6 was profiled further. Kinase selectivity of 6 was evaluated at 1 μM in the “Eurofins kinase panel”. It showed significant inhibition (>80% inhibition) on only 7 kinases out of 125 kinases: CDK9 (98%), GSK3α (101%), GSK3β (100%), CDK1 (96%), CDK2 (93%), DYRK2 (87%), and CK1γ1 (87%). The selectivity among the CDK family was further assessed in assays recapitulating the typical ATP concentration in cells ([ATP] of 5 mM). The overall profile is summarized in Table 3, supporting that 6 is a potent CDK9 inhibitor with >10-fold selectivity against CDK1–7 and CDK12, except CDK3 (2-fold).

The binding kinetics of 6 to CDK9 were determined by surface plasmon resonance. Compound 6 showed a dissociation rate constant (*k_d*) of 3.64 × 10⁻³ s⁻¹, which resulted in a dissociation half-life (*t_{1/2}*) of 6.3 min (see Table 4) and was classified as “fast-off” binding kinetics. The reversibility of pSer2-RNAP2 inhibition was also investigated in the MCF-7 cell line by incubation of 6 followed by cell washout and measurement of pSer2-RNAP2 inhibition at 30 min and 2 h after washout of the inhibitor. Compound 6 showed reversible inhibition with an increased IC₅₀ at both time points following washout (IC₅₀ > 3 μM at both time points vs IC₅₀ 0.11 μM without cell washout). The reversibility of pSer2-RNAP2 inhibition (in line with the “fast-off” binding kinetics of 6 to CDK9) was seen as a desirable feature for a CDK9 inhibitor to deliver short target engagement.

The solubility of compound 6 was further assessed from a crystalline batch: 94 mg/L in 1× PBS buffer pH 7.4 and 210 mg/L in 0.1 M acetate buffer pH 4 (from crystalline Form B⁴⁴). The

Scheme 3^a

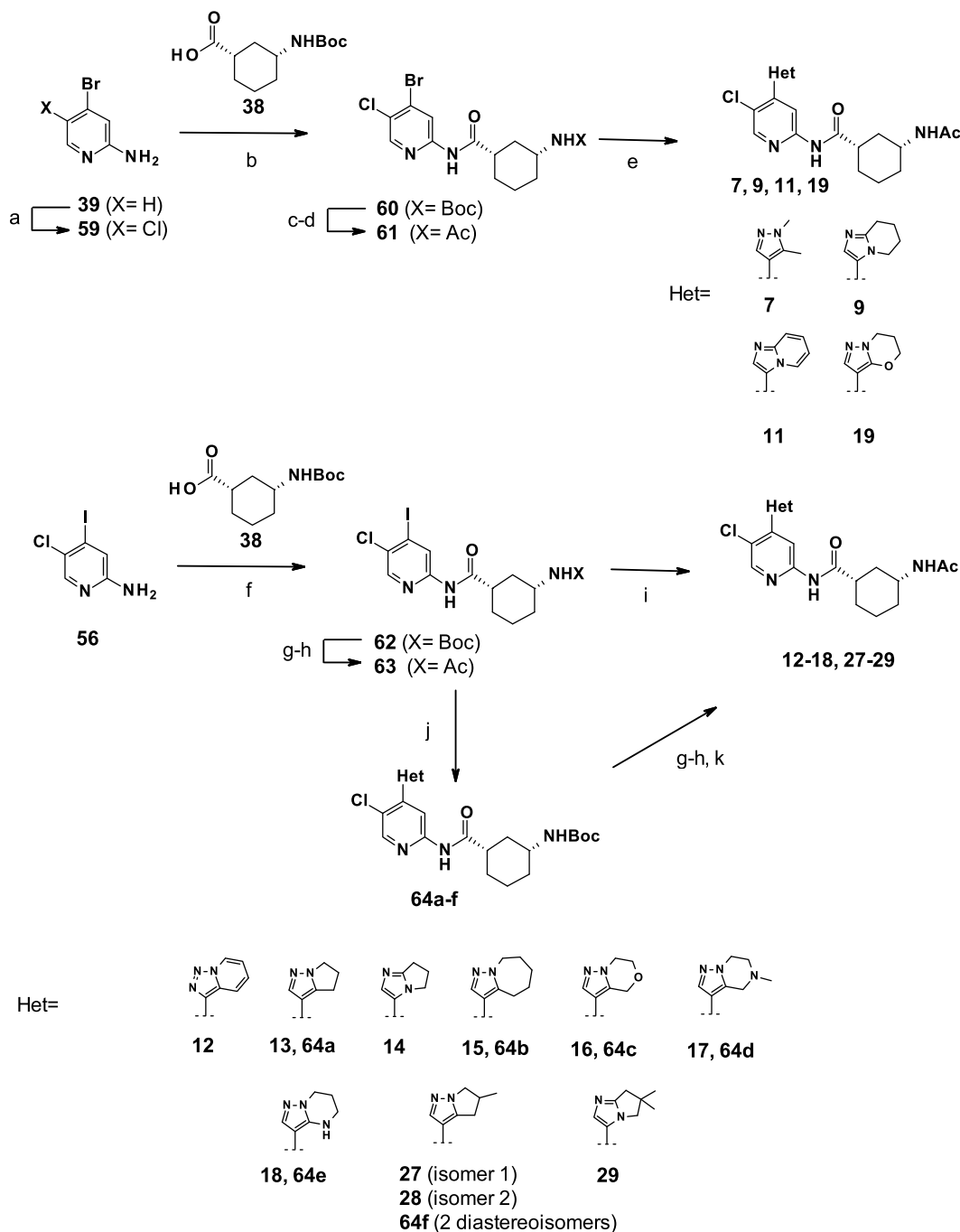
^aReagents: (a) Het-BPin, second generation XPhos precatalyst, K_3PO_4 , dioxane–water, 90 °C; (b) 47, $Pd(PPh_3)_4$, xantphos, CS_2CO_3 , dioxane, 120 °C; (c) TFA, DCM, rt; (d) Ac_2O , NEt_3 , DMAP (optional), DCM, rt; (e) Het-BPin, $Pd(PPh_3)_4$, CS_2CO_3 , dioxane–water, 100 °C (for 53a); (f) 1,2-dimethylimidazole, $Pd(OAc)_2$, PPh_3 , CS_2CO_3 , dioxane, 120 °C (for 53b).

Scheme 4^a

^aReagents: (a) conc. aq. ammonia, NMP, 100 °C (microwave); (b) 41, $PdCl_2(dppf)$, CS_2CO_3 , dioxane–water, 95 °C; (c) 38, 1-chloro-*N,N*,2-trimethylprop-1-en-1-amine, DCM, 0 °C, then 57, pyridine, DCM, 0 °C to rt; (d) HCl, dioxane–DCM–MeOH, 0 °C; (e) AcCl, pyridine, DCM, 0 °C.

pharmacokinetics of compound **6** were subsequently evaluated in multiple species to facilitate prediction of its human pharmacokinetics. In mouse, rat, and dog, compound **6** showed a moderate volume of distribution typical of its neutral ionic state.⁴⁵ Clearance was high in rats and moderate in dogs with the observed plasma clearance values in both species being

accurately predicted by scaling the intrinsic clearance derived from isolated hepatocyte incubations. Overall, this resulted in short half-lives of less than 1 h in all three species. Compound **6** was, however, metabolized much more slowly in human microsomes and hepatocytes, resulting a predicted human clearance of <2.8 mL/min/kg. The predicted human

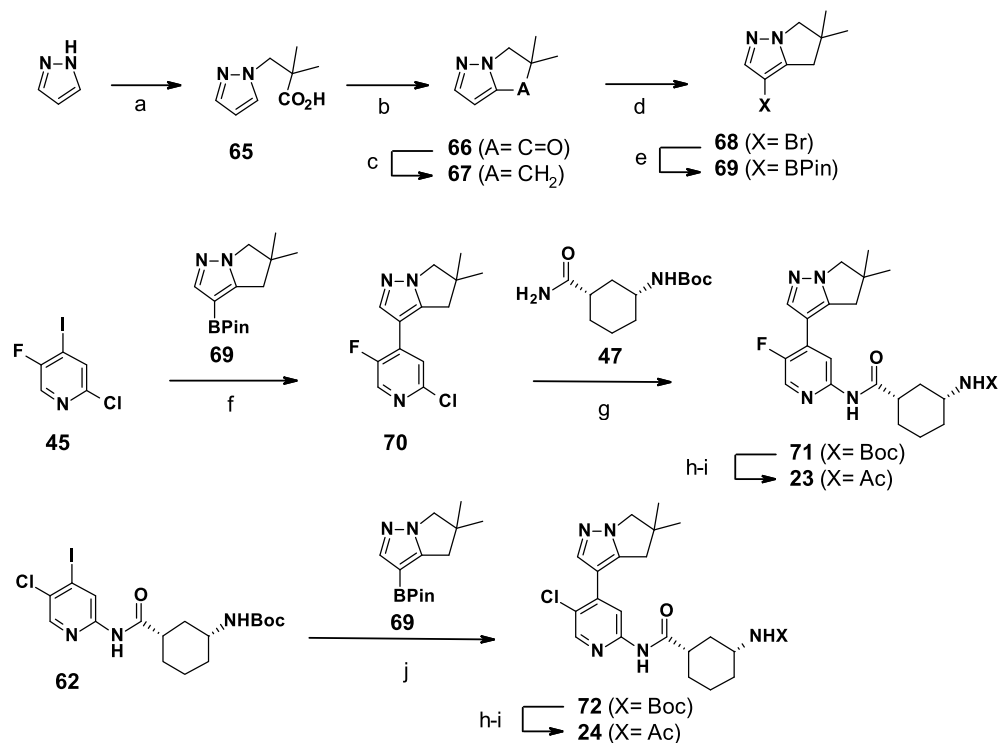
Scheme 5^a

^aReagents: (a) NCS, DMF, -78°C to rt; (b) **38**, 1-chloro-*N,N*,2-trimethylprop-1-en-1-amine, DCM, 0°C , then **57**, pyridine, DCM, THF, 0°C to rt; (c) HCl, dioxane-MeOH, 0°C ; (d) Ac_2O , DMAP, NEt_3 , DCM, rt; (e) Het-BPin, second-generation XPhos precatalyst, K_3PO_4 , dioxane-water, rt (for **7** and **19**) or Het-H, $\text{Pd}(\text{OAc})_2$, PPh_3 , NEt_3 , Cs_2CO_3 , dioxane, 100°C (for **9** and **11**); (f) **38**, 1-chloro-*N,N*,2-trimethylprop-1-en-1-amine, DCM, 0°C , then **56**, pyridine, rt; (g) HCl, dioxane-DCM, rt; (h) Ac_2O , DMAP (optional), NEt_3 , DCM, rt; (i) Het-BPin, second generation XPhos precatalyst, K_3PO_4 , dioxane-water, 60°C (for **12** from **63**) or Het-B(OH)₂, $\text{PdCl}_2(\text{dppf})$, $\text{Ba}(\text{OH})_2$, dioxane-water, 75°C (for **14** from **63**) or $\text{Pd}(\text{OAc})_2$, KOAc, DMA, 150°C (microwave) (for **29** from **63**); (j) Het-BPin, second generation XPhos precatalyst, K_2HPO_4 or K_3PO_4 , dioxane-water, rt to $50\text{--}80^{\circ}\text{C}$ (for **13**, **15**–**18**, **27**–**28** from **62**); (k) chiral purification (for **27**–**28** only).

pharmacokinetic parameters, when integrated into a PBPK model, resulted in a predicted $t_{1/2}$ in humans of >2.8 h (see Table 5), which was longer than we were seeking to achieve.

Despite concerns that the human pharmacokinetic properties of compound **6** might not be optimal for a short target engagement CDK9 inhibitor, compound **6** was a promising lead. Another hypothetical concern with the series was the potential

for pharmacologically active metabolites with longer human half-lives that would result in more sustained target engagement. Therefore, metabolite identification studies were conducted with compound **6** in HLM (and human hepatocytes) resulting in the identification of three oxidative metabolites: **6-M1**, **6-M2**, and **6-M3**. **6-M1** was identified as the major metabolite. Open

Scheme 6^a

^aReagents: (a) $\text{BrCH}_2\text{C}(\text{Me})_2\text{CO}_2\text{Et}$, Cs_2CO_3 , DMA, 80 °C; aq. NaOH, MeOH, rt; (b) *n*-BuLi, 2-MeTHF, -78 °C to rt; (c) hydrazine hydrate, 2,2'-oxidiethanol, 180 °C, then NaOH, 150 °C; (d) NBS, DCM, rt; (e) $\text{Pd}(\text{P}(\text{Cy})_3)_2\text{Cl}_2$, (BPin)₂, KOAc, $\text{PdCl}_2(\text{dppf})$, DMA, 85 °C; (f) **69**, second generation XPhos precatalyst, K_2HPO_4 , dioxane–water, 80 °C; (g) **47**, $\text{Pd}(\text{PPh}_3)_4$, xantphos, Cs_2CO_3 , dioxane, 120 °C; (h) HCl, dioxane–DCM–MeOH, rt; (i) Ac_2O , pyridine or NEt_3 , DMAP (optional), DCM, rt; (j) **69**, second generation XPhos precatalyst, K_2HPO_4 , dioxane–water, 50 °C.

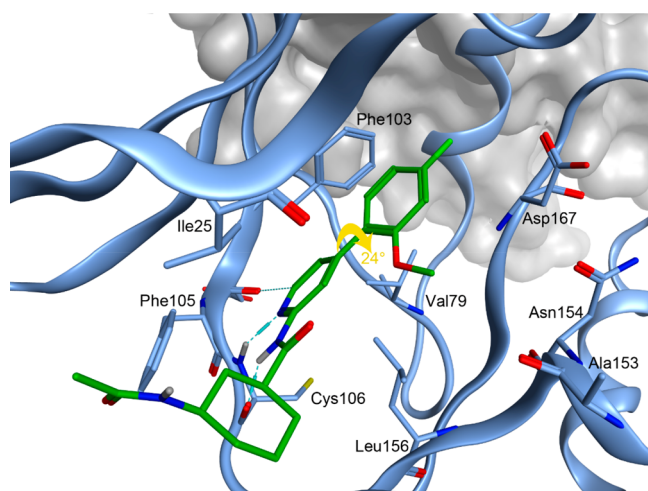


Figure 2. Compound **2** (green) docked into the ATP binding site of a publicly available crystal structure of CDK9–cyclinT1 (PDB: 4BCF), with CDK9 shown as a blue ribbon and CyclinT1 as a gray surface.

chain primary alcohol **6-M2** was detected as a trace metabolite, and **6-M3** as a minor carboxylic acid metabolite (see Figure 3).

The structures of **6-M1** and **6-M2** were subsequently confirmed by chemical synthesis of authentic standards (see Supporting Information). Pharmacological evaluation of **6-M1** and **6-M2** showed that they were significantly less potent (6.5-fold for **6-M1** and >18-fold for **6-M2** in the pSer2-RNAP2 cellular assay) than compound **6** (see Table 6). In addition, **6-M1** also showed a high rate of metabolism in human

hepatocytes, and **6-M2** was present only as a trace metabolite in HLM. Therefore, it was considered unlikely that either would have sufficient exposure to significantly contribute to CDK9 inhibition in the clinic.

Having established the potential for five-membered and [5,6]-bicyclic systems at the C-4 position of the pyridine to balance CDK9 potency with aqueous solubility, and the potential to further improve potency through C-5 substitution of the pyridine, we decided to further mine this SAR by again varying the C-4 position. From the initial exploration of the C-4 substituent, the pyrazolopiperidine headgroup (compound **6**) combined acceptable CDK9 potency and high solubility. 1,5-Dimethyl-3-pyrazole **7** was significantly less potent against CDK9, whereas pyrazolopyridine **8** kept comparable potency to **6**, but was much less soluble. Initial compounds comparing an imidazole group to the pyrazole group (e.g., imidazopyridine **9** vs pyrazolopiperidine **6**, 1,2-dimethyl-5-imidazole **10** vs 1,5-dimethyl-3-pyrazole **7**, and imidazopyridine **11** vs pyrazolopyridine **8**) showed reduced CDK9 potency by about 10-fold, but provided some evidence of increased solubility (probably related to the lower lipophilicity). Finally, triazolopiperidine **12** gave much reduced potency (ca. 100-fold) against CDK9 vs pyrazolopiperidine **6**.

We then explored modifications of the piperidine portion of the pyrazolopiperidine headgroup in compound **6**. Pyrrolidine **13** showed slightly reduced potency (ca. 5-fold) when compared to piperidine **6**, but surprisingly, imidazopyrrolidine **14** was nearly equipotent compared vs pyrazolopyrrolidine **13** (potency reduced by only ca. 2-fold). Azepane **15** showed comparable potency (CDK9 5 mM [ATP], IC_{50} : 0.023 μM ; pSer2-RNAP2,

Table 2. Structure, CDK9 Enzyme and Cell Inhibitory Potencies, and Other Properties of Compounds 2–34

Cpd	Core	X	Het or R	A		B		Log D _{7.4} ^b	Sol. (μM) ^c	Rat heps Cl _{lim} ^d	HLM Cl _{lim} ^e	Hu. heps Cl _{lim} ^d
				CDK9 enz. [ATP] 5 mM IC ₅₀ (μM) ^a	pSer2 cell IC ₅₀ (μM) ^a	MV-411 caspase EC ₅₀ (μM) ^a	EC ₅₀ (μM) ^a					
2	A	H		0.029	0.13	0.22	3.0	33	58	12	1.4	
3	A	H		0.38	0.92	0.66 ^f	1.9	660	7.4	3.6	-	
4	A	H		0.23	0.52	0.44 ^f	2.4	730	33	<3	-	
5	A	F		0.051	0.10	0.16 ^f	2.9	>1000	73	<3	-	
6	A	Cl		0.039	0.11	0.13	3.2	310	46	17	<1.2	
7	A	Cl		0.27	0.44	0.56	2.6	960	10	3.3	<1	
8	A	Cl		0.061	0.14	0.15	3.6	45	-	-	-	
9	A	Cl		0.66	1.2	1.2	2.7	600	12	16	-	
10	A	Cl		5.3	>3	-	2.2	>1000	-	-	-	
11	A	Cl		0.75	1.6	-	3.0	120	-	-	-	
12	A	Cl		4.4	>2.6	-	2.0	530	-	-	-	
13	A	Cl		0.18	0.53	0.33 ^f	2.9	160	72	<3	-	
14	A	Cl		0.31	0.76	0.70	2.6	490	19	9.7	-	
15	A	Cl		0.023	0.092	0.18	3.6	104	51	39	4.6	
16	A	Cl		1.0	2.1	1.9 ^f	2.4	220	18	<3	-	
17	A	Cl		0.22	0.80	0.91 ^f	2.1	870	7.7	<3	-	
18	A	Cl		0.35	0.86	0.67	2.4	860	10	6.2	-	
19	A	Cl		0.11	0.35	0.26	2.6	110	34	<3	-	
20	A	H		0.008	0.048	0.039	3.1	640	35	29	4.3	

Table 2. continued

Cpd	Core	X	Het or R	CDK9 enz. [ATP] 5 mM IC ₅₀ (μM) ^a	pSer2 cell IC ₅₀ (μM) ^a	MV-4-11 caspase EC ₅₀ (μM) ^a	Log D _{7.4} ^b	Sol. (μM) ^c	Rat heps Cl _{int} ^d	HLM Cl _{int} ^e	Hu. heps Cl _{int} ^d
21	A	F		<0.003	0.010	0.015	3.6	160	42	178	23
22	A	H		0.029	0.15	0.10 ^f	2.8	970	45	<3	<1
23	A	F		0.004	0.025	0.029	3.3	550	81	19	2.6
24	A	Cl		<0.004	0.0134	0.0137	3.8	150	73	50	5.5
25	A	CN		0.062	0.15	0.14	3.2	380	47	26	<1
26	A	Me		0.022	0.040	0.074	3.1	600	53	19	-
27	A	Cl		0.027	0.077	0.077	3.4	159	85	18	-
			Isomer 1								
28	A	Cl		0.026	0.036	0.092	3.4	79	97	13	-
			Isomer 2								
29	A	Cl		0.011	0.036	0.054	3.6	280	28	63	2.5
30	B	Cl		0.29	0.31	0.42	-	-	-	-	-
31	B	Cl		6.8	2.4	4.8	-	-	-	-	-
			Trans, isomer 1								
32	B	Cl		0.017	0.049	0.068	-	-	-	-	-
			Trans, isomer 2								
33	B	Cl		0.003	0.040	0.015	3.5	35	97	38	5.8
34	B	Cl		0.025	0.044	0.038	3.2	15	157	25	106

^aGeometric means of at least two IC₅₀ determinations per compound. ^bMeasured using shake-flask methodology with a buffer/octanol volume ratio of 100:1. ^cSolubility from phosphate buffer (pH: 7.4); sample from dried DMSO solution. ^dIntrinsic clearance measured from fresh rat hepatocytes and cryopreserved human hepatocytes, Cl_{int}; μL·min⁻¹·10⁶ cells⁻¹. ^eHuman liver microsome intrinsic clearance (HLM Cl_{int}); μL·min⁻¹·mg⁻¹.

Table 3. Selectivity of Compounds 6 and 23 against Kinases within the CDK Family

kinase	compound 6 IC ₅₀ (μM) ^a [ATP] 5 mM	compound 23 IC ₅₀ (μM) ^a [ATP] 5 mM
CDK9	0.039	0.004
CDK1	0.44	0.095
CDK2	0.61	0.066
CDK3	0.084	0.020
CDK4	2.1	0.334
CDK5	4.1	2.78
CDK6	2.5	0.532
CDK7	5.9	0.548
CDK12	>30	9.85

^a[ATP] 5 mM: concentration of ATP used in the kinase assay 5 mM.

IC₅₀: 0.092 μM) to piperidine 6. In addition, 15 exhibited an increased rate of metabolism in HLM and human hepatocytes, although its solubility was slightly lower. Introduction of heteroatoms to the piperidine ring of compound 6 (e.g., compounds 16–19) showed reduced potency against CDK9 (range of 3–30-fold) compared to compound 6. It is noteworthy that only a very small number of basic compounds (e.g., compound 17) were investigated. Despite the good solubility

Table 4. Binding Kinetics of 6, 23, and 24 to CDK9 Determined by Surface Plasmon Resonance

	compound 6	compound 23	compound 24
equilibrium dissociation constant K _D (nM)	0.295	0.123	0.0894
association rate constant k _a (μM ⁻¹ ·s ⁻¹)	8.93	4.62	7.95
dissociation rate constant k _d (10 ⁻⁶ ·s ⁻¹)	3640	569	711
dissociation half-life t _{1/2} (min)	6.3	20.3	16.2

observed with them, we were concerned by the potential higher volume of distribution associated with this ion class and the consequence on the pharmacokinetic half-life. We then looked at adding substituents on the piperidine in an attempt to further interact with the P-loop. Indeed, gem-dimethylpiperidine 20 showed significantly increased potency (about 10–20-fold, CDK9 5 mM [ATP], IC₅₀: 0.008 μM; pSer2-RNAP2, IC₅₀: 0.048 μM) versus the unsubstituted piperidine 4. In addition, 20 was highly soluble and showed an increased rate of metabolism in HLM and human hepatocytes. Introduction of a 5-fluoro on the pyridine led to a further increase in potency (compound 21: CDK9 5 mM [ATP], IC₅₀: < 0.003 μM; pSer2-RNAP2, IC₅₀:

Table 5. Pharmacokinetic Properties of Compound 6 in Preclinical Species and Predicted Human Parameters

	mouse	rat	dog	human
hepatocytes Cl_{int} ($\mu\text{L}/\text{min}/10^6$ cells) ^a	27	46	14	<1.2
plasma Cl ($\text{mL}/\text{min}/\text{kg}$) ^b	65	78	30	<2.8 ^c
V_{ss} (L/kg) ^b	0.65	0.75	0.90	0.68 ^c
$t_{1/2}$ (h)	0.45	0.25	0.50	>2.8 ^c

^aIntrinsic clearance measured from hepatocytes, Cl_{int} . ^bFor mouse and Han Wistar rat studies ($n \geq 2$), the compound was administered respectively at a dose of 4.8 $\mu\text{mol}/\text{kg}$ and 1.2 $\mu\text{mol}/\text{kg}$ i.v. as a solution formulation. For Beagle dogs ($n = 2$), the compound was administered by intravenous infusion over 0.25 h at a dose of 5.2 $\mu\text{mol}/\text{kg}$ as a solution in 5% DMSO and made to volume with 0.9% sodium chloride. ^cItalicized text indicated human PK predictions (see Supporting Information for methods).

0.010 μM) while showing an increased rate of metabolism in HLM and human hepatocytes with only a modest reduction in solubility. Similarly, substitution of the pyrrolidine with *gem*-dimethyl (compounds 22–24) was very fruitful. Compound 22 was significantly more potent than 4. Again, introduction of a 5-fluoro or a 5-chloro on the pyridine further improved potency (respectively compound 23: CDK9 5 mM [ATP], IC_{50} : 0.004 μM ; pSer2-RNAP2, IC_{50} : 0.025 μM and 24: CDK9 5 mM [ATP], IC_{50} < 0.004 μM ; pSer2-RNAP2, IC_{50} : 0.0134 μM), while introduction of a 5-cyano (compound 25) or a 5-methyl (compound 26) was less favorable. In addition, 23 and 24 were highly soluble (550 and 150 μM , solubility at pH 7.4 phosphate buffer, data obtained from dried DMSO sample method) and showed a higher rate of metabolism in HLM and human hepatocytes than compound 22. *Gem*-dimethyl substitution provided more CDK9 potency than a single methyl substituent (see compound 24 vs compounds 27 and 28). The imidazopyrrolidine analogue of 24 (compound 29) also displayed high potency against CDK9 (CDK9 5 mM [ATP], IC_{50} 0.011 μM ; pSer2-RNAP2, IC_{50} : 0.036 μM) and showed high solubility and a similar rate of metabolism in HLM to compound 24.

The C-2 position of the pyridine had been previously optimized, following a library on a less optimized scaffold

Table 6. CDK9 Enzymatic and Cellular Potencies and in Vitro Intrinsic Clearance of 6 and Its Metabolites 6-M1 and 6-M2 in HLM and Human Hepatocytes

Cpd	CDK9 enz. [ATP] 5 mM IC_{50} (μM) ^a	pSer2 cell IC_{50} (μM) ^a	HLM Cl_{int}	Hu. heps Cl_{int}
6	0.039	0.11	17	<1.2
6-M1	0.060	0.72	18	33
6-M2	0.085	>2	15	2.9

^aGeometric means of at least two IC_{50} determinations per compound.

^bHuman liver microsome intrinsic clearance (HLM Cl_{int}); $\mu\text{L}\cdot\text{min}^{-1}\cdot\text{mg}^{-1}$. ^cIntrinsic clearance measured from human hepatocytes, Cl_{int} ; $\mu\text{L}\cdot\text{min}^{-1}\cdot 10^6$ cells⁻¹.

(data not shown), but we were keen to explore the subtleties of the SAR in this position, following the extensive optimization in other areas of the molecule. The different stereoisomers of the 3-acetamido-cyclohexane-1-carboxamide substituent were evaluated (compounds 30–32 vs 24), confirming the initial observation on related compounds that the (*R,R*)-diastereoisomer was the most potent. Finally, further modification of this region (e.g., compounds 33 and 34) did not improve activity versus the 3-acetamido-cyclohexane-1-carboxamide group (compound 24).

The cocrystallographic structure of 24 bound to CDK9 in complex with cyclin T1 confirmed the ligand binding mode (Figure 4). The cyclin is bound as expected near the αC -helix of CDK9, with no direct interaction with the ATP binding site or the ligand. Consistent with the predicted binding mode of 2 (Figure 2), Cys106 makes two hydrogen-bonds with the pyridyl amide core, and the cyclohexyl ring of solvent channel group is orthogonal to this motif. The pyrazole–pyridine biaryl system is twisted out of plane by 37 deg, such that one of the *gem*-dimethyl substituents of 24 fills a small pocket formed near Asp167 of the activation loop, in close proximity to the aliphatic portion C β of its side chain, the C α of Asn154 and the side chain of Ala166.

Selected compounds (e.g., compounds 23 and 24) were further profiled. Kinase selectivity of 23 was evaluated at 1 μM in the “Eurofins kinase panel”. It showed significant inhibition (>80% inhibition) on 8 kinases out of 125 kinases in the

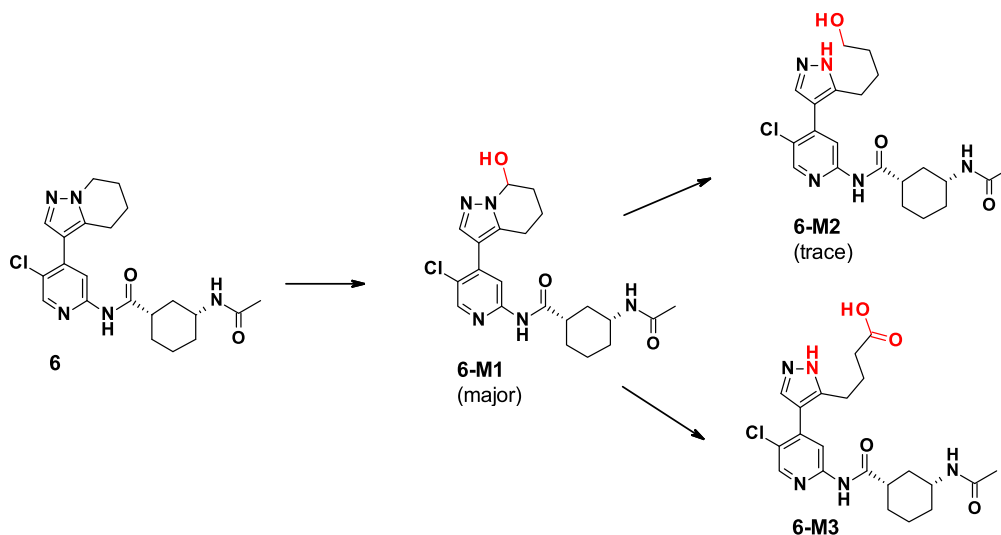


Figure 3. Metabolites of 6 after incubation in HLM. Metabolites shown were considered to have the potential to retain pharmacological activity and do not represent a complete metabolic scheme.

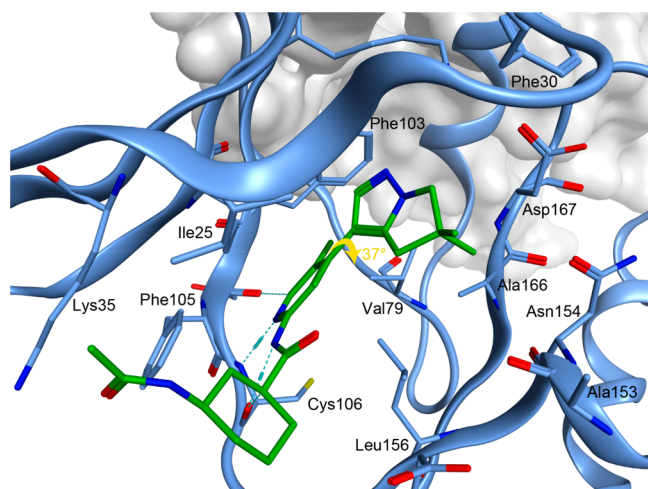


Figure 4. Crystal structure of **24** bound to the complex of CDK9 (blue) and cyclin T1 (gray) (PDB: 6Z45). The ligand carbon atoms are shown in green.

“Eurofins kinase panel”: CDK9 (100%), GSK3 α (101%), GSK3 β (101%), CDK1 (100%), CDK2 (100%), CDK7 (92%), CK1 γ 1 (91%), and DYRK2 (89%). The selectivity of **23** among the CDK family was further assessed in assays recapitulating the typical ATP concentration in cells ([ATP] of 5 mM), supporting that **23** is a potent CDK9 inhibitor with at least 16-fold selectivity against CDK1-7 and CDK12, except CDK3 (5-fold); see Table 2. Kinase selectivity of **24** was evaluated at 1 μ M in the “Eurofins kinase panel” and at 0.1 μ M in the “Thermofisher kinase panel”. It showed significant inhibition (>80% inhibition) on 8 kinases outside the CDK family out of 125 kinases in the “Eurofins kinase panel”: GSK3 β (104%), DYRK2 (100%), GSK3 α (100%), CK1 γ 1 (94%), Jnk1 (90%), MAP2K7 (85%), INSR (83%), and MAP3K9 (82%). In the “Thermofisher kinase panel”, only 7 kinases outside the CDK family out of 362 kinases tested were significantly inhibited (>80% inhibition): GSK3 β (100%), GSK3 α (96%), DYRK2 (85%), MAP4K4 (85%), Jnk1 (84%), ERK7 (83%), and DYRK1A (80%). The selectivity among the CDK family and other kinase hits was further assessed in assays recapitulating the typical ATP concentration in cells ([ATP] of 5 mM). The overall profile is summarized in Table 7, supporting that **24** is a potent CDK9 inhibitor with >10-fold selectivity against CDK1-7 and CDK12, except CDK3 (>5.8-fold) and >47-fold selectivity for other non-CDK kinases. This selectivity profile among the CDK family was confirmed in cells, showing that **24** exhibited >25-fold cellular selectivity for CDK9 over CDK1, CDK2, CDK4, CDK6, and CDK7 upon short-term treatment.⁴⁶

The binding kinetics of **23** and **24** to CDK9 was determined by surface plasmon resonance (Table 4). Both compounds showed a short dissociation half-life: 20.3 min for compound **23** and 16.2 min for compound **24**. The reversibility of pSer2-RNAP2 inhibition in the MCF-7 cell line was investigated by incubation of **23** and **24** followed by cell washout and measurement of pSer2-RNAP2 inhibition at 30 min and 2 h after wash-out. Compounds **23** and **24** showed reversibility, where inhibition was very significantly reduced at 30 min (IC_{50} reduced by 19-fold for **23** and 32-fold for **24**) and at 2 h (IC_{50} > 3 μ M), which was expected from the “fast-off” binding kinetics of **23** and **24** to CDK9 measured by surface plasmon resonance.

Thermodynamic solubilities of **23** and **24** were further assessed from crystalline batches: 30 mg/L in 1 \times PBS buffer pH

Table 7. Selectivity of Compound **24** against Selected Kinases

kinase	IC_{50} (μ M) ^a [ATP] 5 mM
CDK9	<0.004
CDK1	0.117
CDK2	0.052
CDK3	0.023
CDK4	0.499
CDK5	1.27
CDK6	0.363
CDK7	1.37
CDK12	8.07
CK1 γ 1	5.52
CK1 γ 2	6.66
DYRK2	8.62
GSK3 α	0.187
GSK3 β	0.247
JNK1	2.80

^a[ATP] 5 mM: concentration of ATP used in the kinase assay 5 mM.

7.4 and 57 mg/L in 0.1 M acetate buffer pH 4 for compound **23** (from crystalline Form B⁴⁴); 17 mg/L in 1 \times PBS buffer pH 7.4 and 50 mg/L in 0.1 M acetate buffer pH 4 for compound **24** (from crystalline Form A⁴⁴). In addition, evaluation of common pharmaceutical excipients suitable for i.v. clinical formulation demonstrated further solubility enhancement. As a result, development of a suitable clinical formulation for i.v. administration was seen as a highly viable option, especially given the anticipated lower therapeutic dose resulting from the increased CDK9 potency of compound **24** compared to compounds **2** and **6**.

The pharmacokinetic properties were evaluated in mouse, rat, and dog for compound **23** and in mouse, rat, dog, and cynomolgus monkey for compound **24**: in all species evaluated, compounds **23** and **24** showed a moderate volume of distribution, as anticipated from their neutral ionic state. Clearance was high in all preclinical species, with the observed plasma clearance values being accurately predicted by scaling the intrinsic clearance derived from isolated hepatocyte incubations. Overall, the high clearance combined with the low/medium volume of distribution resulted in short half-lives (below 1 h) in all species. Scaling of in vitro intrinsic clearances values from human hepatocytes resulted in similar predicted human clearance values for both compounds, which, when combined with the predicted human volume of distribution, resulted in a predicted human $t_{1/2}$ value of 1.5 h for compound **23** (predicted human PK parameters: Cl 4.8 mL/min/kg, V_{ss} 0.61 L/kg, mean $t_{1/2}$ 1.5 h, see Table 8) and 1.6 h for compound **24** (predicted human PK parameters: Cl 5.3 mL/min/kg, V_{ss} 0.73 L/kg, mean $t_{1/2}$ 1.6 h, see Table 9) respectively.

Metabolite identification studies were performed in HLM (and human hepatocytes) for compounds **23** and **24**. Both compounds showed analogous metabolic pathways to those observed with compound **6**, leading to the formation of **23-M1**, **23-M2**, and **23-M3** from compound **23** and **24-M1**, **24-M2**, and **24-M3** from compound **24** (see Figure 5), the M1 metabolite being the most abundant. The structures of **24-M1** and **24-M2** were subsequently confirmed by chemical synthesis of authentic standards. From their biological activity and their properties (Table 10), the risk that the metabolites formed from **24** would contribute to significant CDK9 activity in the clinical setting was viewed as low. The detailed metabolism of **24** in vitro and in vivo will be the subject of a separate publication in due course.

Table 8. Pharmacokinetic Properties of Compound 23 in Preclinical Species and Predicted Human Parameters

	mouse	rat	dog	human
hepatocytes Cl_{int} ($\mu\text{L}/\text{min}/10^6$ cells) ^a	75	81	23	2.6
plasma Cl ($\text{mL}/\text{min}/\text{kg}$) ^b	70	104	53	4.8 ^c
V_{ss} (L/kg) ^b	0.49	0.80	1.2	0.61 ^c
$t_{1/2}$ (h)	0.16	0.18	0.43	1.5 ^c

^aIntrinsic clearance measured from hepatocytes, Cl_{int} . ^bFor mouse and Han Wistar rat studies ($n \geq 2$), the compound was administered respectively at a dose of 2.4 $\mu\text{mol}/\text{kg}$ and 1.2 $\mu\text{mol}/\text{kg}$ i.v. as a solution formulation. For Beagle dogs ($n = 2$), the compound was administered by intravenous infusion over 0.25 h at a dose of 0.24 $\mu\text{mol}/\text{kg}$ as a solution in 10/90 DMSO/10% captisol (w/v) at the concentration of 0.2 mg/mL. ^cItalicized text indicates human PK predictions (see Supporting Information for methods).

Table 9. Pharmacokinetic Properties of Compound 24 in Preclinical Species and Predicted Human Parameters

	mouse	rat	dog	monkey	human
hepatocytes Cl_{int} ($\mu\text{L}/\text{min}/10^6$ cells) ^a	98	73	11	32	5.5
plasma Cl ($\text{mL}/\text{min}/\text{kg}$) ^b	55	71	16	19	5.3 ^c
V_{ss} (L/kg) ^b	0.45	0.68	0.67	1.3	0.73 ^c
$t_{1/2}$ (h)	0.18	0.18	0.66	0.89	1.6 ^c

^aIntrinsic clearance measured from hepatocytes, Cl_{int} . ^bFor mouse and Han Wistar rat studies ($n \geq 2$), the compound was administered respectively at a dose of 2.3 $\mu\text{mol}/\text{kg}$ and 1.2 $\mu\text{mol}/\text{kg}$ i.v. as a solution formulation. Male Beagle dogs ($n = 2$) were administered 0.23 $\mu\text{mol}/\text{kg}$ by intravenous infusion over 0.25 h formulated as a solution in 10% dimethyl sulfoxide (DMSO)/90% sterile water for injection (adjusted to pH 7–9). For cynomolgus monkeys ($n = 2$), the compound was administered by intravenous infusion over 0.25 h at a dose of 0.46 $\mu\text{mol}/\text{kg}$ as a solution in 2% dimethylacetamide (DMA)/30% polyethylene glycol 400 (PEG400)/68%, 1% (w/v) Tween 80 in sterile water for injection. ^cItalicized text indicates human PK predictions (see Supporting Information for methods).

Table 10. CDK9 Enzymatic and Cellular Potencies and In Vitro Intrinsic Clearance of 24 and Its Metabolites 24-M1 and 24-M2 in HLM and Human Hepatocytes

Cpd	CDK9 enz. [ATP] 5 mM IC_{50} (μM) ^a	pSer2 cell IC_{50} (μM) ^a	HLM Cl_{int} ^b	Hu. heps Cl_{int} ^c
24	<0.004	0.0134	50	5.5
24-M1	0.020	0.17	14	48
24-M2	0.139	>2.3	24	<1

^aGeometric means of at least two IC_{50} determinations per compound. ^bHuman liver microsome intrinsic clearance (HLM Cl_{int}); $\mu\text{L}\cdot\text{min}^{-1}\cdot\text{mg}^{-1}$. ^cIntrinsic clearance measured from human hepatocytes, Cl_{int} ; $\mu\text{L}\cdot\text{min}^{-1}\cdot 10^6$ cells⁻¹.

The activity of compound 24 was recently reported in multiple AML cell lines in vitro and multiple AML xenograft models in vivo.⁴⁶ Consistent with the expected mode of action of a CDK9 inhibitor, compound 24 showed inhibition of pSer2-RNAP2, reduction of Mcl-1 protein and induction of caspase 3/7 activation in the acute myeloid leukemia cell lines MV-4-11⁴⁶ and Nomo-1 (see Figure 6) in a dose- and time-dependent manner.

In the MV-4-11 xenograft mouse model, compound 24 showed a dose-dependent cell death driven antitumor efficacy when dosed intermittently (BID 2 h apart by i.p. administration, 2 days on 5 days off) at 5 mg/kg (97% tumor growth inhibition, measurement taken 33 days after commencement of dosing) and 15 mg/kg (100% complete tumor regression that was sustained out to more than 125 days). This antitumor response was driven by cell death as evidenced by induction of caspase 3/7. A concomitant reduction in pSer2-RNAP2 and Mcl-1 demonstrated that this effect is indeed mediated by inhibition of CDK9.⁴⁶ Here we report the in vivo activity of compound 24 in the Nomo-1 AML xenograft model. Compound 24 resulted in a similar extent of cell death driven antitumor efficacy using the same doses and schedules, with the 5 mg/kg BID schedule resulting in 65% tumor growth inhibition, and the 15 mg/kg BID

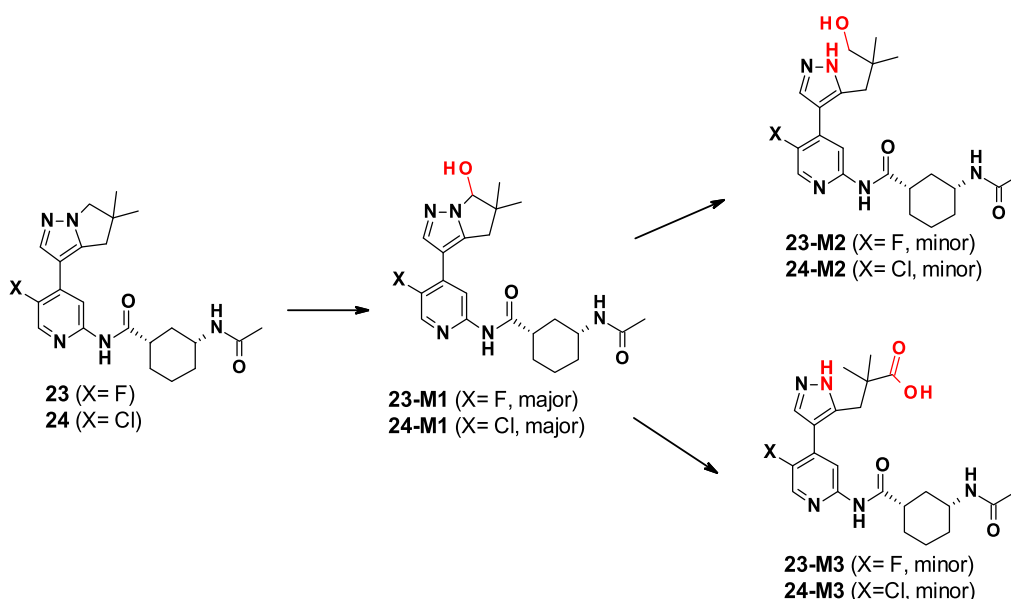
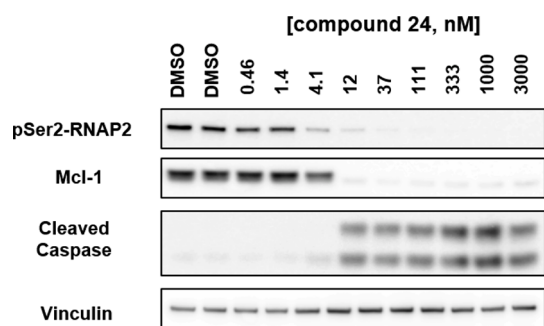


Figure 5. Metabolite identification of 23 and 24 after incubation in HLM. Metabolites shown were considered to have the potential to retain pharmacological activity and do not represent a complete metabolic scheme.



Nomo-1 cell line, 6 h in vitro exposure

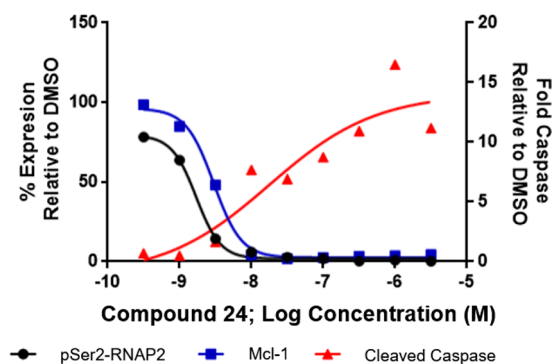


Figure 6. Inhibition of pSer2-RNAP2, depletion of Mcl-1 protein, and induction of caspase 3/7 activation after a 6-h incubation of compound 24 (dose response) in the acute myeloid leukemia Nomo-1 cell line. Top panel: Western blot; bottom panel: quantification.

schedule resulting in 65% tumor volume regression (assessed 12 days after the commencement of dosing), **Figure 7**. The extent and duration of reduction of pSer2-RNAP2 in the Nomo-1 xenograft tumors (**Figure 8**) were also similar to that observed in MV-4-11 tumors at both dose levels.

As the half-maximal effective concentration (EC_{50}) for caspase activation in MV-4-11 cells closely aligns with other

Nomo-1 AML Xenograft Efficacy

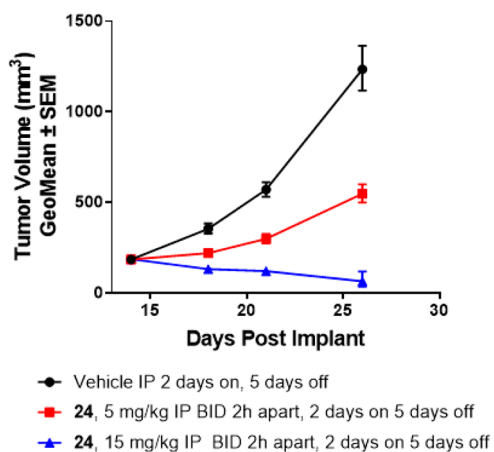


Figure 7. Dose-dependent cell death driven antitumor efficacy in the acute myeloid leukemia Nomo-1 xenograft model of compound 24 by i.p. administration, twice daily 2 h apart, 2 days on 5 days off.

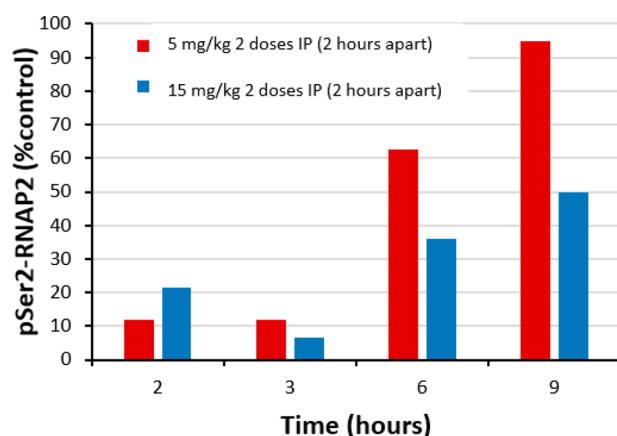


Figure 8. Dose-dependent reduction of pSer2-RNAP2 in the acute myeloid leukemia Nomo-1 xenograft model by i.p. administration of compound 24, two doses 2 h apart by i.p. administration.

sensitive AML cell lines screened with compound 24,⁴⁶ MV-4-11 was selected as a representative AML cell line for the purposes of predicting the efficacious dose in clinical AML. The quantitative PKPD/antitumor efficacy model, derived from mouse MV-4-11 xenograft study data (described previously⁴⁶) was translated to the clinical AML setting (by adjusting system parameter values and replacing the mouse PK model for compound 24 with a predicted human PBPK model; see **Supporting Information**) and used to predict clinical efficacy. Clinical i.v. dose was optimized such that each 2 h i.v. infusion was predicted to result in a 60% reduction in the leukemic cell burden. This extent of antitumor efficacy (per dosing occasion) was similar to what had been achieved in mouse MV-4-11 xenograft models when dosing compound 24 and was predicted to be sufficient to drive a sustained progressive reduction in leukemic cell burden in AML patients when utilizing a 2 days-on/12 days-off dosing schedule (assuming a 10 day doubling time). The predicted clinical dose of compound 24 that would be required to achieve this extent of antitumor efficacy was 44 mg. The predicted time-course of free concentration in plasma for a typical patient, at this dose, is shown in **Figure 9**.

Preclinical in vivo toxicological evaluation of compound 24 supported dosing to patients, and 24 (AZD4573) is currently in phase 1 clinical trials in patients with relapsed or refractory

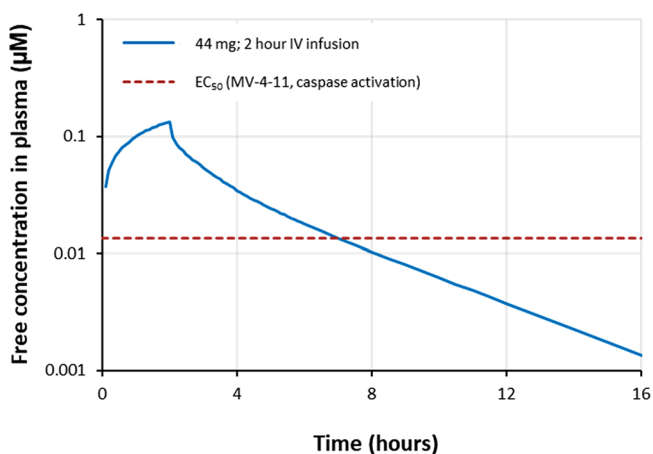


Figure 9. Simulated human pharmacokinetic profile of compound 24 following a 44 mg dose administered by a 2 h continuous i.v. infusion.

hematological malignancies (ClinicalTrials.gov Identifier: NCT03263637).

CONCLUSION

Here we report the optimization of a series of pyrimidine amides as potent and selective CDK9 inhibitors having suitable pharmacokinetic and physicochemical properties for an intravenous agent with short duration of target engagement. Starting from **2**, a highly selective inhibitor of CDK9 but with physical and pharmacokinetic properties that appeared to be unsuitable for the desired profile, we identified compound **24** (also known as AZD4573). Compound **24** is a potent inhibitor of CDK9 (IC_{50} of $<0.004 \mu\text{M}$) with fast-off binding kinetics ($t_{1/2}$ 16 min) and high selectivity versus other kinases, including other CDK family members. Compound **24** exhibited a short pharmacokinetic half-life in multiple preclinical species (less than 1 h in rat, dog, and monkey), and PBPK modeling predicted a short half-life in humans. While the predictions of human PK may never be completely accurate due to species differences, the predictions for compounds relative to one another are useful in providing a rank order in order to select the most appropriate clinical candidate. Compound **24** also exhibited suitable solubility for intravenous administration. Short-term treatment with compound **24** led to a rapid dose- and time-dependent decrease in pSer2-RNAP2 and Mcl-1 in cells, resulting in activation of caspase 3/7 and cell apoptosis in a broad range of hematological cancer cell lines. In vivo efficacy was demonstrated in xenograft models derived from multiple hematological tumors (e.g., regression at 15 mg/kg, i.p administration, BID 2 days on 5 days off, in acute myeloid lymphoma MV-4-11 and Nomo-1 xenografts), with evidence of a decrease of pharmacologically relevant biomarkers (e.g., pSer2-RNAP2). Compound **24** is currently in phase 1 clinical trials for the treatment of hematological malignancies.

EXPERIMENTAL SECTION

General Methods. All experiments were carried out at ambient temperature under an inert atmosphere. Evaporations were carried out by rotary evaporation or utilizing Genevac equipment or a Biotage v10 evaporator *in vacuo*, and workup procedures were carried out after the removal of residual solids by filtration. Flash chromatography purifications were performed on an automated Teledyne Isco CombiFlash Rf or Teledyne Isco CombiFlash Companion using prepacked RediSep Rf Gold Silica Columns (20–40 μm , spherical particles), GraceResolv Cartridges (Davisil silica), or Silicycle cartridges (40–63 μm). Ion exchange purification was generally performed using an SCX-2 (Biotage) cartridge. Preparative chromatography was performed on a Gilson prep HPLC instrument with UV collection or on a Waters AutoPurification HPLC-MS instrument with MS- and UV- triggered collection. The purities of the compounds for biological testing were assessed by NMR and mass spectral techniques following liquid chromatography (LCMS or UPLC) and are consistent with the proposed structures characterized; purity was at least 95%. Proton NMR were determined using a Bruker Avance 500 (500 MHz) or Bruker Avance 400 (400 MHz) instrument. Measurements were taken at ambient temperature unless otherwise specified; the following abbreviations have been used: s, singlet; d, doublet; t, triplet; q, quartet; m, multiplet; dd, doublet of doublets; ddd, doublet of doublet of doublet; dq, double of quartets; dt, doublet of triplets; tt, triplet of triplets; p, pentet; br, broad signal. UPLC was carried out using a Waters UPLC fitted with Waters SQ mass spectrometer (column temp 40, UV = 220–300 nm, mass spec = ESI with positive/negative switching) at a flow rate of 1 mL/min using a solvent system of 97% A + 3% B to 3% A to 97% B over 1.50 min (total run time with equilibration back to starting conditions back to starting conditions 1.70 min), where

A = 0.1% formic acid in water (for acid work) or 0.1% ammonia in water (for base work) B = acetonitrile. For acid analysis, the column used was Waters Acquity HSS T3 1.8 μm 2.1 \times 50 mm, and for base analysis the column used was Waters Acquity BEH 1.7 μm 2.1 \times 50 mm. Alternatively, UPLC was carried out using a Waters UPLC fitted with a Waters SQ mass spectrometer (column temp 30, UV = 210–400 nm, mass spec = ESI with positive/negative switching) at a flow rate of 1 mL/min using a solvent gradient of 2–98% B over 1.5 min (total runtime with equilibration back to starting conditions: 2 min), where A = 0.1% formic acid in water and B = 0.1% formic acid in acetonitrile (for acid work) or A = 0.1% ammonium hydroxide in water and B = acetonitrile (for base work). For acid analysis, the column used was a Waters Acquity HSS T3 1.8 μm 2.1 \times 30 mm, and for base analysis the column used was a Waters Acquity BEH C18 1.7 μm 2.1 \times 30 mm; LCMS was carried out using a Waters Alliance HT (2795) fitted with a Waters ZQ_ESCi mass spectrometer and a Phenomenex Gemini – NX (5 μm \times 2.1 mm) column at a flow rate of 1.1 mL/min 95% A to 95% B over 4 min with a 0.5 min hold. The modifier was kept at a constant 5% C (50:50 acetonitrile/water 0.1% formic acid) or D (50:50 acetonitrile/water 0.1% ammonium hydroxide depending on whether it was an acidic or basic method. Intermediates were not fully purified, but their structure and purity were assessed by NMR, HPLC, or UPLC and mass techniques (unless stated otherwise) and are consistent with the proposed structures.

All experimental activities involving animals were carried out in accordance with AstraZeneca animal welfare protocols, which are consistent with the American Chemical Society Publications rules and ethical guidelines.

(1*S*,3*R*)-3-Acetamido-*N*-[4-(1-isopropyl-2-methyl-1*H*-imidazol-5-yl)-2-pyridinyl]cyclohexanecarboxamide (**3**). A mixture of 4-(4,4,5,5-tetramethyl-1,3,2-dioxaborolan-2-yl)pyridin-2-amine (**35**, 0.650 g, 2.95 mmol), potassium phosphate (0.941 g, 4.43 mmol), and 5-bromo-1-isopropyl-2-methyl-1*H*-imidazole (**36**, 0.30 g, 1.5 mmol) in water (8 mL) and 1,4-dioxane (24 mL) was degassed using a stream of nitrogen for 20 min. Then, chloro(2-dicyclohexylphosphino-2',4',6'-triisopropyl-1,1'-biphenyl)[2-(2'-amino-1,1'-biphenyl)]palladium(II) (0.12 g, 0.15 mmol) was added to the mixture, and the reaction was heated at 110 °C for 3 h. After concentration under reduced pressure, the resulting residue was suspended in MeOH (10 mL) and DCM (30 mL), and the mixture was filtered and concentrated under reduced pressure to give crude 4-(1-isopropyl-2-methyl-1*H*-imidazol-5-yl)pyridin-2-amine (**37**, 137 mg, 42%), which was used without purification. MS-ESI m/z 217 [MH⁺].

1-Chloro-*N,N,N*-trimethylprop-1-en-1-amine (0.232 g, 1.73 mmol) was added to (1*S*,3*R*)-3-((*tert*-butoxycarbonyl)amino)-cyclohexanecarboxylic acid (**38**, 0.337 g, 1.39 mmol) in DCM (8 mL) at 0 °C. The solution was stirred at room temperature for 30 min. A solution of **37** (0.25 g, 1.2 mmol) and pyridine (0.14 mL, 1.7 mmol) in THF (8 mL) was then added. The mixture was stirred at room temperature for 18 h. The mixture was then partitioned between EtOAc (50 mL) and water (50 mL), and the layers were separated. The organic layer was concentrated under reduced pressure. The resulting residue was purified by flash silica chromatography, eluting with 10–20% MeOH in DCM to afford *tert*-butyl ((1*R*,3*S*)-3-((4-(1-isopropyl-2-methyl-1*H*-imidazol-5-yl)pyridin-2-yl)carbamoyl)cyclohexyl)-carbamate (62 mg, 12%). MS-ESI m/z 442 [MH⁺].

Hydrochloric acid in dioxane (4 M; 0.49 mL, 14.0 mmol) was added to a solution of *tert*-butyl ((1*R*,3*S*)-3-((4-(1-isopropyl-2-methyl-1*H*-imidazol-5-yl)pyridin-2-yl)carbamoyl)cyclohexyl)-carbamate (0.062 g, 0.14 mmol) in MeOH (2 mL). The reaction was stirred at room temperature for 18 h. After concentration under reduced pressure, the resulting residue was diluted in DCM (5 mL) and DIPEA (0.098 mL, 0.56 mmol). Acetyl chloride (0.020 mL, 0.28 mmol) was then added. The reaction was stirred at room temperature for 10 min. The reaction was then concentrated under reduced pressure, and the resulting residue was purified by preparative HPLC (column: Xbridge Phenyl 19 mm \times 150 mm 5 μm), eluting with 25–45% acetonitrile in water containing 0.2% NH₄OH (pH 10). Product fractions were concentrated under reduced pressure to give **3** (26 mg, 48%) as a solid. ¹H NMR (400 MHz, DMSO-*d*₆): 1.01–1.17 (1*H*, m), 1.21–1.39 (3*H*, m),

1.44 (6H, d, $J = 7.0$ Hz), 1.73–1.82 (6H, m), 1.89 (1H, br d, $J = 11.5$ Hz), 2.47 (3H, s), 2.58–2.70 (1 H, m), 3.52–3.61 (1H, m), 4.50 (1H, td, $J = 7.0, 14.1$ Hz), 6.89 (1H, s), 7.05 (1H, dd, $J = 1.4, 5.1$ Hz), 7.77 (1H, d, $J = 8.0$ Hz), 8.10 (1H, s), 8.34 (1H, d, $J = 5.0$ Hz) 10.53 (1 H, s); MS-ESI m/z 384 [MH⁺]. HRMS-ESI: m/z found 384.2390 [MH⁺], C₂₂H₂₉ClN₅O₂ requires 384.2394.

(1*S*,3*R*)-3-Acetamido-*N*-(4-(4,5,6,7-tetrahydropyrazolo[1,5-*a*]pyridin-3-yl)pyridin-2-yl)cyclohexanecarboxamide (4). 1-Chloro-*N,N,N*,2-trimethylprop-1-en-1-amine (0.57 mL, 4.33 mmol) was added to a solution of 38 (1.01 g, 4.16 mmol) in DCM (40 mL) at 0 °C. After 1.5 h, a mixture of 4-bromopyridin-2-amine 39 (0.60 g, 3.5 mmol) and pyridine (1.1 mL, 14 mmol) in DCM (33 mL) was added via cannula. The resulting yellow mixture was allowed to warm to room temperature and was stirred under these conditions for 72 h. The now white mixture was filtered and rinsed with a cold DCM wash, and the white precipitate was dried under a vacuum at 70 °C for 30 min to afford *tert*-butyl ((1*R*,3*S*)-3-((4-bromopyridin-2-yl)carbamoyl)cyclohexyl)carbamate 40 (1.38 g, 100%) as a white solid. ¹H NMR (300 MHz, DMSO-*d*₆): 0.99–1.35 (4H, m) 1.38 (9H, s) 1.68–1.80 (3H, m) 1.88 (1H, d) 2.53–2.64 (1H, m) 3.15–3.35 (1H, m) 6.76 (1H, d) 7.34 (1H, dd) 8.21 (1H, d) 8.33 (1H, d) 10.63 (1H, s). MS-ESI m/z 398, 400 [MH⁺].

Chloro(2-dicyclohexylphosphino-2',4',6'-triisopropyl-1,1'-biphenyl)[2-(2'-amino-1,1'-biphenyl)]palladium(II) (9.88 mg, 0.01 mmol) was added in one portion to a degassed mixture of 40 (100 mg, 0.25 mmol), 3-(4,4,5,5-tetramethyl-1,3,2-dioxaborolan-2-yl)-4,5,6,7-tetrahydropyrazolo[1,5-*a*]pyridine 41 (93 mg, 0.38 mmol), potassium phosphate (160 mg, 0.75 mmol), 1,4-dioxane (2 mL), and water (0.2 mL) at 21 °C under nitrogen. The resulting mixture was stirred at 100 °C for 16 h. The reaction mixture was diluted with EtOAc (10 mL) and washed with saturated NaHCO₃ (10 mL). The aqueous layer was extracted with EtOAc (2 × 10 mL), and the combined organic layers were dried over Na₂SO₄, filtered, and concentrated under reduced pressure to afford crude product. The crude product was purified by flash silica chromatography, elution gradient 20–80% EtOAc in heptane. Pure fractions were evaporated to dryness to afford *tert*-butyl ((1*R*,3*S*)-3-((4-(4,5,6,7-tetrahydropyrazolo[1,5-*a*]pyridin-3-yl)pyridin-2-yl)carbamoyl)cyclohexyl)carbamate (42, 70 mg, 63%) as a white powder. ¹H NMR (400 MHz, DMSO-*d*₆): 1.12 (1H, d), 1.21–1.33 (3H, m), 1.39 (9H, s), 1.76 (3H, s), 1.82–1.95 (3H, m), 2.00 (2H, d), 2.59 (1H, s), 2.97 (2H, t), 3.89 (1H, s), 4.12 (2H, t), 6.75 (1H, s), 7.19 (1H, dd), 7.85 (1H, s), 8.22 (2H, d), 10.32 (1H, s). MS-ESI m/z 440 [MH⁺].

Hydrochloric acid in dioxane (4 M; 0.20 mL, 0.80 mmol) was added dropwise to 42 (70 mg, 0.16 mmol) in DCM (2 mL) at 21 °C under nitrogen. The resulting mixture was stirred at 21 °C for 16 h. MeOH (1 mL) was added, and the mixture was purified directly by ion exchange chromatography, using an SCX-2 column. The desired product was eluted using 1 M NH₃ in MeOH, and product fractions were concentrated under reduced pressure to afford (1*S*,3*R*)-3-amino-*N*-(4-(4,5,6,7-tetrahydropyrazolo[1,5-*a*]pyridin-3-yl)pyridin-2-yl)cyclohexanecarboxamide (47 mg, 87%) as a white crystalline solid. ¹H NMR (400 MHz, CD₃OD): 0.95–1.08 (1H, m), 1.2–1.4 (3H, m), 1.76–1.91 (5H, m), 1.99 (3H, dt), 2.44 (1H, ddd), 2.61 (1H, tt), 2.95 (2H, t), 3.25 (1H, s), 4.07 (2H, t), 7.11 (1H, dd), 7.74 (1H, s), 8.07–8.16 (2H, m), NH₂ peak not observed. MS-ESI m/z 340 [MH⁺].

Acetic anhydride (0.016 mL, 0.17 mmol) was added to (1*S*,3*R*)-3-amino-*N*-(4-(4,5,6,7-tetrahydropyrazolo[1,5-*a*]pyridin-3-yl)pyridin-2-yl)cyclohexanecarboxamide (47 mg, 0.14 mmol) and triethylamine (0.023 mL, 0.17 mmol) in DCM (1 mL) at 21 °C under nitrogen. The resulting solution was stirred under these conditions for 60 h. The reaction mixture was loaded directly onto silica and purified by flash silica chromatography, elution gradient 1–10% MeOH in DCM. Product fractions were concentrated under reduced pressure to afford 4 (43 mg, 81%) as a white solid. ¹H NMR (400 MHz, CDCl₃): 1.07–1.23 (1H, m), 1.37–1.53 (3H, m), 1.87–2.03 (8H, m), 2.03–2.11 (2H, m), 2.25 (1H, d), 2.39–2.51 (1H, m), 3.06 (2H, t), 3.88 (1H, dtq), 4.20 (2H, t), 5.40 (1H, d), 7.10 (1H, dd), 7.80 (1H, s), 8.17 (1H, dd), 8.32 (1H, s), 8.35 (1H, s). MS-ESI m/z 382 [MH⁺]. HRMS-ESI: m/z found 382.2248 [MH⁺], C₂₁H₂₈N₅O₂ requires 382.2238.

(1*S*,3*R*)-3-Acetamido-*N*-(5-fluoro-4-(4,5,6,7-tetrahydropyrazolo[1,5-*a*]pyridin-3-yl)pyridin-2-yl)cyclohexanecarboxamide (5). Chloro(2-dicyclohexylphosphino-2',4',6'-triisopropyl-1,1'-biphenyl)-[2-(2'-amino-1,1'-biphenyl)]palladium(II) (0.092 g, 0.12 mmol) was added to a degassed mixture of 41 (0.347 g, 1.40 mmol), 2-chloro-5-fluoro-4-iodopyridine 45 (0.30 g, 1.2 mmol) and potassium phosphate, tribasic (0.61 g, 3.5 mmol) in 1,4-dioxane (10 mL), and water (2 mL). The mixture was degassed and stirred at 90 °C for 2 h under nitrogen. The reaction mixture was concentrated under reduced pressure, and the resulting residue was taken up in water (20 mL). The mixture was extracted with DCM (3 × 20 mL). The combined organic layers were dried over MgSO₄, filtered, and concentrated under reduced pressure. The resulting residue was purified by flash silica chromatography, elution gradient 0–60% EtOAc in heptane. Product fractions were concentrated under reduced pressure to afford 3-(2-chloro-5-fluoropyridin-4-yl)-4,5,6,7-tetrahydropyrazolo[1,5-*a*]pyridine 46 (200 mg, 68%) as a yellow gum. MS-ESI m/z 252 [MH⁺].

Tetrakis(triphenylphosphine)palladium(0) (0.092 g, 0.080 mmol) was added to a mixture of 46 (0.20 g, 0.79 mmol), *tert*-butyl ((1*R*,3*S*)-3-carbamoylcyclohexyl)carbamate 47 (0.231 g, 0.95 mmol, see Supporting Information), 9,9-dimethyl-4,5-bis(diphenylphosphino)-xanthene (0.092 g, 0.16 mmol), and cesium carbonate (0.777 g, 2.38 mmol) in 1,4-dioxane (6 mL). The mixture was degassed (vacuum) and backfilled with nitrogen, and the resulting suspension was stirred at 120 °C for 2 h in the microwave reactor. The reaction mixture was partitioned between water (20 mL) and DCM (40 mL) and separated using a phase separation cartridge. The organic layer was adsorbed onto silica and purified by flash silica chromatography, elution gradient 0–60% EtOAc in heptane. Product fractions were concentrated under reduced pressure to afford *tert*-butyl ((1*R*,3*S*)-3-((5-fluoro-4-(4,5,6,7-tetrahydropyrazolo[1,5-*a*]pyridin-3-yl)pyridin-2-yl)carbamoyl)-cyclohexyl)carbamate 48 (136 mg). This material was used directly in the next step without further purification. MS-ESI m/z 458 [MH⁺].

Trifluoroacetic acid (0.17 mL, 2.2 mmol) was added to 48 (0.10 g, 0.22 mmol) in DCM (5 mL). The resulting solution was stirred at room temperature for 1 h. The reaction mixture was purified by ion exchange chromatography using an SCX-2 column. The desired product was eluted from the column using 1 M NH₃ in MeOH, and product fractions were concentrated under reduced pressure to afford (1*S*,3*R*)-3-amino-*N*-(5-fluoro-4-(4,5,6,7-tetrahydropyrazolo[1,5-*a*]pyridin-3-yl)pyridin-2-yl)cyclohexanecarboxamide as a yellow gum. This material was used directly in the next step without further purification. MS-ESI m/z 358 [MH⁺]. Acetic anhydride (0.032 mL, 0.34 mmol) was added to (1*S*,3*R*)-3-amino-*N*-(5-fluoro-4-(4,5,6,7-tetrahydropyrazolo[1,5-*a*]pyridin-3-yl)pyridin-2-yl)cyclohexanecarboxamide (0.10 g, 0.28 mmol), triethylamine (0.12 mL, 0.84 mmol), and *N,N*-dimethylpyridin-4-amine (2 mg, 0.01 mmol) in DCM (5 mL) at room temperature under air. The resulting solution was stirred at room temperature for 2 h. The reaction mixture was quenched with saturated aqueous ammonium chloride (20 mL) and extracted with DCM (2 × 20 mL). The combined organic layers were dried over MgSO₄, filtered, and concentrated under reduced pressure. The resulting residue was purified by preparative HPLC (Waters XBridge Prep C18 OBD column, 5 μ silica, 30 mm diameter, 100 mm length), using decreasingly polar mixtures of water (containing 1% NH₃) and MeCN as eluents. Fractions containing the desired compound were concentrated under reduced pressure to afford 5 (0.047 g, 42%) as a gum. ¹H NMR (500 MHz, DMSO-*d*₆): 1.03–1.15 (1H, m), 1.23–1.37 (3H, m), 1.74–1.82 (6H, m), 1.83–1.94 (3H, m), 2.00–2.08 (2H, m), 2.56–2.68 (1H, m), 2.91 (2H, t), 3.58–3.61 (1H, m), 4.15 (2H, t), 7.73–7.78 (2H, m), 8.26 (1H, d), 8.30 (1H, d), 10.48 (1H, s). MS-ESI m/z 400 [MH⁺]. HRMS-ESI: m/z found 400.2144 [MH⁺], C₂₁H₂₇FN₅O₂ requires 400.2143.

(1*S*,3*R*)-3-Acetamido-*N*-(5-chloro-4-(4,5,6,7-tetrahydropyrazolo[1,5-*a*]pyridin-3-yl)pyridin-2-yl)cyclohexanecarboxamide (6). The reaction was split into four separate sealed microwave reaction vessels, each containing 5-chloro-2-fluoro-4-iodopyridine 55 (750 mg, 2.95 mmol), concentrated aqueous ammonium hydroxide (8.4 mL), and NMP (7.5 mL). The reaction vessels were each heated at 100 °C for 17 h. The combined batches were then diluted with water (50 mL) and extracted with EtOAc (3 × 120 mL). The combined organic layers were

dried over MgSO_4 , filtered, and concentrated under reduced pressure to afford a pale-yellow oil. The oil was loaded onto a 20 g SCX-2 column and eluted sequentially with DCM, MeOH, and 1% NH_3 in MeOH. Basic fractions were concentrated to provide 5-chloro-4-iodopyridin-2-amine **56** (2.9 g, 99%) as a colorless solid. $^1\text{H NMR}$ (400 MHz, $\text{DMSO}-d_6$): 6.21 (2H, s), 7.05 (1H, s), 7.93 (1H, s). MS-ESI m/z 255 [MH^+].

Cesium carbonate (13.4 g, 41.2 mmol) and $\text{PdCl}_2(\text{dppf})\cdot\text{CH}_2\text{Cl}_2$ (0.94 g, 1.2 mmol) were added sequentially to a degassed mixture of **56** (4.19 g, 16.5 mmol), **41** (5.72 g, 23.1 mmol), 1,4-dioxane (141 mL), and water (23.5 mL). The resulting red mixture was warmed to 95 °C and became clear. With vigorous stirring, some precipitate formed which gradually redissolved. After 4 h, another 800 mg of **41** were added; after another 40 min, the reaction was cooled to room temperature and stirred under these conditions for 18 h. The mixture was then diluted with ethyl acetate, and the layers were separated. The organic layer was washed with saturated aqueous sodium chloride, dried over sodium sulfate, filtered, and concentrated under reduced pressure. The resulting oil was purified by flash silica chromatography, elution gradient 0–10% methanol in ethyl acetate. Product fractions were combined, concentrated under reduced pressure, and the resulting residue was stirred vigorously in 1:1 DCM: hexane for 20 min. The mixture was then diluted with hexane and filtered with a hexane wash. The resulting solid was dried under vacuum to afford 5-chloro-4-(4,5,6,7-tetrahydropyrazolo[1,5-*a*]pyridin-3-yl)pyridin-2-amine **57** (2.79 g, 68%) as light orange-beige needles. $^1\text{H NMR}$ (300 MHz, $\text{DMSO}-d_6$): 1.74–1.88 (2H, m), 1.96–2.06 (2H, m), 2.76 (2H, t), 4.12 (2H, t), 6.03 (2H, br. s), 6.43 (1H, s), 7.63 (1H, s), 7.94 (1H, s). MS-ESI m/z 249 [MH^+].

1-Chloro-*N,N*,2-trimethylprop-1-en-1-amine (1.1 mL, 8.4 mmol) was added to a solution of **38** (2.01 g, 8.24 mmol) in DCM (50 mL) at 0 °C. The reaction was maintained under these conditions for 100 min. During this time, **58** (1.64 g, 6.59 mmol), pyridine (2.1 mL, 26 mmol), and DCM (20 mL) were combined in a separate flask. The resulting mixture was warmed gently (~40 °C) until all solids dissolved. The resulting solution was then cooled to 0 °C, whereupon a homogeneous light-yellow mixture formed. This mixture was added via cannula rapidly to the previously prepared solution of **38** and 1-chloro-*N,N*,2-trimethylprop-1-en-1-amine, resulting in a darker yellow solution. The reaction was allowed to warm to room temperature overnight and was then evaporated to dryness to afford *tert*-butyl ((1*R*,3*S*)-3-((5-chloro-4-(4,5,6,7-tetrahydropyrazolo[1,5-*a*]pyridin-3-yl)pyridin-2-yl)-carbamoyl)cyclohexyl)carbamate **58** as a gray mixture (3.12 g). This crude material was taken on to the next step without further purification. MS-ESI m/z 474 [MH^+].

Hydrochloric acid in dioxane (4 M; 10 mL, 40 mmol) was added to a mixture of crude **58** (3.12 g, 6.59 mmol) in DCM (5 mL) and methanol (5 mL) at 0 °C. The mixture became an amber solution. After 1 h, the amber solution was concentrated under reduced pressure, and the resulting residue was dried under a vacuum to afford (1*S*,3*R*)-3-amino-*N*-(5-chloro-4-(4,5,6,7-tetrahydropyrazolo[1,5-*a*]pyridin-3-yl)pyridin-2-yl)cyclohexanecarboxamide as a beige/gray foam solid. This material was carried on to the next step without further purification. MS-ESI m/z 374 [MH^+]. Acetyl chloride (1.0 mL, 14.5 mmol) was added dropwise to a mixture of (1*S*,3*R*)-3-amino-*N*-(5-chloro-4-(4,5,6,7-tetrahydropyrazolo[1,5-*a*]pyridin-3-yl)pyridin-2-yl)cyclohexanecarboxamide (2.46 g, 6.59 mmol) and pyridine (6.4 mL, 79 mmol) in DCM (58 mL) at 0 °C. After 45 min, the mixture was washed with saturated aqueous sodium hydrogen carbonate and saturated aqueous sodium chloride before being dried over sodium sulfate, filtered, and concentrated under reduced pressure. The resulting dark amber oil was purified by flash silica chromatography, elution gradient 0–10% methanol in DCM. Product fractions were concentrated under reduced pressure to afford **6** (2.6 g, 93% yield over three steps, 96% e.e.) as a light beige foam solid. This material was further purified by preparative SFC conditions (Chiralpak IA column, 5 μm , 30 mm diameter, 250 mm length, 40 °C column temperature, 100 bar outlet pressure, 120 mL/min flow rate), eluting with 40% methanol containing 0.1% dimethylethylamine in CO_2 , to afford faster eluting **6** and the slower eluting (1*R*,3*S*) enantiomer. Product fractions for **6** were concentrated under reduced pressure to afford an amber-pink solid (2.3

g). This solid was repurified by flash silica (plug) chromatography, elution gradient 0–10% MeOH in ethyl acetate, to afford a white foam solid. The solid was treated with 20 mL of acetonitrile, and the resulting mixture was warmed to reflux conditions before being allowed to cool to rt. Additional acetonitrile (~5 mL) was added, and the process was repeated until all solid dissolved. The resulting faint yellow solution was cooled to rt, and a precipitate formed. After 1 h the precipitate was filtered and washed with acetonitrile before being dried under vacuum at 65 °C for 1 h. The solid was cooled to rt to afford **6** (1.76 g, > 98% e.e.).

6: $^1\text{H NMR}$ (300 MHz, $\text{DMSO}-d_6$): 0.97–1.17 (1H, m), 1.20–1.38 (3H, m), 1.68–1.94 (9H, m), 1.96–2.07 (2H, m), 2.54–2.68 (1H, m), 2.80 (2H, t), 3.46–3.65 (1H, m), 4.14 (2H, t), 7.73 (1H, d), 7.76 (1H, s), 8.14 (1H, s), 8.38 (1H, s), 10.57 (1H, s). $^{13}\text{C NMR}$ (126 MHz, $\text{DMSO}-d_6$): 20.13, 22.89, 22.96, 23.22, 24.49, 28.69, 32.38, 35.64, 43.91, 47.39, 48.22, 113.46, 114.37, 123.66, 138.38, 138.62, 141.16, 148.10, 151.40, 168.56, 174.98. MS-ESI m/z 416 [MH^+]. HRMS-ESI: m/z found 416.1851 [MH^+], $\text{C}_{21}\text{H}_{27}\text{ClN}_5\text{O}_2$ requires 416.1848. Analytical SFC: flow: 1 mL/min, column: Chiralpak IA, 5 μm , 4.6 \times 150 mm, eluent: 40% methanol in CO_2 containing 0.1% dimethylethylamine), t_{R} : (6, 1.42 min), ((1*R*,3*S*), 2.42 min). $[\alpha]_{\text{D}}^{25}$ °C: + 70.2° in MeOH.

(1*S*,3*R*)-3-Acetamido-*N*-(4-bromo-5-chloropyridin-2-yl)-cyclohexanecarboxamide (**7**). *N*-Chloro-succinimide (3.70 g, 27.7 mmol) dissolved in DMF (20 mL) was added dropwise to 4-bromopyridin-2-amine **39** (4.40 g, 25.4 mmol) in DMF (50 mL) at –78 °C over a period of 30 min under nitrogen. The resulting suspension was then allowed to warm to room temperature. After stirring under these conditions for 24 h, the reaction mixture was diluted with Et_2O (50 mL) and washed sequentially with aqueous NaOH (1 M; 2 \times 50 mL), water (50 mL), and saturated aqueous sodium chloride (25 mL). The organic layer was dried over MgSO_4 , filtered, and concentrated under reduced pressure. The resulting residue was purified by flash silica chromatography, elution gradient 0–25% EtOAc in DCM. Product fractions were concentrated under reduced pressure to afford 4-bromo-5-chloropyridin-2-amine **59** (2.30 g, 43.7%) as a cream-colored solid. $^1\text{H NMR}$ (400 MHz, $\text{DMSO}-d_6$): 6.35 (2H, s), 6.82 (1H, s), 8.01 (1H, s). MS-ESI m/z 207, 209 [MH^+].

A solution of **38** (1.50 g, 6.15 mmol) dissolved in DCM (20 mL) at 0 °C was treated with 1-chloro-*N,N*,2-trimethylprop-1-en-1-amine (0.976 mL, 7.38 mmol). The mixture was stirred at room temperature for 1.5 h before **59** (1.02 g, 4.92 mmol) and pyridine (0.59 mL, 7.4 mmol) were added sequentially. The resulting solution was stirred at room temperature for 16 h. The reaction mixture was diluted with DCM (25 mL) and washed sequentially with water (2 \times 25 mL) and saturated aqueous sodium chloride (25 mL). The organic layer was dried over MgSO_4 , filtered, and concentrated under reduced pressure. The resulting crude product was purified by ion exchange chromatography, using an SCX-2 column. The desired product was eluted from the column using methanol to afford *tert*-butyl ((1*R*,3*S*)-3-((4-bromo-5-chloropyridin-2-yl)carbamoyl)cyclohexyl)carbamate **60** (2.34 g, quantitative) as a white solid. $^1\text{H NMR}$ (400 MHz, $\text{DMSO}-d_6$): 1.12 (1H, dd), 1.22–1.32 (3H, m), 1.38 (9H, s), 1.72 (3H, dd), 1.83–1.94 (2H, m), 2.11 (1H, dt), 8.48 (1H, s), 8.50 (1H, s), 10.77 (1H, s), one proton not observed. MS-ESI m/z 430, 432 [M^-].

Hydrochloric acid in dioxane (4 M; 5.9 mL, 24 mmol) was added to **60** (1.20 g, 2.77 mmol) in MeOH (7.0 mL) under air. The resulting solution was stirred at ambient temperature for 16 h. The reaction mixture was concentrated under reduced pressure to afford crude (1*S*,3*R*)-3-amino-*N*-(4-bromo-5-chloropyridin-2-yl)-cyclohexanecarboxamide dihydrochloride as a white solid. This solid was taken up in DCM (8.4 mL), and 4-dimethylaminopyridine (0.014 g, 0.11 mmol) and triethylamine (1.0 mL, 7.1 mmol) were added sequentially. Then acetic anhydride (0.26 mL, 2.7 mmol) was added dropwise. The resulting solution was stirred at room temperature for 18 h before being quenched with saturated aqueous NH_4Cl (50 mL) and extracted with DCM (2 \times 50 mL). The combined organic layers were dried over MgSO_4 , filtered, and concentrated under reduced pressure to afford (1*S*,3*R*)-3-acetamido-*N*-(4-bromo-5-chloropyridin-2-yl)-cyclohexanecarboxamide **61** (0.96 g, 95%) as a white solid. The

product was used in the next step without further purification. ^1H NMR (400 MHz, DMSO- d_6): 1.23–1.41 (4H, m), 1.67–1.85 (4H, m), 2.39 (3H, t), 2.75–2.92 (1H, m), 3.53 (1H, d), 7.59–7.83 (1H, m), 8.50 (2H, dd), 10.80 (1H, d). MS-ESI m/z 374, 376 [MH^+].

61 (0.10 g, 0.27 mmol) was added to a mixture of 1,5-dimethyl-4-(4,4,5,5-tetramethyl-1,3,2-dioxaborolan-2-yl)-1H-pyrazole (0.065 g, 0.29 mmol), chloro(2-dicyclohexylphosphino-2',4',6'-triisopropyl-1,1'-biphenyl)[2-(2'-amino-1,1'-biphenyl)]palladium(II) (0.021 g, 0.03 mmol), and potassium phosphate (0.170 g, 0.80 mmol) in 1,4-dioxane (2.3 mL) and water (0.23 mL). The reaction mixture was then degassed with a stream of nitrogen for 5 min. The resulting mixture was stirred at room temperature for 16 h and subsequently purified by ion exchange chromatography, using an SCX-2 column and eluting first with methanol and then with 1 M NH_3 in methanol. Product fractions were concentrated under reduced pressure to afford a yellow oil. This oil was further purified by preparative HPLC (Waters XBridge Prep C18 OBD column, 5 μ silica, 50 mm diameter, 100 mm length), using decreasingly polar mixtures of water (containing 1% NH_3) and MeCN as eluents. Fractions containing the desired compound were concentrated under reduced pressure to afford **7** (0.011 g, 11%) as a colorless solid. ^1H NMR (500 MHz, DMSO- d_6): 0.91–1.17 (1H, m), 1.19–1.4 (3H, m), 1.78 (6H, s), 1.89 (1H, d, $J = 12.2$ Hz), 2.28 (3H, s), 2.54–2.69 (1H, m), 3.45–3.65 (1H, m), 3.82 (3H, s), 7.60 (1H, s), 7.75 (1H, d, $J = 7.9$ Hz), 8.08 (1H, s), 8.41 (1H, s), 10.60 (1H, s). MS-ESI m/z 390 [MH^+]. HRMS-ESI: m/z found 390.1704 [MH^+], $\text{C}_{19}\text{H}_{25}\text{ClN}_5\text{O}_2$ requires 390.1691.

(1*S*,3*R*)-3-Acetamido-*N*-(5-chloro-4-(pyrazolo[1,5-*a*]pyridin-3-yl)pyridin-2-yl)cyclohexanecarboxamide (**8**). Pd(PPh_3) $_4$ (0.21 g, 0.18 mmol) was added to 3-(4,4,5,5-tetramethyl-1,3,2-dioxaborolan-2-yl)pyrazolo[1,5-*a*]pyridine (0.490 g, 2.01 mmol), 2,5-dichloro-4-iodopyridine (**52**, 0.500 g, 1.83 mmol), and Cs_2CO_3 (1.78 g, 5.48 mmol) in dioxane (2 mL) and water (0.2 mL) under nitrogen. The resulting mixture was stirred at 100 °C for 1 h. The reaction mixture was then concentrated under reduced pressure. The resulting mixture was diluted with EtOAc (100 mL) and washed sequentially with water (100 mL) and saturated aqueous sodium chloride (100 mL). The organic layer was dried over sodium sulfate, filtered, and concentrated under reduced pressure. The resulting residue was purified by flash silica chromatography, elution gradient 0–25% EtOAc in petroleum ether. Product fractions were concentrated under reduced pressure to afford 3-(2,5-dichloropyridin-4-yl)pyrazolo[1,5-*a*]pyridine (**53a**, 0.310 g, 64%) as a white solid. ^1H NMR (300 MHz, DMSO- d_6): 7.09 (1H, dt, $J = 1.3, 6.9$ Hz), 7.46 (1H, ddd, $J = 1.1, 6.8, 9.0$ Hz), 7.74 (1H, s), 7.80 (1H, td, $J = 1.2, 9.0$ Hz), 8.44 (1H, s), 8.60 (1H, s), 8.84 (1H, td, $J = 1.1, 7.0$ Hz). MS-ESI m/z 264 [MH^+].

Pd(PPh_3) $_4$ (0.02 g, 0.02 mmol) was added to a mixture of **53a** (0.054 g, 0.21 mmol), **47** (0.05 g, 0.21 mmol), 4,5-bis(diphenylphosphino)-9,9-dimethylxanthene (0.024 g, 0.04 mmol), and Cs_2CO_3 (0.202 g, 0.62 mmol) in dioxane (2 mL) under nitrogen. The resulting mixture was stirred at 120 °C for 2 h. In a separate flask, Pd(PPh_3) $_4$ (0.05 g, 0.04 mmol) was added to a mixture of **53a** (0.109 g, 0.41 mmol), **47** (0.10 g, 0.41 mmol), 4,5-bis(diphenylphosphino)-9,9-dimethylxanthene (0.048 g, 0.08 mmol), and Cs_2CO_3 (0.403 g, 1.24 mmol) in dioxane (2 mL) under nitrogen. The resulting mixture was stirred at 120 °C for 2 h. Both reactions were then combined and filtered through a plug of silica with ethyl acetate wash. The filtrate was concentrated under reduced pressure, and the resulting residue was redissolved in EtOAc (100 mL) before being washed sequentially with water (100 mL) and saturated aqueous sodium chloride (100 mL). The organic layer was dried over sodium sulfate, filtered, and concentrated under reduced pressure. The resulting residue was purified by preparative TLC (eluting with 50% EtOAc in petroleum ether), to afford *tert*-butyl ((1*R*,3*S*)-3-((5-chloro-4-(pyrazolo[1,5-*a*]pyridin-3-yl)pyridin-2-yl)carbamoyl)cyclohexyl)carbamate (**54a**, 0.13 g, 44%) as a white solid. ^1H NMR (400 MHz, DMSO- d_6): 1.06–1.13 (1H, m), 1.26–1.30 (3H, m), 1.39 (9H, s), 1.73–1.80 (3H, m), 1.86–1.94 (1H, m), 2.56–2.63 (1H, m), 3.17–3.32 (1H, m), 6.82 (1H, d, $J = 8.2$ Hz), 7.09 (1H, t, $J = 6.8$ Hz), 7.45–7.54 (1H, m), 7.80 (1H, d, $J = 9.0$ Hz), 8.37 (1H, s), 8.45 (1H, s), 8.48 (1H, s), 8.85 (1H, d, $J = 6.9$ Hz), 10.67 (1H, s). MS-ESI m/z 470 [MH^+].

TFA (2.0 mL, 26 mmol) was added to **54a** (0.12 g, 0.26 mmol) in DCM (10 mL). The resulting mixture was stirred at room temperature for 16 h and then concentrated under reduced pressure. The resulting crude yellow gum (100 mg) was dissolved in DCM (2 mL), and then TEA (0.11 mL, 0.81 mmol) and acetic anhydride (0.051 mL, 0.54 mmol) were added sequentially. The resulting mixture was stirred at room temperature for 1 h and was then concentrated under reduced pressure. The crude product was purified by preparative HPLC (Waters XBridge Prep C18 OBD column, 5 μ silica, 19 mm diameter, 150 mm length), using decreasingly polar mixtures of water (containing 0.1% NH_4HCO_3) and MeCN as eluents. Fractions containing the desired compound were concentrated under reduced pressure to afford impure **8** (0.050 g, 45%) as a white solid. This material was repurified by preparative HPLC (Waters XBridge Prep C18 OBD column, 5 μ silica, 19 mm diameter, 150 mm length), using decreasingly polar mixtures of water (containing 0.05% TFA) and MeCN as eluents. Product fractions were concentrated under reduced pressure to afford **8** (0.030 g, 27%) as a white solid. ^1H NMR (300 MHz, DMSO- d_6): 1.02–1.12 (1H, m), 1.19–1.40 (3H, m), 1.74–1.80 (6H, m), 1.85–1.95 (1H, m), 2.59–2.65 (1H, m), 3.52–3.58 (1H, m), 7.07 (1H, dt, $J = 1.3, 6.9$ Hz), 7.47 (1H, ddd, $J = 1.1, 6.8, 9.0$ Hz), 7.73–7.84 (2H, m), 8.35 (1H, s), 8.44 (1H, s), 8.47 (1H, s), 8.84 (1H, td, $J = 1.1, 7.0$ Hz), 10.68 (1H, s). HRMS-ESI: m/z found 412.1537 [MH^+], $\text{C}_{21}\text{H}_{23}\text{ClN}_5\text{O}_2$ requires 412.1535.

(1*S*,3*R*)-3-Acetamido-*N*-(5-chloro-4-(5,6,7,8-tetrahydroimidazo[1,2-*a*]pyridin-3-yl)pyridin-2-yl)cyclohexanecarboxamide (**9**). **61** (0.20 g, 0.53 mmol), 5,6,7,8-tetrahydroimidazo[1,2-*a*]pyridine (47 mg, 0.38 mmol), cesium carbonate (0.14 g, 0.42 mmol), triethylamine (0.11 mL, 0.76 mmol), triphenylphosphine (0.02 g, 0.06 mmol) and diacetoxypalladium (6.85 mg, 0.030 mmol) were suspended in 1,4-dioxane (5 mL) and sealed in a microwave tube. The reaction was heated to 100 °C for 16 h in a microwave reactor and then cooled to room temperature. The reaction was concentrated under reduced pressure, and the resulting residue was purified by ion exchange chromatography using an SCX-2 column. The desired product was eluted from the column using 1 M NH_3 in MeOH, and product fractions were concentrated under reduced pressure. The resulting residue was further purified by preparative HPLC (Waters XBridge Prep C18 OBD column, 5 μ silica, 50 mm diameter, 100 mm length), using decreasingly polar mixtures of water (containing 1% NH_3) and MeCN as eluents. Fractions containing the desired compound were concentrated under reduced pressure to afford **9** (0.069 g, 44%) as a yellow gum. ^1H NMR (500 MHz, DMSO- d_6): 0.95–1.16 (1H, m), 1.19–1.39 (3H, m), 1.78 (3H, s), 1.83–1.97 (2H, m), 2.55–2.68 (1H, m), 2.84 (2H, s), 3.18 (2H, dd), 3.31 (3H, s), 3.57 (1H, dt), 3.83 (2H, s), 4.08 (1H, q), 7.13 (1H, s), 7.75 (1H, d), 8.16 (1H, s), 8.47 (1H, s), 10.70 (1H, s). MS-ESI m/z 416 [MH^+]. HRMS-ESI: m/z found 416.1851 [MH^+], $\text{C}_{21}\text{H}_{27}\text{ClN}_5\text{O}_2$ requires 416.1848.

(1*S*,3*R*)-3-Acetamido-*N*-(5-chloro-4-(1,2-dimethyl-1H-imidazol-5-yl)pyridin-2-yl)cyclohexanecarboxamide (**10**). Pd(OAc) $_2$ (0.041 g, 0.18 mmol) was added to 1,2-dimethyl-1H-imidazole (0.175 g, 1.83 mmol), **52** (0.5 g, 1.83 mmol), Cs_2CO_3 (1.78 g, 5.48 mmol), and PPh $_3$ (0.048 g, 0.18 mmol) in dioxane (10 mL) under nitrogen. The resulting mixture was stirred at 120 °C for 16 h and then filtered with an ethyl acetate wash. The filtrate was concentrated under reduced pressure and redissolved in EtOAc (50 mL). This mixture was washed sequentially with water (2 \times 50 mL) and saturated aqueous sodium chloride (50 mL). The organic layer was dried over sodium sulfate, filtered, and concentrated under reduced pressure. The resulting residue was purified by flash silica chromatography, elution gradient 0–30% EtOAc in petroleum ether. Product fractions were concentrated under reduced pressure, and the resulting oil was crystallized from hexane to afford 2,5-dichloro-4-(1,2-dimethyl-1H-imidazol-5-yl)pyridine (**53b**, 0.170 g, 38.5%) as a yellow solid. ^1H NMR (400 MHz, DMSO- d_6): 3.17 (3H, s), 3.48 (3H, s), 7.16 (1H, s), 7.65 (1H, s), 8.64 (1H, s). MS-ESI m/z 242 [MH^+].

Pd(PPh_3) $_4$ (0.05 g, 0.04 mmol) and 4,5-bis(diphenylphosphino)-9,9-dimethylxanthene (0.05 g, 0.08 mmol) were added to a mixture of **53b** (0.20 g, 0.41 mmol), **47** (0.10 g, 0.41 mmol), and Cs_2CO_3 (0.403 g, 1.24 mmol) in dioxane (3 mL) under nitrogen. The resulting mixture

was stirred at 120 °C for 30 min. The reaction was then filtered with an ethyl acetate wash, and the filtrate was concentrated under reduced pressure. The resulting residue was purified by preparative TLC (100% EtOAc), to afford *tert*-butyl ((1*R*,3*S*)-3-((5-chloro-4-(1,2-dimethyl-1*H*-imidazol-5-yl)pyridin-2-yl)carbamoyl)cyclohexyl)carbamate (**54b**, 0.140 g, 76%) as a pale yellow solid. ¹H NMR (400 MHz, DMSO-*d*₆): 1.08–1.12 (1*H*, m), 1.22–1.35 (3*H*, m), 1.38 (9*H*, s), 1.73–1.77 (3*H*, m), 1.85–1.93 (1*H*, m), 2.38 (3*H*, s), 2.57–2.61 (1*H*, m), 3.23–3.31 (1*H*, m), 3.44 (3*H*, s), 6.77–6.83 (1*H*, m), 7.01 (1*H*, s), 8.12 (1*H*, s), 8.48 (1*H*, s), 10.72 (1*H*, s). MS-ESI *m/z* 448 [MH⁺].

TFA (1 mL, 13 mmol) was added to **54b** (0.14 g, 0.31 mmol) in DCM (5 mL). The resulting mixture was stirred at room temperature for 1 h and then concentrated under reduced pressure to afford a yellow gum (110 mg). This gum was taken up in DCM (5 mL), and TEA (0.13 mL, 0.95 mmol) was added. Then acetic anhydride (0.032 g, 0.32 mmol) was added dropwise. The resulting mixture was stirred at rt for 1 h and was then concentrated under reduced pressure. The resulting residue was purified by preparative HPLC (Waters XBridge Prep C18 OBD column, 5 μ silica, 19 mm diameter, 150 mm length), using decreasingly polar mixtures of water (containing 0.1% NH₄HCO₃) and MeCN as eluents. Product fractions were concentrated under reduced pressure to afford **10** (40 mg) as a white solid. This solid was repurified by chiral reverse phase HPLC (Chiralpak IA column, 5 μ silica, 20 mm diameter, 250 mm length; flow rate 20 mL/min), eluting with isocratic 30% IPA in hexanes, to afford **10** (0.030 g, 25%) as a white solid. ¹H NMR (400 MHz, DMSO-*d*₆): 1.01–1.14 (1*H*, m), 1.19–1.38 (3*H*, m), 1.69–1.84 (6*H*, m), 1.85–1.92 (1*H*, m), 2.38 (3*H*, s), 2.60–2.64 (1*H*, m), 3.44 (3*H*, s), 3.51–3.63 (1*H*, m), 7.01 (1*H*, s), 7.78 (1*H*, d, *J* = 7.9 Hz), 8.13 (1*H*, s), 8.48 (1*H*, s), 10.74 (1*H*, s). HRMS-ESI: *m/z* found 390.1701 [MH⁺], C₁₉H₂₅ClN₅O₂ requires 390.1691.

(1*S*,3*R*)-3-Acetamido-*N*-(5-chloro-4-(imidazo[1,2-*a*]pyridin-3-yl)pyridin-2-yl)cyclohexanecarboxamide (**11**). Imidazo[1,2-*a*]pyridine (0.045 mL, 0.45 mmol), **61** (0.235 g, 0.63 mmol), cesium carbonate (0.161 g, 0.49 mmol), triethylamine (0.125 mL, 0.90 mmol), triphenylphosphine (0.019 g, 0.07 mmol), and diacetoxypalladium (8.05 mg, 0.04 mmol) were suspended in 1,4-dioxane (5 mL) in a microwave tube. The reaction was heated at 100 °C for 2 h in a microwave reactor and then cooled to rt. The reaction was then resubjected to microwave conditions (100 °C) for another 4 h and cooled. The reaction mixture was diluted with DCM (20 mL) and washed with water (3 × 25 mL). The organic layer was dried over sodium sulfate, filtered, and concentrated under reduced pressure. The resulting residue was purified by flash silica chromatography, elution gradient 0–2% MeOH in EtOAc. Product fractions were concentrated under reduced pressure to afford (0.078 g, 42%) as a colorless solid. ¹H NMR (400 MHz, CDCl₃): 1.08–1.28 (1*H*, m), 1.32–1.58 (3*H*, m), 1.87–1.97 (3*H*, m), 1.98 (3*H*, s), 2.26 (1*H*, d, *J* = 12.3 Hz), 2.54 (1*H*, ddd, *J* = 3.4, 8.2, 11.6 Hz), 3.88 (1*H*, dtd, *J* = 4.1, 7.9, 11.7 Hz), 5.69 (1*H*, d, *J* = 8.1 Hz), 6.91 (1*H*, td, *J* = 1.1, 6.9 Hz), 7.29 (1*H*, ddd, *J* = 1.2, 6.8, 9.1 Hz), 7.72 (1*H*, dt, *J* = 1.0, 9.1 Hz), 7.95 (1*H*, s), 8.15 (1*H*, dt, *J* = 1.1, 6.9 Hz), 8.38 (1*H*, s), 8.43 (1*H*, s), 8.70 (1*H*, s). MS-ESI *m/z* 412 [MH⁺]. HRMS-ESI: *m/z* found 412.1545 [MH⁺], C₂₁H₂₃ClN₅O₂ requires 412.1535.

(1*S*,3*R*)-3-Acetamido-*N*-(5-chloro-4-(4,5,6,7-tetrahydro-[1,2,3]-triazolo[1,5-*a*]pyridin-3-yl)pyridin-2-yl)cyclohexanecarboxamide (**12**). 1-Chloro-*N,N*,2-trimethylpropenylamine (1.149 mL, 8.68 mmol) was added to a stirred solution of **38** (1.41 g, 5.79 mmol) in DCM (25 mL) cooled in an ice bath under a nitrogen atmosphere. The resulting mixture was stirred at ambient temperature for 1 h. **56** (1.47 g, 5.79 mmol) and pyridine (0.70 mL, 8.7 mmol) were added, and the resulting mixture was stirred at ambient temperature for 16 h. The reaction was quenched by the addition of saturated aqueous NH₄Cl (50 mL). The resulting mixture was extracted with DCM (3 × 75 mL), and the combined organic layers were dried over MgSO₄, filtered, and concentrated under reduced pressure. The resulting pale-yellow solid was slurried with Et₂O (10 mL) and filtered to yield *tert*-butyl ((1*R*,3*S*)-3-((5-chloro-4-iodopyridin-2-yl)carbamoyl)cyclohexyl)carbamate **62** (1.79 g, 3.73 mmol, 64%) as a cream-colored solid. ¹H NMR (400 MHz, CDCl₃): 1.04–1.18 (1*H*, m), 1.24–1.41 (2*H*, m), 1.44 (9*H*, s), 1.92 (2*H*, dq), 2.00 (1*H*, d), 2.28 (1*H*, d), 2.31–2.41 (1*H*, m), 3.27–

3.62 (2*H*, m), 4.44 (1*H*, s), 7.80 (1*H*, s), 8.19 (1*H*, s), 8.81 (1*H*, s). MS-ESI *m/z* 478 [M – H⁻].

62 (1 g, 2.08 mmol) was suspended in DCM (15 mL) at ambient temperature. Hydrochloric acid in dioxane (4*M*; 2.61 mL, 10.4 mmol) was added, and the resulting mixture stirred for 16 h. The reaction mixture was then loaded onto a 50 g SCX-2 column and eluted sequentially with DCM, MeOH, and 1% NH₃ in MeOH. Basic fractions were concentrated under reduced pressure to afford crude 3-amino-*N*-(5-chloro-4-iodopyridin-2-yl)cyclohexanecarboxamide as a colorless amorphous solid (782 mg). This solid was dissolved in triethylamine (0.632 mL, 4.53 mmol) in DCM (10 mL) at ambient temperature. Then acetic anhydride (0.214 mL, 2.27 mmol) was added dropwise. The reaction mixture was stirred for 5 days under these conditions before being filtered with a DCM wash to provide (1*S*,3*R*)-3-acetamido-*N*-(5-chloro-4-iodopyridin-2-yl)cyclohexanecarboxamide **63** (480 mg, 55%) as a colorless solid. The filtrate was concentrated under reduced pressure, and the resulting residue was purified by flash silica chromatography, elution gradient 20 to 60% EtOAc in heptane. Product fractions were concentrated under reduced pressure to afford additional **63** (193 mg, 22%) as a colorless crystalline solid (combined yield: 77%). ¹H NMR (400 MHz, DMSO-*d*₆): 1.01–1.17 (1*H*, m), 1.18–1.39 (3*H*, m), 1.68–1.84 (2*H*, m), 1.78 (3*H*, s), 1.89 (1*H*, m), 2.51 (2*H*, m), 3.48–3.65 (1*H*, m), 7.74 (1*H*, d), 8.38 (1*H*, s), 8.71 (1*H*, s), 10.66 (1*H*, s). MS-ESI *m/z* 422 [MH⁺].

Crude 3-(4,4,5,5-tetramethyl-1,3,2-dioxaborolan-2-yl)-4,5,6,7-tetrahydro-[1,2,3]triazolo[1,5-*a*]pyridine (approximately 0.3 mL solution; see Supporting Information) was added to a mixture of **63** (10 mg, 0.02 mmol), Cs₂CO₃ (15 mg, 0.05 mmol), and chloro(2-dicyclohexylphosphino-2',4',6'-triisopropyl-1,1'-biphenyl)[2-(2'-amino-1,1'-biphenyl)]palladium(II) (1.9 mg, 2.4 μmol) in 1,4-dioxane (2 mL) and water (0.5 mL) under nitrogen. The resulting mixture was warmed to 60 °C and maintained under these conditions for 45 min. This reaction was then allowed to cool to room temperature. In a separate flask the remaining suspension mixture containing crude 3-(4,4,5,5-tetramethyl-1,3,2-dioxaborolan-2-yl)-4,5,6,7-tetrahydro-[1,2,3]triazolo[1,5-*a*]pyridine (approximately 2.0 mL) was added to a mixture of **63** (70 mg, 0.17 mmol), Cs₂CO₃ (325 mg, 1.00 mmol) and chloro(2-dicyclohexylphosphino-2',4',6'-triisopropyl-1,1'-biphenyl)[2-(2'-amino-1,1'-biphenyl)]palladium(II) (26 mg, 0.03 mmol) in 1,4-dioxane (16 mL) and water (4 mL) under nitrogen. The resulting mixture was stirred at 60 °C for 45 min. This reaction was then allowed to cool to room temperature. Both cooled reaction mixtures were combined and then diluted with saturated aqueous sodium chloride (100 mL). The resulting mixture was extracted with EtOAc (3 × 100 mL), and the combined organic layers were dried over Na₂SO₄, filtered, and concentrated under reduced pressure. The resulting residue was purified by flash silica chromatography, using an elution gradient of 0 to 100% EtOAc in petroleum ether followed by an elution gradient of 0 to 20% MeOH in EtOAc. Pure fractions were concentrated under reduced pressure. The resulting residue was further purified by preparative HPLC (XBridge Prep C18 OBD column, 5 μ silica, 19 mm diameter, 150 mm length), using decreasingly polar mixtures of water (containing 0.8% NH₄HCO₃) and MeCN as eluents. Fractions containing the desired compound were concentrated under reduced pressure to afford **12** (20 mg, 25%) as a white solid. ¹H NMR (DMSO-*d*₆, 400 MHz): 1.00–1.14 (1*H*, m), 1.19–1.37 (3*H*, m), 1.68–1.81 (6*H*, m), 1.81–1.92 (3*H*, m), 1.99–2.10 (2*H*, m), 2.56–2.70 (1*H*, m), 2.82 (2*H*, t), 3.51–3.63 (1*H*, m), 4.42 (2*H*, t), 7.80 (1*H*, d), 8.26 (1*H*, s), 8.48 (1*H*, s), 10.73 (1*H*, s). MS-ESI *m/z* 417 [MH⁺]. HRMS-ESI: *m/z* found 417.1795 [MH⁺], C₂₀H₂₆ClN₆O₂ requires 417.1800.

(1*S*,3*R*)-3-Acetamido-*N*-(5-chloro-4-(5,6-dihydro-4*H*-pyrrolo[1,2-*b*]pyrazol-3-yl)pyridin-2-yl)cyclohexanecarboxamide (**13**). A mixture of 3-(4,4,5,5-tetramethyl-1,3,2-dioxaborolan-2-yl)-5,6-dihydro-4*H*-pyrrolo[1,2-*b*]pyrazole (0.14 g, 0.58 mmol; see Supporting Information), **62** (0.18 g, 0.38 mmol), chloro(2-dicyclohexylphosphino-2',4',6'-triisopropyl-1,1'-biphenyl)[2-(2'-amino-1,1'-biphenyl)]palladium(II) (0.03 g, 0.04 mmol), potassium phosphate, dibasic (0.200 g, 1.15 mmol), 1,4-dioxane (4 mL), and water (0.8 mL) was stirred at 21 °C for 18 h. The mixture was then heated at 40 °C for 17 h, and then at 50 °C for another 2 h. The mixture was diluted with EtOAc

(30 mL) and then washed with water (10 mL). The organic layer was concentrated under reduced pressure, and the resulting crude product was purified by flash silica chromatography, elution gradient 0 to 70% EtOAc in heptane. Product fractions were concentrated under reduced pressure to afford *tert*-butyl ((1*R*,3*S*)-3-((5-chloro-4-(5,6-dihydro-4*H*-pyrrolo[1,2-*b*]pyrazol-3-yl)pyridin-2-yl)carbamoyl)cyclohexyl)carbamate **64a** (0.119 g, 67%) as a white solid. ¹H NMR (400 MHz, CDCl₃): 1.04–1.17 (1H, m), 1.34–1.41 (2H, m), 1.44 (9H, s), 1.89–2.03 (4H, m), 2.29 (1H, d), 2.33–2.44 (1H, m), 2.69 (2H, p), 3.14–3.21 (2H, m), 3.45–3.59 (1H, m), 4.17–4.24 (2H, m), 4.44 (1H, s), 7.93 (1H, s), 8.15 (1H, s), 8.23 (1H, s), 8.33 (1H, s). MS-ESI *m/z* 460 [MH⁺].

To a solution of **64a** (0.12 g, 0.26 mmol) dissolved in DCM (3 mL) was added hydrochloric acid in dioxane (4 M; 1.29 mL, 5.17 mmol). The mixture was stirred at rt for 30 min before being concentrated under reduced pressure. The resulting residue was dissolved in DCM (2 mL) and treated with triethylamine (0.079 mL, 0.57 mmol) followed by acetic anhydride (0.029 mL, 0.31 mmol). The reaction mixture was stirred at rt for 0.5 h and then washed with water. The organic layer was concentrated under reduced pressure and purified by flash silica chromatography, elution gradient 0–10% MeOH in DCM. Product fractions were concentrated under reduced pressure to afford **13** (0.075 g, 72%) as a white solid. ¹H NMR (400 MHz, CDCl₃): 1.09–1.22 (1H, m), 1.38–1.58 (2H, m), 1.88–2.03 (6H, m), 2.26 (1H, d), 2.43–2.56 (1H, m), 2.69 (2H, p), 3.14–3.21 (2H, m), 3.49 (1H, s), 3.87 (1H, dt), 4.21 (2H, t), 5.59 (1H, d), 8.14 (1H, s), 8.22 (1H, s), 8.33 (1H, s), 8.43 (1H, s). MS-ESI *m/z* 402 [MH⁺]. HRMS-ESI: *m/z* found 402.1681 [MH⁺], C₂₀H₂₅ClN₅O₂ requires 402.1691.

(1*S*,3*R*)-3-Acetamido-*N*-(5-chloro-4-(6,7-dihydro-5*H*-pyrrolo[1,2-*a*]imidazol-3-yl)pyridin-2-yl)cyclohexanecarboxamide (**14**). **63** (130 mg, 0.31 mmol), (6,7-dihydro-5*H*-pyrrolo[1,2-*a*]imidazol-3-yl)-boronic acid hydrochloride (145 mg, 0.77 mmol; see [Supporting Information](#)), barium hydroxide (211 mg, 1.23 mmol) and PdCl₂(dppf) (22 mg, 0.030 mmol) were suspended in dioxane (2 mL) and water (0.4 mL) and sealed into a microwave tube. The reaction was heated to 75 °C in a microwave reactor and maintained under these conditions for 2 h before being cooled to rt. The reaction mixture was filtered with a methanol wash, and the filtrate was then concentrated under reduced pressure. The resulting residue was purified by preparative HPLC (Waters XBridge Prep C18 OBD column, 5 μm silica, 19 mm diameter, 100 mm length), using decreasingly polar mixtures of water (containing 1% NH₃) and MeCN as eluents. Fractions containing the desired compound were evaporated to dryness to afford **14** (21 mg, 17%) as a solid. ¹H NMR (500 MHz, DMSO-*d*₆): 1.09 (1H, d), 1.30 (3H, q), 1.76–1.80 (5H, m), 1.91 (1H, d), 2.57–2.73 (4H, m), 2.85 (2H, t), 3.58 (1H, dd), 4.16 (2H, t), 7.55 (1H, s), 7.75 (1H, d), 8.35 (1H, s), 8.42 (1H, s), 10.67 (1H, s). MS-ESI *m/z* 402 [MH⁺]. HRMS-ESI: *m/z* found 402.1707 [MH⁺], C₂₀H₂₅ClN₅O₂ requires 402.1691.

(1*S*,3*R*)-3-Acetamido-*N*-(5-chloro-4-(5,6,7,8-tetrahydro-4*H*-pyrazolo[1,5-*a*]azepin-3-yl)pyridin-2-yl)cyclohexanecarboxamide (**15**). Chloro(2-dicyclohexylphosphino-2',4',6'-triisopropyl-1,1'-biphenyl)[2-(2'-amino-1,1'-biphenyl)]palladium(II) (0.16 g, 0.21 mmol) was added to a degassed mixture of 3-(4,4,5,5-tetramethyl-1,3,2-dioxaborolan-2-yl)-5,6,7,8-tetrahydro-4*H*-pyrazolo[1,5-*a*]azepine (0.656 g, 2.50 mmol; see [Supporting Information](#)), **62** (1.00 g, 2.08 mmol) and potassium phosphate, tribasic (1.09 g, 6.25 mmol) in 1,4-dioxane (20 mL) and water (2 mL). The mixture was again degassed and was stirred at 85 °C for 24 h under nitrogen. The reaction mixture was allowed to cool, and silica added. This new mixture was concentrated under reduced pressure, and the resulting residue was purified by flash silica chromatography, eluting with 50% ethyl acetate in heptane to give *tert*-butyl ((1*R*,3*S*)-3-((5-chloro-4-(5,6,7,8-tetrahydro-4*H*-pyrazolo[1,5-*a*]azepin-3-yl)pyridin-2-yl)carbamoyl)cyclohexyl)carbamate (**64b**, 0.70 g, 69%) as a solid. This material was carried on to the next step without further purification. MS-ESI *m/z* 488 [MH⁺].

TFA (2 mL) was added to a stirred solution of **64b** (700 mg, 1.43 mmol) in DCM (10 mL). The reaction was stirred at rt for 24 h, the volatiles removed under a vacuum, and the resulting residue was

purified by ion exchange chromatography using an SCX-2 column, eluting with 7 N ammonia in methanol. Product fractions were concentrated under reduced pressure to afford crude (1*S*,3*R*)-3-amino-*N*-(5-chloro-4-(5,6,7,8-tetrahydro-4*H*-pyrazolo[1,5-*a*]azepin-3-yl)pyridin-2-yl)cyclohexanecarboxamide (550 mg) as a solid. A portion of this solid (450 mg, 1.16 mmol) was dissolved in DCM (10 mL) and triethylamine (0.34 mL, 2.4 mmol). Acetic anhydride (0.13 mL, 1.4 mmol) was added. The reaction mixture was stirred at rt for 4 h. Silica was added, and the mixture was concentrated under reduced pressure. The resulting residue was purified by flash silica chromatography, eluting with 0.5% methanol in ethyl acetate, to give **15** (260 mg, 52%) as a white solid. ¹H NMR (400 MHz, DMSO-*d*₆): 1.05–1.12 (1H, m), 1.17–1.37 (3H, m), 1.57–1.66 (2H, m), 1.69–1.95 (11H, m), 2.56–2.65 (1H, m), 2.70–2.77 (2H, m), 3.50–3.61 (1H, m), 4.21–4.45 (2H, m), 7.48 (1H, s), 7.73 (1H, d), 8.05 (1H, s), 8.40 (1H, s), 10.58 (1H, s). MS-ESI *m/z* 430 [MH⁺]. HRMS-ESI: *m/z* found 430.2007 [MH⁺], C₂₂H₂₉ClN₅O₂ requires 430.2004.

(1*S*,3*R*)-3-Acetamido-*N*-(5-chloro-4-(6,7-dihydro-4*H*-pyrazolo[5,1-*c*][1,4]oxazin-3-yl)pyridin-2-yl)cyclohexanecarboxamide (**16**). A mixture of 3-(4,4,5,5-tetramethyl-1,3,2-dioxaborolan-2-yl)-6,7-dihydro-4*H*-pyrazolo[5,1-*c*][1,4]oxazine (0.094 g, 0.38 mmol; see [Supporting Information](#)), **62** (0.120 g, 0.25 mmol), chloro(2-dicyclohexylphosphino-2',4',6'-triisopropyl-1,1'-biphenyl)[2-(2'-amino-1,1'-biphenyl)]palladium(II) (0.020 g, 0.03 mmol) and potassium phosphate dibasic (0.131 g, 0.75 mmol) in 1,4-dioxane (4 mL), and water (0.8 mL) was stirred at 50 °C for 1 h. The mixture was then diluted with EtOAc (30 mL). The resulting mixture was washed with water (10 mL), and the organic layer was concentrated under reduced pressure. The resulting residue was purified by flash silica chromatography, elution gradient 0 to 70% EtOAc in heptane. Product fractions were concentrated under reduced pressure to afford *tert*-butyl ((1*R*,3*S*)-3-((5-chloro-4-(6,7-dihydro-4*H*-pyrazolo[5,1-*c*][1,4]oxazin-3-yl)pyridin-2-yl)carbamoyl)cyclohexyl)carbamate **64c** (0.081 g, 68%). ¹H NMR (400 MHz, DMSO-*d*₆): 1.22–1.35 (4H, m), 1.38 (9H, s), 1.75 (3H, s), 1.90 (1H, d), 2.54–2.63 (1H, m), 4.12–4.26 (4H, m), 4.90 (2H, s), 5.75 (1H, s), 6.76 (1H, d), 7.89 (1H, s), 8.01 (1H, s), 8.39 (1H, s), 10.58 (1H, s). MS-ESI *m/z* 476 [MH⁺].

To a mixture of **64c** (0.072 g, 0.15 mmol) suspended in DCM (3 mL) at room temperature was added HCl in dioxane (4 M; 0.756 mL, 3.03 mmol). The mixture became a solution which was stirred at room temperature for 30 min. The reaction was concentrated under reduced pressure to yield a solid. This solid was dissolved in DCM (2 mL), and the resulting solution was treated sequentially with triethylamine (0.047 mL, 0.33 mmol) and acetic anhydride (0.017 mL, 0.18 mmol) at room temperature. The reaction mixture was stirred at room temperature for 30 min and then concentrated under reduced pressure. The resulting residue was purified by flash silica chromatography, elution gradient 50 to 100% EtOAc in heptane, then 0 to 10% MeOH in DCM. Product fractions were concentrated under reduced pressure to afford **16** (0.056 g, 88%) as a white solid. ¹H NMR (400 MHz, DMSO-*d*₆): 1.08 (1H, d), 1.29 (4H, q), 1.78 (1H, s), 1.91 (3H, s), 2.61 (2H, s), 3.57 (1H, dt), 4.08–4.27 (4H, m), 4.89 (2H, s), 7.74 (1H, d), 7.88 (1H, s), 8.01 (1H, s), 8.39 (1H, s), 10.59 (1H, s), 11.90 (1H, s). MS-ESI *m/z* 418 [MH⁺]. HRMS-ESI: *m/z* found 418.1640 [MH⁺], C₂₀H₂₅ClN₅O₃ requires 418.1640.

(1*S*,3*R*)-3-Acetamido-*N*-(5-chloro-4-(5-methyl-4,5,6,7-tetrahydropyrazolo[1,5-*a*]pyrazin-3-yl)pyridin-2-yl)cyclohexanecarboxamide (**17**). A mixture of **62** (0.200 g, 0.42 mmol), 5-methyl-3-(4,4,5,5-tetramethyl-1,3,2-dioxaborolan-2-yl)-4,5,6,7-tetrahydropyrazolo[1,5-*a*]pyrazine (0.197 g, 0.750 mmol; see [Supporting Information](#)), chloro(2-dicyclohexylphosphino-2',4',6'-triisopropyl-1,1'-biphenyl)[2-(2'-amino-1,1'-biphenyl)]palladium(II) (0.033 g, 0.040 mmol), potassium phosphate dibasic (0.218 g, 1.25 mmol), 1,4-dioxane (4 mL), and water (0.8 mL) was stirred at 45 °C for 18 h. More chloro(2-dicyclohexylphosphino-2',4',6'-triisopropyl-1,1'-biphenyl)-[2-(2'-amino-1,1'-biphenyl)]palladium(II) (0.033 g, 0.04 mmol) was added, and the reaction temperature was raised to 60 °C for 1 h. The reaction mixture was then cooled and passed through an SCX-2 column. The desired product was eluted from the column using 1 M NH₃ in MeOH, and product fractions were concentrated under

reduced pressure. The resulting residue was purified by flash silica chromatography, elution gradient 0 to 100% EtOAc in heptane, then 0–10% MeOH in DCM. Product fractions were concentrated under reduced pressure to afford *tert*-butyl ((1*R*,3*S*)-3-((5-chloro-4-(5-methyl-4,5,6,7-tetrahydropyrazolo[1,5-*a*]pyridin-3-yl)pyridin-2-yl)-carbamoyl)cyclohexyl)carbamate **64d** (0.054 g, 27%). ¹H NMR (400 MHz, CDCl₃, 30 °C): 1.04–1.19 (1H, m), 1.44 (12H, s), 1.87–2.02 (3H, m), 2.29 (1H, d), 2.33–2.46 (1H, m), 2.53 (3H, s), 2.95–3.00 (2H, m), 3.50 (1H, s), 3.76 (2H, s), 4.28 (2H, t), 4.52 (1H, s), 7.85 (1H, s), 8.12 (2H, s), 8.26 (1H, s). MS-ESI *m/z* 489 [MH⁺].

To a solution of **64d** (0.042 g, 0.090 mmol) dissolved in DCM (2 mL) was added HCl in dioxane (4 M; 0.429 mL, 1.72 mmol). The mixture was stirred at room temperature for 2 h before being concentrated under reduced pressure to afford a solid (33 mg). This solid was dissolved in DCM (2 mL) and triethylamine (0.026 mL, 0.19 mmol). Then acetic anhydride (9.6 μL, 0.10 mmol) was added. The mixture was stirred at room temperature for 30 min and then concentrated under reduced pressure. The resulting residue was purified by flash silica chromatography, elution gradient 0 to 100% EtOAc in (10% MeOH in DCM). Product fractions were concentrated under reduced pressure to afford **17** (0.027 g, 74%, 94% purity by HPLC) as a colorless dry film. ¹H NMR (400 MHz, CDCl₃): 1.09–1.24 (1H, m), 1.41–1.56 (3H, m), 1.87–2.04 (6H, m), 2.25 (1H, d), 2.51 (4H, s), 2.9–2.98 (2H, m), 3.73 (2H, s), 3.87 (1H, dtd), 4.26 (2H, t), 5.60 (1H, d), 7.84 (1H, s), 8.11 (1H, s), 8.25 (1H, d), 8.30 (1H, s). MS-ESI *m/z* 431 [MH⁺]. HRMS-ESI: *m/z* found 431.1955 [MH⁺], C₂₁H₂₈ClN₆O₂ requires 431.1957.

(1*S*,3*R*)-3-Acetamido-*N*-(5-chloro-4-(4,5,6,7-tetrahydropyrazolo[1,5-*a*]pyrimidin-3-yl)pyridin-2-yl)cyclohexanecarboxamide (**18**). Crude 3-(4,4,5,5-tetramethyl-1,3,2-dioxaborolan-2-yl)-4,5,6,7-tetrahydropyrazolo[1,5-*a*]pyrimidine (see Supporting Information) was added to **62** (0.160 g, 0.33 mmol), chloro(2-dicyclohexylphosphino-2',4',6'-triisopropyl-1,1'-biphenyl)[2-(2'-amino-1,1'-biphenyl)]palladium(II) (0.026 g, 0.03 mmol) and potassium phosphate tribasic (0.175 g, 1.00 mmol) in 1,4-dioxane (4 mL) and water (0.8 mL) at 50 °C. The resulting mixture was stirred at 50 °C for 2 h and then at 80 °C for 16 h. The reaction mixture was concentrated under reduced pressure, and the resulting residue was redissolved in DCM (20 mL) and washed with water (20 mL). The organic layer was dried over MgSO₄, filtered, and concentrated under reduced pressure. The resulting residue was purified by flash silica chromatography, elution gradient 0 to 30% EtOAc in heptane. Product fractions were concentrated under reduced pressure to afford *tert*-butyl ((1*R*,3*S*)-3-((5-chloro-4-(4,5,6,7-tetrahydropyrazolo[1,5-*a*]pyrimidin-3-yl)pyridin-2-yl)carbamoyl)cyclohexyl)carbamate **64e** (0.082 g, 52%) as a yellow gum. ¹H NMR (400 MHz, CDCl₃): 1.44 (12H, s), 1.82–2.46 (8H, m), 3.27–3.36 (3H, m), 4.12 (3H, t), 5.33 (1H, d), 7.80 (1H, s), 8.13 (1H, s), 8.19 (1H, s), 8.20 (1H, s). MS-ESI *m/z* 475 [MH⁺].

64e (0.086 g, 0.18 mmol) and HCl in dioxane (4 M; 0.362 mL, 1.45 mmol) were dissolved in methanol (2 mL) at room temperature under air. The resulting solution was stirred at room temperature for 3 h before being concentrated under reduced pressure. The resulting material (66 mg) was dissolved in triethylamine (0.081 mL, 0.58 mmol) in DCM (1 mL) at room temperature under nitrogen. Then 4-dimethylaminopyridine (1.14 mg, 9.3 μmol) was added followed by dropwise addition of acetic anhydride (0.021 mL, 0.22 mmol). The resulting solution was stirred at room temperature for 2 h before being quenched with saturated aqueous NH₄Cl (10 mL). The resulting mixture was extracted with DCM (2 × 10 mL). The combined organic layers were dried over MgSO₄, filtered, and concentrated under reduced pressure. The resulting white solid was purified by flash silica chromatography, elution gradient 0 to 100% EtOAc in heptane. Fractions were concentrated under reduced pressure to afford semipure product, which was further purified by preparative HPLC (Waters XBridge Prep C18 OBD column, 5 μm silica, 30 mm diameter, 100 mm length) using decreasingly polar mixtures of water (containing 1% NH₃) and MeCN as eluents. Fractions containing the desired compound were concentrated under reduced pressure to afford **18** (9.8 mg, 13%, 94% purity by HPLC). ¹H NMR (400 MHz, CDCl₃): 1.13 (1H, dd), 1.31–1.52 (4H, m), 1.87–1.95 (2H, m), 1.96 (4H, s),

2.20 (3H, dd), 2.39–2.5 (1H, m), 3.39–3.45 (2H, m), 4.16 (2H, t), 4.81 (1H, s), 5.49 (1H, d), 7.79 (1H, s), 8.14 (1H, s), 8.19 (1H, s), 8.30 (1H, s). MS-ESI *m/z* 417 [MH⁺]. HRMS-ESI: *m/z* found 417.1796 [MH⁺], C₂₀H₂₆ClN₆O₂ requires 417.1800.

(1*S*,3*R*)-3-Acetamido-*N*-(5-chloro-4-(6,7-dihydro-5*H*-pyrazolo[5,1-*b*][1,3]oxazin-3-yl)pyridin-2-yl)cyclohexanecarboxamide (**19**). **61** (0.100 g, 0.27 mmol) was added in one portion to a degassed mixture of 3-(4,4,5,5-tetramethyl-1,3,2-dioxaborolan-2-yl)-6,7-dihydro-5*H*-pyrazolo[5,1-*b*][1,3]oxazine (0.067 g, 0.27 mmol; see Supporting Information), chloro(2-dicyclohexylphosphino-2',4',6'-triisopropyl-1,1'-biphenyl)[2-(2'-amino-1,1'-biphenyl)]palladium(II) (0.021 g, 0.03 mmol), potassium phosphate (0.170 g, 0.80 mmol), 1,4-dioxane (2.3 mL) and water (0.45 mL) at room temperature. The resulting mixture was stirred at room temperature for 16 h and then concentrated under reduced pressure before being purified by ion exchange chromatography using an SCX-2 cartridge. The desired product was eluted from the column using 1 M NH₃ in MeOH, and product fractions were concentrated under reduced pressure. The resulting residue was purified by preparative HPLC (Waters XBridge Prep C18 OBD column, 5 μm silica, 30 mm diameter, 100 mm length) using decreasingly polar mixtures of water (containing 1% NH₃) and MeCN as eluents. Fractions containing the desired compound were concentrated under reduced pressure to afford **19** (0.017 g, 16%) as a white gum. ¹H NMR (500 MHz, DMSO-*d*₆): 1.21–1.32 (1H, m), 1.4–1.53 (3H, m), 1.95 (1H, s), 1.96 (3H, s), 2.06 (1H, d), 2.39–2.48 (2H, m), 2.7–2.85 (3H, m), 3.74 (1H, dt), 4.34 (2H, t), 4.53–4.68 (2H, m), 7.93 (1H, d), 8.05 (1H, s), 8.48 (1H, d), 8.58 (1H, s), 10.62 (1H, s). MS-ESI *m/z* 418 [MH⁺]. HRMS-ESI: *m/z* found 418.1639 [MH⁺], C₂₀H₂₅ClN₅O₃ requires 418.1640.

(1*S*,3*R*)-3-Acetamido-*N*-(4-(5,5-dimethyl-4,5,6,7-tetrahydropyrazolo[1,5-*a*]pyridin-3-yl)pyridin-2-yl)cyclohexanecarboxamide (**20**). **40** (1.50 g, 3.77 mmol), potassium acetate (1.11 g, 11.3 mmol), 4,4,4',4',5,5,5',5'-octamethyl-2,2'-bi-(1,3,2-dioxaborolane) (1.44 g, 5.65 mmol), and PdCl₂(dppf) (0.276 g, 0.380 mmol) were charged to a flask. 1,4-Dioxane (30 mL) was added, and the mixture was heated at 90 °C under nitrogen for 3 h. The mixture was allowed to cool, and the solids were removed by filtration. Ethyl acetate (100 mL) and water (50 mL) were added, and the layers were separated. The aqueous layer was extracted with EtOAc (2 × 50 mL), and the combined organic layers were dried over Na₂SO₄ and concentrated under reduced pressure to afford *tert*-butyl ((1*R*,3*S*)-3-((4-(4,4,5,5-tetramethyl-1,3,2-dioxaborolan-2-yl)pyridin-2-yl)carbamoyl)cyclohexyl)carbamate **43** (2.76 g) as a dark brown oil. This oil was used directly in the next step without further purification. MS-ESI *m/z* 446 [MH⁺].

Dichloro[1,1'-bis(di-*t*-butylphosphino)ferrocene]palladium(II) (44 mg, 0.070 mmol) was added to a degassed solution of **43** (300 mg, 0.67 mmol), 3-iodo-5,5-dimethyl-4,5,6,7-tetrahydropyrazolo[1,5-*a*]pyridine (242 mg, 0.88 mmol; see Supporting Information) and potassium phosphate, tribasic (429 mg, 2.02 mmol) in 1,4-dioxane (10 mL), and water (1 mL). The resulting mixture was stirred at 90 °C for 18 h. The crude reaction was cooled and purified by ion exchange chromatography using an SCX-2 column. The desired product was eluted from the column using 1 M NH₃ in MeOH, and product fractions were concentrated under reduced pressure to afford a brown oil. This oil was purified by flash silica chromatography, elution gradient 0–100% EtOAc in heptane. Product fractions were concentrated under reduced pressure to afford *tert*-butyl ((1*R*,3*S*)-3-((4-(5,5-dimethyl-4,5,6,7-tetrahydropyrazolo[1,5-*a*]pyridin-3-yl)pyridin-2-yl)carbamoyl)cyclohexyl)carbamate (**44a**, 170 mg, 54%) as a solid. ¹H NMR (400 MHz, DMSO-*d*₆): 1.03 (6H, s), 1.04–1.15 (1H, m), 1.21–1.41 (12H, m), 1.72–1.81 (3H, m), 1.83–1.92 (3H, m), 2.53–2.62 (1H, m), 2.65–2.69 (2H, m), 3.30 (2H, m), 4.16 (2H, t), 6.76 (1H, br d), 7.76 (1H, d), 8.19 (1H, d), 8.29 (1H, d), 10.43 (1H, s). MS-ESI *m/z* 468 [MH⁺].

Trifluoroacetic acid (1 mL) was added to **44a** (170 mg, 0.36 mmol) in DCM (10 mL). The resulting mixture was stirred at rt for 6 h. The reaction was then concentrated under reduced pressure, and the resulting residue was subjected to ion exchange chromatography using an SCX-2 column. The desired product was eluted from the column

using 2 M NH₃ in MeOH. Product fractions were concentrated under reduced pressure, and the resulting residue was purified by flash silica chromatography, eluting with 7% (1% ammonia in methanol) in DCM to afford (1*S*,3*R*)-3-amino-*N*-(4-(5,5-dimethyl-4,5,6,7-tetrahydropyrazolo[1,5-*a*]pyridin-3-yl)pyridin-2-yl)cyclohexanecarboxamide (70 mg, 52%) as a solid. MS-ESI *m/z* 368 [MH⁺].

Acetic anhydride (0.022 mL, 0.23 mmol) was added to a stirred solution of (1*S*,3*R*)-3-amino-*N*-(4-(5,5-dimethyl-4,5,6,7-tetrahydropyrazolo[1,5-*a*]pyridin-3-yl)pyridin-2-yl)cyclohexanecarboxamide (70 mg, 0.19 mmol), triethylamine (0.056 mL, 0.40 mmol), and *N,N*-dimethylpyridin-4-amine (1.2 mg, 9.5 μmol) in DCM (10 mL). The reaction mixture was stirred at rt for 4 h, and the crude reaction was purified by ion exchange chromatography using an SCX-2 column. The desired product was eluted from the column using 1 M NH₃ in MeOH and product fractions were concentrated under reduced pressure. The resulting residue was further purified by preparative HPLC (Waters XBridge Prep C18 OBD column, 5 μ silica, 30 mm diameter, 100 mm length), using decreasingly polar mixtures of water (containing 1% NH₃) and MeCN as eluents. Fractions containing the desired compound were concentrated under reduced pressure to afford **20** (44 mg, 56%) as a solid. ¹H NMR (500 MHz, DMSO-*d*₆): 1.04 (6H, s), 1.06–1.15 (1H, m), 1.32–1.38 (3H, m), 1.66–1.82 (6H, m), 1.83–1.94 (3H, m), 2.58–2.64 (1H, m), 2.78 (2H, s), 3.54–3.62 (1H, m), 4.14 (2H, t), 7.16 (1H, dd), 7.76 (1H, d), 7.84 (1H, s), 8.18 (1H, s), 8.24 (1H, d), 10.34 (1H, s). MS-ESI *m/z* 410 [MH⁺]. HRMS-ESI: *m/z* found 410.2547 [MH⁺], C₂₃H₃₂N₅O₂ requires 410.2551.

(1*S*,3*R*)-3-Acetamido-*N*-(4-(5,5-dimethyl-4,5,6,7-tetrahydropyrazolo[1,5-*a*]pyridin-3-yl)-5-fluoropyridin-2-yl)cyclohexanecarboxamide (**21**). 45 (1.55 g, 6.03 mmol), 5,5-dimethyl-3-(4,4,5,5-tetramethyl-1,3,2-dioxaborolan-2-yl)-4,5,6,7-tetrahydropyrazolo[1,5-*a*]pyridine (**49**, 2.0 g, 7.2 mmol; see [Supporting Information](#)), chloro(2-dicyclohexylphosphino-2',4',6'-triisopropyl-1,1'-biphenyl)[2-(2'-amino-1,1'-biphenyl)]palladium(II) (0.48 g, 0.60 mmol) and potassium phosphate, dibasic (3.15 g, 18.1 mmol) were dissolved in degassed dioxane (20 mL) and water (1 mL) at 21 °C. The mixture was stirred at 90 °C for 24 h and then allowed to cool to room temperature. The mixture was diluted with EtOAc (30 mL), washed with water (10 mL), and the organic layer was concentrated under reduced pressure. The resulting residue was purified by flash silica chromatography, elution gradient 0–50% EtOAc in heptane. Product fractions were concentrated under reduced pressure to afford 3-(2-chloro-5-fluoropyridin-4-yl)-5,5-dimethyl-4,5,6,7-tetrahydropyrazolo[1,5-*a*]pyridine **50** (1.3 g, 77%) as a white solid. ¹H NMR (400 MHz, CDCl₃): 1.10 (6H, s), 1.89 (2H, m), 2.68 (2H, s), 4.26 (2H, t), 7.27 (1H, d), 7.80 (1H, d), 8.23 (1H, d). MS-ESI *m/z* 280 [MH⁺].

Tetrakis(triphenylphosphine)palladium(0) (0.496 g, 0.43 mmol) was added to **50** (1.2 g, 4.29 mmol), **47** (1.04 g, 4.29 mmol), 9,9-dimethyl-4,5-bis(diphenylphosphino)xanthene (0.496 g, 0.86 mmol), and cesium carbonate (4.19 g, 12.9 mmol) in 1,4-dioxane (10 mL). The resulting mixture was degassed for 5 min under nitrogen and then subjected to microwave conditions (120 °C; 17 h). The reaction mixture was diluted with water (20 mL) and ethyl acetate (100 mL) before being filtered. The layers were separated, and the organic layer was adsorbed onto silica and purified by flash silica chromatography, eluting with isocratic 50% EtOAc in heptane. Product fractions were concentrated under reduced pressure to afford *tert*-butyl ((1*R*,3*S*)-3-((4-(5,5-dimethyl-4,5,6,7-tetrahydropyrazolo[1,5-*a*]pyridin-3-yl)-5-fluoropyridin-2-yl)carbamoyl)cyclohexyl)carbamate **51** (1.1 g, 53%) as a white solid. ¹H NMR (400 MHz, DMSO-*d*₆): 1.03 (6H, s), 1.02–1.14 (1H, m), 1.20–1.35 (3H, m), 1.39 (9H, s), 1.70–1.79 (3H, br m), 1.82–1.92 (3H, m), 2.54–2.63 (1H, m), 2.68 (2H, s), 4.16 (2H, t), 6.76 (1H, br d), 7.76 (1H, d), 8.19 (1H, d), 8.29 (1H, d), 10.43 (1H, s). 1H multiplet under water peak. MS-ESI *m/z* 486 [MH⁺].

TFA (2 mL) was added to a solution of **51** (1.1 g, 2.27 mmol) in DCM (20 mL). The resulting mixture was stirred at ambient temperature for 24 h, and then the reaction was concentrated under reduced pressure. The resulting residue was purified by ion exchange chromatography using an SCX-2 column. The desired product was

eluted from the column with 7 N NH₃ in MeOH. Product fractions were concentrated under reduced pressure to afford (1*S*,3*R*)-3-amino-*N*-(4-(5,5-dimethyl-4,5,6,7-tetrahydropyrazolo[1,5-*a*]pyridin-3-yl)-5-fluoropyridin-2-yl)cyclohexanecarboxamide (0.87 g, 100%) as a solid. ¹H NMR (400 MHz, CDCl₃): 1.01–1.12 (7H, m), 1.31–1.49 (3H, m), 1.83–1.99 (5H, m), 2.14 (1H, d), 2.35 (1H, td), 2.66–2.85 (3H, m), 4.23 (2H, t), 7.85 (1H, d), 7.99–8.18 (2H, m), 8.29 (1H, d). NH₂ signal not observed. MS-ESI *m/z* 386 [MH⁺].

Acetic anhydride (0.088 mL, 0.93 mmol) was added to a stirred solution of (1*S*,3*R*)-3-amino-*N*-(4-(5,5-dimethyl-4,5,6,7-tetrahydropyrazolo[1,5-*a*]pyridin-3-yl)-5-fluoropyridin-2-yl)cyclohexanecarboxamide (300 mg, 0.78 mmol), triethylamine (0.23 mL, 1.6 mmol) and DCM (10 mL). The reaction mixture was stirred at ambient temperature for 4 h. Silica was added, and the volatiles were removed by concentration under reduced pressure. The resulting residue was purified by flash silica chromatography, eluting with 0.5% methanol in ethyl acetate, to afford **21**. ¹H NMR (400 MHz, DMSO-*d*₆): 1.03 (6H, s), 1.02–1.14 (1H, m), 1.24–1.38 (3H, m), 1.72–1.81 (6H, m), 1.86–1.91 (3H, m), 2.55–2.64 (1H, m), 2.69 (2H, s), 3.52–3.64 (1H, m), 4.16 (2H, t), 7.64–7.81 (2H, m), 8.19 (1H, d), 8.29 (1H, d), 10.45 (1H, s). MS-ESI *m/z* 428 [MH⁺]. ¹³C NMR (126 MHz, DMSO-*d*₆): 22.75, 24.03, 27.03, 27.06, 28.29, 28.49, 31.91, 34.37, 35.12, 36.14, 43.38, 44.81, 46.93, 109.90, 112.12, 129.97, 135.67, 137.69, 138.80, 148.78, 152.23, 168.07, 174.12. HRMS-ESI: *m/z* found 428.2459 [MH⁺], C₂₃H₃₁FN₅O₂ requires 428.2456.

(1*S*,3*R*)-3-Acetamido-*N*-(4-(5,5-dimethyl-5,6-dihydro-4*H*-pyrrolo[1,2-*b*]pyrazol-3-yl)pyridin-2-yl)cyclohexanecarboxamide (**22**). Dichloro[1,1'-bis(di-*t*-butylphosphino)ferrocene]palladium(II) (45.5 mg, 0.07 mmol) was added to a degassed solution of **43** (518 mg, 0.70 mmol), 3-bromo-5,5-dimethyl-5,6-dihydro-4*H*-pyrrolo[1,2-*b*]pyrazole (**68**, 150 mg, 0.70 mmol; see preparation as an intermediate in the synthesis of **23**), and potassium phosphate tribasic (444 mg, 2.09 mmol) in 1,4-dioxane (5 mL) and water (0.5 mL). The resulting mixture was stirred at 90 °C for 18 h and then purified by ion exchange chromatography using an SCX-2 column. The desired product was eluted from the column using 1 M NH₃ in MeOH, and pure fractions were concentrated under reduced pressure to afford crude product as a brown oil. This oil was purified by flash silica chromatography, elution gradient 0–100% EtOAc in heptane. Product fractions were concentrated under reduced pressure to afford *tert*-butyl ((1*R*,3*S*)-3-((4-(5,5-dimethyl-5,6-dihydro-4*H*-pyrrolo[1,2-*b*]pyrazol-3-yl)pyridin-2-yl)carbamoyl)cyclohexyl)carbamate **44b** (100 mg, 31%) as a white solid. MS-ESI *m/z* 454 [MH⁺].

44b (93 mg, 0.21 mmol) was dissolved in HCl in dioxane (4 M; 0.436 mL, 1.74 mmol) and MeOH (5 mL), and the reaction mixture was stirred at room temperature for 18 h. The reaction mixture was then purified by ion exchange chromatography using an SCX-2 column. The desired product was eluted from the column using 1 M NH₃ in MeOH, and product fractions were concentrated under reduced pressure. The resulting residue was further purified by flash silica chromatography, elution gradient 0–10% (7 N ammonia in methanol) in DCM. Product fractions were concentrated under reduced pressure to afford (1*S*,3*R*)-3-amino-*N*-(4-(5,5-dimethyl-5,6-dihydro-4*H*-pyrrolo[1,2-*b*]pyrazol-3-yl)pyridin-2-yl)cyclohexanecarboxamide (68 mg, 94%) as a white solid. MS-ESI *m/z* 354 [MH⁺]. To a stirred solution of (1*S*,3*R*)-3-amino-*N*-(4-(5,5-dimethyl-5,6-dihydro-4*H*-pyrrolo[1,2-*b*]pyrazol-3-yl)pyridin-2-yl)cyclohexanecarboxamide (65 mg, 0.18 mmol), triethylamine (0.054 mL, 0.39 mmol) and *N,N*-dimethylpyridin-4-amine (1.12 mg, 9.2 μmol) in DCM (5 mL) was added acetic anhydride (0.021 mL, 0.22 mmol). The reaction mixture was stirred at room temperature for 1 h and then purified by ion exchange chromatography using an SCX-2 column. The desired product was eluted from the column using 1 M NH₃ in MeOH, and product fractions were concentrated under reduced pressure to afford **22** (60.0 mg, 82.0%) as a colorless oil which was crystallized from an ether/heptane mix to afford a white solid. ¹H NMR (400 MHz, DMSO-*d*₆): 1.10 (1H, t), 1.29 (9H, s), 1.79 (6H, s), 1.85–1.94 (1H, m), 2.57–2.66 (1H, m), 2.93 (2H, s), 3.58 (1H, dt), 3.90 (2H, s), 7.21 (1H, dd), 7.74 (1H, d), 7.96 (1H, s), 8.18–8.24 (2H, m), 10.32 (1H, s). MS-ESI *m/z* 396 [MH⁺]. HRMS-ESI: *m/z* found 396.2393 [MH⁺], C₂₂H₃₀N₅O₂ requires 396.2394.

(1*S*,3*R*)-3-Acetamido-*N*-(4-(5,5-dimethyl-5,6-dihydro-4*H*-pyrrolo[1,2-*b*]pyrazol-3-yl)-5-fluoropyridin-2-yl)cyclohexanecarboxamide (**23**). 1*H*-Pyrazole (20 g, 293.78 mmol), ethyl 3-bromo-2,2-dimethylpropanoate (61.4 g, 293.78 mmol), and cesium carbonate (144 g, 440.68 mmol) in DMA (200 mL) were stirred at 80 °C for 16 h. The mixture was then poured into water (400 mL) and extracted with ethyl acetate (150 mL). The organic layer was concentrated under reduced pressure to give a colorless oil. This oil was purified by flash silica chromatography, elution gradient 10 to 40% ethyl acetate in heptane). Product fractions were concentrated under reduced pressure to afford ethyl 2,2-dimethyl-3-(1*H*-pyrazol-1-yl)propanoate (46.0 g, 80.0%), as a colorless oil. ¹H NMR (400 MHz, CDCl₃): 0.97 (6H, s), 1.02 (3H, t), 3.93 (2H, q), 4.10 (2H, s), 6.00 (1H, t), 7.16 (1H, d), 7.26 (1H, d). MS-ESI *m/z* 197 [MH⁺].

Aqueous sodium hydroxide (5 M; 94 mL, 46 mmol) was added portion-wise to a stirred solution of ethyl 2,2-dimethyl-3-(1*H*-pyrazol-1-yl)propanoate (46 g, 234 mmol) dissolved in methanol (250 mL) at room temperature. The mixture was allowed to exotherm to 37 °C during addition. The resulting solution was stirred under these conditions for 30 min and then cooled to room temperature before being concentrated under reduced pressure to 1/3 volume. This new solution was acidified to ~pH 3 with concentrated aqueous HCl. A colorless oil separated from the mixture. The flask was swirled in an ice bath, and a colorless solid crystallized. The mixture was allowed to stand overnight at room temperature. The solid was isolated by filtration and dried under reduced pressure to afford 2,2-dimethyl-3-(1*H*-pyrazol-1-yl)propanoic acid **65** (30.0 g, 76%) as a colorless crystalline solid. ¹H NMR (400 MHz, DMSO-*d*₆): 1.05 (6H, s), 4.23 (2H, s), 6.21 (1H, t), 7.35–7.44 (1H, m), 7.54–7.67 (1H, m), 12.41 (1H, br s). MS-ESI *m/z* 169 [MH⁺].

n-BuLi in hexane (9.03 mL, 24.4 mmol) was added dropwise to **65** (2.0 g, 12 mmol) in 2-methyl tetrahydrofuran (40 mL) at –78 °C over a period of 20 min under nitrogen. The resulting suspension was stirred at –78 °C for 15 min, and then the reaction was stirred at approximately –45 °C for 1 h. The mixture was allowed to warm to 15 °C before the reaction was quenched slowly onto ice-cold saturated ammonium chloride (100 mL). The reaction mixture was diluted with EtOAc (100 mL), and the ammonium chloride layer was separated and extracted with EtOAc (50 mL). The combined organic layers were washed with saturated aqueous sodium chloride (50 mL), dried over MgSO₄, filtered, and concentrated under reduced pressure to afford 5,5-dimethyl-5,6-dihydro-4*H*-pyrrolo[1,2-*b*]pyrazol-4-one **66** (0.97 g, 54%) as a pale-yellow oil which crystallized on standing. ¹H NMR (400 MHz, DMSO-*d*₆): 1.29 (6H, s), 4.36 (2H, s), 6.77 (1H, d), 7.89 (1H, d). MS-ESI *m/z* 151 [MH⁺].

Hydrazine hydrate (4.13 mL, 85.2 mmol) was added to a stirred solution of **66** (2.56 g, 17.1 mmol) dissolved in 2,2'-oxydiethanol (48.5 mL, 511 mmol). The resulting solution was stirred at 180 °C for 1 h. Potassium hydroxide (3.35 mL, 59.7 mmol) was carefully added to the mixture, and the resulting suspension was stirred at 150 °C for 2 h. After being cooled to room temperature, the reaction mixture was diluted with water (50 mL), and the pH was adjusted to 4.5 with aqueous HCl (2 N). Following extraction with Et₂O (5 × 50 mL), the combined organic layers were washed with water (2 × 20 mL) and then saturated aqueous sodium chloride (20 mL). The organic layers were dried over MgSO₄, filtered, and concentrated under reduced pressure to give 5,5-dimethyl-5,6-dihydro-4*H*-pyrrolo[1,2-*b*]pyrazole **67** (0.922 g, 40%) as a clear yellow oil. ¹H NMR (400 MHz, CDCl₃): 1.21 (6H, s), 2.61 (2H, s), 3.80 (2H, s), 5.82–5.93 (1H, m), 7.41 (1H, d).

N-Bromosuccinimide (1.17 g, 6.55 mmol) was added to a stirred solution of **67** (892 mg, 6.55 mmol) dissolved in DCM (10 mL) at 23 °C. The resulting mixture was stirred at 23 °C for 16 h before being diluted with DCM (20 mL) and washed sequentially with water (2 × 20 mL) and saturated aqueous sodium chloride (20 mL). The organic layer was dried over MgSO₄, filtered, and concentrated under reduced pressure to afford 3-bromo-5,5-dimethyl-5,6-dihydro-4*H*-pyrrolo[1,2-*b*]pyrazole **68** (1.39 g, 99%) as a yellow oil. ¹H NMR (400 MHz, CDCl₃): 1.23 (6H, s), 2.58 (2H, s), 3.83 (2H, s), and 7.35 (1H, s).

Pd(P(Cy)₃)₂Cl₂ (0.25 g, 0.33 mmol) was added to 4,4',4',5',5',5'-octamethyl-2,2'-bi(1,3,2-dioxaborolane) (1.70 g, 6.69 mmol), **68**

(0.720 g, 3.35 mmol), and potassium acetate (1.15 g, 11.7 mmol) in DMA (7 mL). The resulting suspension was degassed and stirred at 85 °C for 5 h. Dichloro[1,1'-bis(diphenylphosphino)ferrocene]palladium DCM adduct (0.273 g, 0.33 mmol) was then added to the reaction mixture, and stirring was continued under these conditions for 18 h before the reaction mixture was cooled to rt. The reaction mixture was diluted with EtOAc (20 mL) and washed sequentially with water (2 × 15 mL), and saturated aqueous sodium chloride (15 mL). The organic layer was dried over MgSO₄, filtered, and concentrated under reduced pressure. The resulting crude product was purified by flash silica chromatography, elution gradient 0–50% EtOAc in heptane. Product fractions were concentrated under reduced pressure to afford 5,5-dimethyl-3-(4,4,5,5-tetramethyl-1,3,2-dioxaborolan-2-yl)-5,6-dihydro-4*H*-pyrrolo[1,2-*b*]pyrazole **69** (0.458 g, 52%) as a cream-colored solid. ¹H NMR (400 MHz, CDCl₃): 1.24 (6H, s), 1.27 (12H, s), 2.79 (2H, s), 3.87 (2H, s), and 7.76 (1H, s).

45 (1.00 g, 3.88 mmol), **69** (1.53 g, 5.83 mmol), chloro(2-dicyclohexylphosphino-2',4',6'-triisopropyl-1,1'-biphenyl)[2-(2'-amino-1,1'-biphenyl)]palladium(II) (0.31 g, 0.39 mmol), and dibasic potassium phosphate (2.03 g, 11.65 mmol) were dissolved in degassed dioxane (10 mL) and water (2 mL) at 21 °C. The reaction mixture was stirred at 80 °C for 3 h, and then the mixture was cooled, diluted with EtOAc (30 mL), and washed with water (10 mL). The organic layer was concentrated under reduced pressure. The resulting residue was purified by flash silica chromatography, elution gradient 0–50% EtOAc in heptane. Product fractions were concentrated under reduced pressure to afford 3-(2-chloro-5-fluoropyridin-4-yl)-5,5-dimethyl-5,6-dihydro-4*H*-pyrrolo[1,2-*b*]pyrazole **70** (1.00 g, 97%) as a white solid. ¹H NMR (500 MHz, CDCl₃): 1.36 (6H, s), 2.95 (2H, d), 3.97 (2H, s), 7.31 (1H, d), 7.94 (1H, d), 8.20 (1H, d). MS-ESI *m/z* 266 [MH⁺].

Tetrakis(triphenylphosphine)palladium(0) (0.13 g, 0.12 mmol) and 4,5-bis(diphenylphosphino)-9,9-dimethylxanthene (0.13 g, 0.23 mmol) were added together in one portion to a degassed mixture of **47** (0.670 g, 2.76 mmol), **70** (0.61 g, 2.3 mmol), cesium carbonate (1.88 g, 5.76 mmol), and 1,4-dioxane (26 mL). The mixture was rapidly heated to reflux. After 20 h, the reaction was cooled, diluted with 50% saturated aqueous sodium chloride, and extracted with ethyl acetate (2×). The combined organic layers were dried over sodium sulfate, filtered, and concentrated under reduced pressure to afford crude *tert*-butyl ((1*R*,3*S*)-3-((4-(5,5-dimethyl-5,6-dihydro-4*H*-pyrrolo[1,2-*b*]pyrazol-3-yl)-5-fluoropyridin-2-yl)carbamoyl)cyclohexyl)carbamate **71** as a light-yellow solid. Hydrochloric acid in dioxane (4 M; 10 mL, 40 mmol) and DCM (5 mL) was added, resulting in a clear orange solution that rapidly became cloudy and yellow. Methanol (~3 mL) was titrated into the reaction until the mixture became mostly clear. After 15 min, the orange mixture was concentrated under reduced pressure to afford an orange solid. Pyridine (3.7 mL, 46 mmol) was added to this solid along with DCM (19 mL). A slight exotherm was noted, and the reaction was immersed in a water bath. Then acetic anhydride (0.43 mL, 4.6 mmol) was added dropwise. After another 10 min, another 200 μL of acetic anhydride was added. After another 30 min, another 600 μL of anhydride and 6 mL of pyridine were added. The reaction was maintained under these conditions for another 45 min and was then poured into saturated aqueous sodium bicarbonate and ethyl acetate. The layers were separated, and the aqueous layer was extracted with ethyl acetate. The combined organic layers were dried over sodium sulfate, filtered, and concentrated under reduced pressure. The resulting orange residue was purified by flash silica chromatography, elution gradient 50 to 100% EtOAc in hexane followed by 0–20% methanol in ethyl acetate, and product fractions were concentrated under reduced pressure to afford **23** (0.89 g, 94%) as a faint yellow foam solid. ¹H NMR (DMSO-*d*₆): 1.00–1.16 (1H, m), 1.22–1.40 (9H, m), 1.74–1.81 (6H, m), 1.83–1.94 (1H, m), 2.55–2.68 (1H, m), 2.93 (2H, s), 3.49–3.65 (1H, m), 3.94 (s, 2H), 7.75 (1H, d), 7.88 (1H, d), 8.28 (1H, d), 8.30 (1H, d), 10.46 (1H, s). ¹³C NMR (126 MHz, DMSO-*d*₆): 22.75, 24.03, 27.55, 28.25, 31.90, 35.21, 42.99, 43.38, 46.94, 60.23, 107.64, 109.96, 129.59, 135.86, 141.88, 144.44, 148.96, 151.91, 168.07, 174.18. HRMS-ESI: *m/z* found 414.2302 [MH⁺], C₂₂H₂₉FN₅O₂ requires 414.2300.

(1*S*,3*R*)-3-Acetamido-*N*-(5-chloro-4-(5,5-dimethyl-5,6-dihydro-4*H*-pyrrolo[1,2-*b*]pyrazol-3-yl)pyridin-2-yl)cyclohexanecarboxamide (**24**). A mixture of **69** (433 mg, 0.83 mmol), **62** (360 mg, 0.75 mmol), chloro(2-dicyclohexylphosphino-2',4',6'-triisopropyl-1,1'-biphenyl)[2-(2'-amino-1,1'-biphenyl)]palladium(II) (59 mg, 0.08 mmol), and potassium phosphate dibasic (392 mg, 2.25 mmol) in 1,4-dioxane (4 mL) and water (0.8 mL) was stirred at 50 °C for 5 h. The reaction mixture was cooled to room temperature and then purified by ion exchange chromatography using an SCX-2 column. The desired product was eluted from the column using 1 M NH₃ in MeOH, and product fractions were concentrated under reduced pressure. The resulting residue was purified by flash silica chromatography, elution gradient 0 to 100% EtOAc in heptane. Product fractions were concentrated under reduced pressure to afford *tert*-butyl ((1*R*,3*S*)-3-(5-chloro-4-(5,5-dimethyl-5,6-dihydro-4*H*-pyrrolo[1,2-*b*]pyrazol-3-yl)pyridin-2-yl)carbamoyl)cyclohexyl)carbamate **72** (188 mg, 51%) as a white solid. ¹H NMR (400 MHz, DMSO-*d*₆): 1.25 (12H, d), 1.37 (7H, s), 1.74 (3H, s), 1.87 (1H, d), 2.52–2.62 (1H, m), 2.88 (2H, s), 3.18–3.29 (1H, m), 3.93 (2H, s), 6.80 (1H, d), 7.99 (1H, s), 8.24 (1H, s), 8.32–8.35 (1H, m), 10.56 (1H, s). MS-ESI *m/z* 488 [MH⁺].

72 (186 mg, 0.380 mmol) was dissolved in HCl in dioxane (4 M; 0.81 mL, 3.2 mmol) and MeOH (5 mL), and the resulting solution was stirred at room temperature for 18 h. The reaction mixture was then purified by ion exchange chromatography using an SCX-2 column. The desired product was eluted from the column using 1 M NH₃ in MeOH, and product fractions were concentrated under reduced pressure to afford (1*S*,3*R*)-3-amino-*N*-(5-chloro-4-(5,5-dimethyl-5,6-dihydro-4*H*-pyrrolo[1,2-*b*]pyrazol-3-yl)pyridin-2-yl)cyclohexanecarboxamide (**114** mg, 77%) as a white solid. This material was used directly in the next step. MS-ESI *m/z* 388 [MH⁺]. This solid was dissolved in DCM (10 mL) and triethylamine (0.084 mL, 0.60 mmol) and *N,N*-dimethylpyridin-4-amine (1.7 mg, 0.010 mmol) were added. Then acetic anhydride (0.032 mL, 0.34 mmol) was added dropwise. The reaction mixture was stirred at room temperature for 4 h and then purified by ion exchange chromatography using an SCX-2 column. The desired product was eluted using 1 M NH₃ in MeOH, and product fractions were concentrated under reduced pressure. The resulting residue was purified by flash silica chromatography, elution gradient 0 to 100% EtOAc in heptane. Product fractions were concentrated under reduced pressure to afford **24** (86 mg, 70%) as a white solid. ¹H NMR (400 MHz, DMSO-*d*₆): 1.09 (1H, d), 1.28 (9H, s), 1.78 (6H, s), 1.90 (1H, d), 2.62 (1H, s), 2.89 (2H, s), 3.57 (1H, dt), 3.95 (2H, s), 7.73 (1H, d), 7.99 (1H, s), 8.25 (1H, s), 8.33–8.36 (1H, m), 10.53 (1H, s). ¹³C NMR (126 MHz, DMSO-*d*₆): 23.23, 24.50, 27.95, 28.72, 32.37, 35.60, 43.63, 43.94, 47.40, 60.74, 111.50, 112.56, 122.30, 140.86, 142.35, 145.18, 148.50, 151.56, 168.56, 174.99. MS-ESI *m/z* 430 [MH⁺]. HRMS-ESI: *m/z* found 430.2003 [MH⁺], C₂₂H₂₉ClN₅O₂ requires 430.2004.

Isomer 1 and Isomer 2 of (1S,3R)-3-acetamido-N-(5-chloro-4-(5-methyl-5,6-dihydro-4H-pyrrolo[1,2-b]pyrazol-3-yl)pyridin-2-yl)cyclohexanecarboxamide (27 and 28). Chloro(2-dicyclohexylphosphino-2',4',6'-triisopropyl-1,1'-biphenyl)[2-(2'-amino-1,1'-biphenyl)]palladium(II) (0.25 g, 0.31 mmol) was added to a degassed mixture of 5-methyl-3-(4,4,5,5-tetramethyl-1,3,2-dioxaborolan-2-yl)-5,6-dihydro-4*H*-pyrrolo[1,2-*b*]pyrazole (1.03 g, 3.75 mmol; see [Supporting Information](#)), **62** (1.50 g, 3.13 mmol), and dibasic potassium phosphate (1.63 g, 9.38 mmol) in 1,4-dioxane (15 mL) and water (3 mL). The resulting mixture was degassed and then stirred at 90 °C for 18 h under nitrogen. The reaction mixture was allowed to cool to rt, diluted with EtOAc (100 mL) and washed sequentially with water (100 mL) and saturated aqueous sodium chloride (50 mL). The organic extract was dried over MgSO₄, filtered, and concentrated under reduced pressure. The resulting residue was purified by flash silica chromatography, elution gradient 0–70% EtOAc in heptane. Product fractions were concentrated under reduced pressure to afford *tert*-butyl ((1*R*,3*S*)-3-(5-chloro-4-(5-methyl-5,6-dihydro-4*H*-pyrrolo[1,2-*b*]pyrazol-3-yl)pyridin-2-yl)carbamoyl)cyclohexyl)carbamate (**64f**, 1.0 g, 69%) as a yellow foam. ¹H NMR (400 MHz, DMSO): 1.08 (2H, s), 1.22–1.3 (6H, m), 1.38 (9H, s), 1.76 (3H, s), 1.90 (1H, d), 2.53–2.75 (2H, m), 3.2–3.3 (2H, m), 3.76 (1H, dd), 4.32 (1H, dd), 6.76 (1H, d),

8.00 (1H, s), 8.27 (1H, s), 8.31–8.38 (1H, m), 10.52 (1H, s). MS-ESI *m/z* 475 [MH⁺].

64f (1.11 g, 2.34 mmol) was dissolved in DCM (20 mL). Trifluoroacetic acid (1.8 mL, 23 mmol) was added, and the reaction mixture was stirred at rt for 18 h. The reaction was purified by ion exchange chromatography using an SCX-2 column. The desired product was eluted from the column using 1 M NH₃ in MeOH, and product fractions were concentrated under reduced pressure to afford (1*S*,3*R*)-3-amino-*N*-(5-chloro-4-(5-methyl-5,6-dihydro-4*H*-pyrrolo[1,2-*b*]pyrazol-3-yl)pyridin-2-yl)cyclohexanecarboxamide (0.68 g, 77%) as a white solid. MS-ESI *m/z* 374 [MH⁺].

Acetic anhydride (0.20 mL, 2.2 mmol) was added to a stirred solution of (1*S*,3*R*)-3-amino-*N*-(5-chloro-4-(5-methyl-5,6-dihydro-4*H*-pyrrolo[1,2-*b*]pyrazol-3-yl)pyridin-2-yl)cyclohexanecarboxamide (670 mg, 1.79 mmol), triethylamine (0.52 mL, 3.8 mmol) and *N,N*-dimethylpyridin-4-amine (11 mg, 0.09 mmol) in DCM (10 mL). The reaction mixture was stirred at rt for 18 h. The mixture was purified by ion exchange chromatography using an SCX-2 column, and the desired product was eluted from the column using 1 M NH₃ in MeOH. Product fractions were concentrated under reduced pressure. The resulting residue was purified by flash silica chromatography, using an elution gradient of 0 to 100% EtOAc in heptane followed by isocratic 10% MeOH in EtOAc. Product fractions were concentrated under reduced pressure to afford (1*S*,3*R*)-3-acetamido-*N*-(5-chloro-4-(5-methyl-5,6-dihydro-4*H*-pyrrolo[1,2-*b*]pyrazol-3-yl)pyridin-2-yl)cyclohexanecarboxamide (693 mg, 93%) as a white solid. ¹H NMR (400 MHz, DMSO-*d*₆): 1.05–1.11 (1H, m), 1.23 (3H, d), 1.27–1.38 (3H, m), 1.72–1.81 (6H, m), 1.89 (1H, br d), 2.52–2.63 (1H, m), 2.67 (1H, dd), 3.13–3.19 (1H, m), 3.20–3.28 (1H, m), 3.50–3.63 (1H, m), 3.76 (1H, dd), 4.27–4.37 (1H, m), 7.75 (1H, d), 8.00 (1H, s), 8.27 (1H, s), 8.35 (1H, s), 10.55 (1H, s). MS-ESI *m/z* 416 [MH⁺].

(1*S*,3*R*)-3-Acetamido-*N*-(5-chloro-4-(5-methyl-5,6-dihydro-4*H*-pyrrolo[1,2-*b*]pyrazol-3-yl)pyridin-2-yl)cyclohexanecarboxamide (670 mg, 1.79 mmol) was resolved by preparative HPLC (Chiral Technologies IA column, 20 μm silica, 100 mm diameter, 250 mm length), using a 70/15/15 mixture of heptane/EtOH/MeOH as eluents and a flow rate of 450 mL/min, fractions containing the desired compounds were concentrated under reduced pressure to give the faster eluting isomer **1** of (1*S*,3*R*)-3-acetamido-*N*-(5-chloro-4-(5-methyl-5,6-dihydro-4*H*-pyrrolo[1,2-*b*]pyrazol-3-yl)pyridin-2-yl)cyclohexanecarboxamide (**27**, 356 mg, 48%, 99.3% e.e.) and the slower eluting isomer **2** of (1*S*,3*R*)-3-acetamido-*N*-(5-chloro-4-(5-methyl-5,6-dihydro-4*H*-pyrrolo[1,2-*b*]pyrazol-3-yl)pyridin-2-yl)cyclohexanecarboxamide (**28**, 348 mg, 47%, 97.5% e.e.).

27: ¹H NMR (400 MHz, DMSO-*d*₆): 1.05–1.15 (1H, m), 1.25 (3H, d), 1.26–1.39 (3H, m), 1.72–1.83 (6H, m), 1.90 (1H, br d), 2.55–2.62 (1H, m), 2.67 (1H, dd), 3.11–3.19 (1H, m), 3.21–3.28 (1H, m), 3.51–3.62 (1H, m), 3.76 (1H, dd), 4.27–4.37 (1H, m), 7.75 (1H, d), 8.00 (1H, s), 8.27 (1H, s), 8.35 (1H, s), 10.55 (1H, s). MS-ESI *m/z* 416 [MH⁺]. HRMS-ESI: *m/z* found 416.1860 [MH⁺], C₂₁H₂₇ClN₅O₂ requires 416.1848.

28: ¹H NMR (400 MHz, DMSO-*d*₆): 1.08–1.13 (1H, m), 1.24 (3H, d), 1.25–1.36 (3H, m), 1.62–1.85 (6H, m), 1.91 (1H, br d), 2.52–2.61 (1H, m), 2.67 (1H, dd), 3.13–3.19 (1H, m), 3.21–3.29 (1H, m), 3.51–3.60 (1H, m), 3.76 (1H, dd), 4.32 (1H, dd), 7.74 (1H, d), 7.98 (1H, s), 8.28 (1H, s), 8.34 (1H, s), 10.54 (1H, s). MS-ESI *m/z* 416 [MH⁺]. HRMS-ESI: *m/z* found 416.1849 [MH⁺], C₂₁H₂₇ClN₅O₂ requires 416.1848.

Analytical HPLC: flow: 2 mL/min, column: Chiral Technologies IA, 5 μm, 4.6 × 250 mm, eluent: 1:1 ethanol/methanol in heptane), *t*_R: (**27**, 7.9 min), (**28**, 9.3 min).

(1*S*,3*R*)-3-Acetamido-*N*-(5-chloro-4-(6,6-dimethyl-6,7-dihydro-5*H*-pyrrolo[1,2-*a*]imidazol-3-yl)pyridin-2-yl)cyclohexanecarboxamide (**29**). **63** (800 mg, 1.90 mmol), 6,6-dimethyl-6,7-dihydro-5*H*-pyrrolo[1,2-*a*]imidazole (825 mg, 5.69 mmol; see [Supporting Information](#)), palladium acetate (171 mg, 0.76 mmol), and potassium acetate (372 mg, 3.79 mmol) were suspended in DMA (15 mL) and sealed into a microwave tube. The tube was degassed and purged with nitrogen (3×). The reaction was then subjected to microwave conditions (150 °C, 16 h) and cooled to rt. The

reaction mixture was purified by preparative HPLC (Waters XBridge Prep C18 OBD column, 5 μ silica, 30 mm diameter, 100 mm length), using decreasingly polar mixtures of water (containing 1% NH₃) and MeCN as eluents. Fractions containing the desired compound were concentrated under reduced pressure. The resulting light brown solid was recrystallized using EtOAc/heptane and dried under a vacuum to give **29** (180 mg, 22%) as a white solid. The filtrate was concentrated under reduced pressure to provide a second batch of **29** (118 mg, 14%). ¹H NMR (500 MHz, DMSO-*d*₆): 1.03–1.16 (1H, m), 1.19–1.41 (9H, m), 1.72–1.81 (6H, m), 1.91 (1H, br. d), 2.57–2.68 (1H, m), 2.71 (2H, s), 3.50–3.62 (1H, m), 3.91 (2H, s), 7.51 (1H, s), 7.75 (1H, d), 8.28 (1H, s), 8.42 (1H, s), 10.66 (1H, s). ¹³C NMR (126 MHz, DMSO-*d*₆): 22.74, 24.01, 27.31, 28.24, 31.86, 35.05, 38.10, 43.14, 43.47, 46.91, 58.27, 111.18, 121.37, 123.87, 134.70, 136.99, 148.20, 151.12, 155.97, 168.09, 174.68. MS-ESI *m/z* 430 [MH⁺]. HRMS-ESI: *m/z* found 430.2006 [MH⁺], C₂₂H₂₅ClN₅O₂ requires 430.2004.

■ ASSOCIATED CONTENT

SI Supporting Information

The Supporting Information is available free of charge at <https://pubs.acs.org/doi/10.1021/acs.jmedchem.0c01754>.

Experimental procedures for the synthesis and characterization of intermediates and metabolites **6-M1**, **6-M2**, **24-M1**, and **24-M2**; crystal structure of compound **24** bound to CDK9 in complex with cyclin T1; ligand docking protocol; procedures for determination of DMPK properties; protocol for human PK predictions and clinical dose projections; biological testing protocol, data, and associated errors (PDF)

Molecular formula strings (CSV)

Accession Codes

The coordinates of the crystal structure of compound **24** bound to CDK9 in complex with cyclin T1 have been deposited under the following code 6Z45. Authors will release the atomic coordinates and experimental data upon article publication.

■ AUTHOR INFORMATION

Corresponding Author

Bernard Barlaam – Oncology R&D, AstraZeneca, Cambridge CB4 0WG, United Kingdom; orcid.org/0000-0002-0904-7556; Phone: +44(0)1625 237335; Email: bernard.barlaam2@astrazeneca.com

Authors

Robert Casella – Advanced Drug Delivery, Pharmaceutical Sciences, R&D, AstraZeneca, Boston, Massachusetts 02451, United States

Justin Cidado – Oncology R&D, AstraZeneca, Boston, Massachusetts 02451, United States

Calum Cook – Oncology R&D, AstraZeneca, Macclesfield SK10 2NA, United Kingdom

Chris De Savi – Oncology R&D, AstraZeneca, Boston, Massachusetts 02451, United States

Allan Dishington – Oncology R&D, AstraZeneca, Cambridge CB4 0WG, United Kingdom

Craig S. Donald – Oncology R&D, AstraZeneca, Cambridge CB4 0WG, United Kingdom

Lisa Drew – Oncology R&D, AstraZeneca, Boston, Massachusetts 02451, United States

Andrew D. Ferguson – Discovery Sciences, AstraZeneca, Boston, Massachusetts 02451, United States; orcid.org/0000-0002-1018-9631

Douglas Ferguson – Oncology R&D, AstraZeneca, Boston, Massachusetts 02451, United States

Steve Glossop – Oncology R&D, AstraZeneca, Cambridge CB4 0WG, United Kingdom

Tyler Grebe – Oncology R&D, AstraZeneca, Boston, Massachusetts 02451, United States

Chungang Gu – Oncology R&D, AstraZeneca, Boston, Massachusetts 02451, United States

Sudhir Hande – Oncology R&D, AstraZeneca, Boston, Massachusetts 02451, United States

Janet Hawkins – Oncology R&D, AstraZeneca, Cambridge CB4 0WG, United Kingdom

Alexander W. Hird – Oncology R&D, AstraZeneca, Boston, Massachusetts 02451, United States

Jane Holmes – Oncology R&D, AstraZeneca, Cambridge CB4 0WG, United Kingdom

James Horstick – Oncology R&D, AstraZeneca, Boston, Massachusetts 02451, United States

Yun Jiang – Pharmaron Beijing Co., Ltd., Beijing 100176, P. R. China

Michelle L. Lamb – Oncology R&D, AstraZeneca, Boston, Massachusetts 02451, United States; orcid.org/0000-0002-3005-8065

Thomas M. McGuire – Oncology R&D, AstraZeneca, Cambridge CB4 0WG, United Kingdom

Jane E. Moore – Oncology R&D, AstraZeneca, Cambridge CB4 0WG, United Kingdom

Nichole O'Connell – Discovery Sciences, AstraZeneca, Boston, Massachusetts 02451, United States

Andy Pike – Oncology R&D, AstraZeneca, Cambridge CB4 0WG, United Kingdom

Kurt G. Pike – Oncology R&D, AstraZeneca, Cambridge CB4 0WG, United Kingdom; orcid.org/0000-0002-9731-7500

Theresa Proia – Oncology R&D, AstraZeneca, Boston, Massachusetts 02451, United States

Bryan Roberts – Oncology R&D, AstraZeneca, Cambridge CB4 0WG, United Kingdom

Maryann San Martin – Oncology R&D, AstraZeneca, Boston, Massachusetts 02451, United States

Ujjal Sarkar – Oncology R&D, AstraZeneca, Boston, Massachusetts 02451, United States

Wenlin Shao – Oncology R&D, AstraZeneca, Boston, Massachusetts 02451, United States

Darren Stead – Oncology R&D, AstraZeneca, Cambridge CB4 0WG, United Kingdom

Neil Sumner – Oncology R&D, AstraZeneca, Cambridge CB4 0WG, United Kingdom

Kumar Thakur – Oncology R&D, AstraZeneca, Boston, Massachusetts 02451, United States

Melissa M. Vashbinder – Oncology R&D, AstraZeneca, Boston, Massachusetts 02451, United States

Jeffrey G. Varnes – Oncology R&D, AstraZeneca, Boston, Massachusetts 02451, United States

Jiyan Wang – Advanced Drug Delivery, Pharmaceutical Sciences, R&D, AstraZeneca, Boston, Massachusetts 02451, United States

Lei Wang – Pharmaron Beijing Co., Ltd., Beijing 100176, P. R. China

Dedong Wu – Advanced Drug Delivery, Pharmaceutical Sciences, R&D, AstraZeneca, Boston, Massachusetts 02451, United States

Liangwei Wu – Pharmaron Beijing Co., Ltd., Beijing 100176, P. R. China

Bin Yang – Oncology R&D, AstraZeneca, Boston, Massachusetts 02451, United States; orcid.org/0000-0002-1499-5569

Tieguang Yao – Pharmaron Beijing Co., Ltd., Beijing 100176, P. R. China

Complete contact information is available at:

<https://pubs.acs.org/10.1021/acs.jmedchem.0c01754>

Author Contributions

The manuscript was written through contributions of all authors. All authors were employees of AstraZeneca at the time of the described work and have given approval to the final version of the manuscript.

Notes

The authors declare no competing financial interest.

ACKNOWLEDGMENTS

The authors would like to acknowledge Matt Peters for assessing the safety risks of this project, Anne Marie Mazzola and Scott Boiko for in vitro and in vivo biology data generation, Tim Ikeda for his input into assay design and data generation, and past and present members of the CDK9 project.

NONSTANDARD ABBREVIATIONS AND ACRONYMS

second-generation XPhos precatalyst, chloro(2-dicyclohexylphosphino-2',4',6'-triisopropyl-1,1'-biphenyl)[2-(2'-amino-1,1'-biphenyl)]palladium(II); 2-MeTHF, 2-methyl tetrahydrofuran; AML, acute myeloid leukemia; Bak, Bcl2 homologous antagonist/killer; Bax, Bcl2-associated X protein; BCL2, B-cell lymphoma 2; BID, bis in die (twice a day); BPIn, boronic pinacol ester; CDK, cyclin dependent kinase; CDT, carboxyl-terminal domain; CSNK1G1, casein kinase 1 gamma 1; DCM, dichloromethane; DIPEA, N-ethyl-N-isopropylpropan-2-amine; DYRK, dual specificity tyrosine phosphorylation regulated kinase; ERK7, extracellular signal-regulated kinase 7; GSK, glycogen synthase kinase; HLM, human liver microsome; INSR, insulin receptor kinase; i.p., intraperitoneal; i.v., intravenous; Jnk1, c-Jun N-terminal kinase 1; MAP2K7, dual specificity mitogen-activated protein kinase kinase 7; MAP3K9, mitogen-activated protein kinase kinase kinase 9; MAP4K4, mitogen-activated protein kinase kinase kinase 4; Mcl-1, myeloid cell leukemia 1; MeCN, acetonitrile; NBS, N-bromosuccinimide; NCS, N-chlorosuccinimide; NMP, N-methylpyrrolidone; PBPK, physiologically based pharmacokinetic; PdCl₂(dppf), [1,1'-bis(diphenylphosphino)ferrocene]dichloropalladium(II); Pd(P(Cy)₃)₂Cl₂, dichlorobis(tricyclohexylphosphine)palladium(II); Puma, p53 upregulated modulator of apoptosis; RNAP2, RNA polymerase II; rt, room temperature; SFC, supercritical fluid chromatography; TEA, triethylamine; V_{ss}, volume of distribution at steady state; xantphos, 4,5-bis(diphenylphosphino)-9,9-dimethylxanthene.

REFERENCES

- (1) Hanahan, D.; Weinberg, R. A. The hallmarks of cancer. *Cell* **2000**, *100*, 57–70.
- (2) Cory, S.; Adams, J. M. The Bcl2 family: regulators of the cellular life-or-death switch. *Nat. Rev. Cancer* **2002**, *2*, 647–656.
- (3) Czabotar, P. E.; Lessene, G.; Strasser, A.; Adams, J. M. Control of apoptosis by the BCL-2 protein family: implications for physiology and therapy. *Nat. Rev. Mol. Cell Biol.* **2014**, *15*, 49–63.
- (4) Beroukhi, R.; Mermel, C. H.; Porter, D.; Wei, G.; Raychaudhuri, S.; Donovan, J.; Barretina, J.; Boehm, J. S.; Dobson, J.; Urashima, M.;

Mc Henry, K. T.; Pinchback, R. M.; Ligon, A. H.; Cho, Y. J.; Haery, L.; Greulich, H.; Reich, M.; Winckler, W.; Lawrence, M. S.; Weir, B. A.; Tanaka, K. E.; Chiang, D. Y.; Bass, A. J.; Loo, A. J.; Hoffman, C.; Prensner, J.; Liefeld, T.; Gao, Q.; Yecies, D.; Signoretti, S.; Maher, E.; Kaye, F. J.; Sasaki, H.; Tepper, J. E.; Fletcher, J. A.; Tabernero, J.; Baselga, J.; Tsao, M. S.; Demicheli, F.; Rubin, M. A.; Janne, P. A.; Daly, M. J.; Nucera, C.; Levine, R. L.; Ebert, B. L.; Gabriel, S.; Rustgi, A. K.; Antonescu, C. R.; Ladanyi, M.; Letai, A.; Garraway, L. A.; Loda, M.; Beer, D. G.; True, L. D.; Okamoto, A.; Pomeroy, S. L.; Singer, S.; Golub, T. R.; Lander, E. S.; Getz, G.; Sellers, W. R.; Meyerson, M. The landscape of somatic copy-number alteration across human cancers. *Nature* **2010**, *463*, 899–905.

(5) Ashkenazi, A. Directing cancer cells to self-destruct with pro-apoptotic receptor agonists. *Nat. Rev. Drug Discovery* **2008**, *7*, 1001–1012.

(6) Wenzel, S. S.; Grau, M.; Mavis, C.; Hailfinger, S.; Wolf, A.; Madle, H.; Deeb, G.; Dörken, B.; Thome, M.; Lenz, P.; Dirnhofer, S.; Hernandez-Ilizaliturri, F. J.; Tzankov, A.; Lenz, G. MCL1 is deregulated in subgroups of diffuse large B-cell lymphoma. *Leukemia* **2013**, *27*, 1381–1390.

(7) Wuillème-Toumi, S.; Robillard, N.; Gomez, P.; Moreau, P.; Le Gouill, S.; Avet-Loiseau, H.; Harousseau, J. L.; Amiot, M.; Bataille, R. Mcl-1 is overexpressed in multiple myeloma and associated with relapse and shorter survival. *Leukemia* **2005**, *19*, 1248–1252.

(8) Gores, G. J.; Kaufmann, S. H.; Glaser, S. P.; Lee, E. F.; Trounson, E. Selectively targeting Mcl-1 for the treatment of acute myelogenous leukemia and solid tumors. *Genes Dev.* **2012**, *26*, 305–311.

(9) Williams, M. M.; Cook, R. S. Bcl-2 family proteins in breast development and cancer: could Mcl-1 targeting overcome therapeutic resistance? *Oncotarget* **2015**, *6*, 3519–3530.

(10) Zhang, B.; Gojo, I.; Fenton, R. G. Myeloid cell factor – 1 is a critical survival factor for multiple myeloma. *Blood* **2002**, *99*, 1885–1893.

(11) Glaser, S. P.; Lee, E. F.; Trounson, E.; Bouillet, P.; Wei, A.; Fairlie, W. D.; Izon, D. J.; Zuber, J.; Rappaport, A. R.; Herold, M. J.; Alexander, W. S.; Lowe, S. W.; Robb, L.; Strasser, A. Anti-apoptotic Mcl-1 is essential for the development and sustained growth of acute myeloid leukemia. *Genes Dev.* **2012**, *26*, 120–125.

(12) Wan, Y.; Dai, N.; Tang, Z.; Fang, H. Small-molecule Mcl-1 inhibitors: emerging anti-tumor agents. *Eur. J. Med. Chem.* **2018**, *146*, 471–482.

(13) Nhu, D.; Lessene, G.; Huang, D. C. S.; Burns, C. J. Small molecules targeting Mcl-1: the search for a silver bullet in cancer therapy. *MedChemComm* **2016**, *7*, 778–787.

(14) Chen, L.; Fletcher, S. Mcl-1 inhibitors: a patent review. *Expert Opin. Ther. Pat.* **2017**, *27*, 163–178.

(15) Kotschy, A.; Szlavik, Z.; Murray, J.; Davidson, J.; Maragno, A. L.; Le Toumelin-Braizat, G.; Chanrion, M.; Kelly, G. L.; Gong, J.-N.; Moujalled, D. M.; Bruno, A.; Csekei, M.; Paczal, A.; Szabo, Z. B.; Sipos, S.; Radics, G.; Prosenyak, A.; Balint, B.; Ondi, L.; Blasko, G.; Robertson, A.; Surgenor, A.; Dokurno, P.; Chen, I.; Matassova, N.; Smith, J.; Pedder, C.; Graham, C.; Studeny, A.; Lysiak-Auvity, G.; Girard, A.-M.; Grave, F.; Segal, D.; Riffkin, C. D.; Pomilio, G.; Galbraith, L. C. A.; Aubrey, B. J.; Brennan, M. S.; Herold, M. J.; Chang, C.; Guasconi, G.; Cauquil, N.; Melchior, F.; Guigal-Stephan, N.; Lockhart, B.; Colland, F.; Hickman, J. A.; Roberts, A. W.; Huang, D. C. S.; Wei, A. H.; Strasser, A.; Lessene, G.; Geneste, O. The MCL1 inhibitor S63845 is tolerable and effective in diverse cancer models. *Nature* **2016**, *538*, 477–482.

(16) Tron, A. E.; Belmonte, M. A.; Adam, A.; Aquila, B. M.; Boise, L. H.; Chiarparin, E.; Cidado, J.; Embrey, K. J.; Gangl, E.; Gibbons, F. D.; Gregory, G. P.; Hargreaves, D.; Hendricks, J. A.; Johannes, J. W.; Johnstone, R. W.; Kazmirski, S. L.; Kettle, J. G.; Lamb, M. L.; Matulis, S. M.; Nooka, A. K.; Packer, M. J.; Peng, B.; Rawlins, P. B.; Robbins, D. W.; Schuller, A. G.; Su, N.; Yang, W.; Ye, Q.; Zheng, X.; Secrist, J. P.; Clark, E. A.; Wilson, D. M.; Fawell, S. E.; Hird, A. W. Discovery of Mcl-1-specific inhibitor AZD5991 and preclinical activity in multiple myeloma and acute myeloid leukemia. *Nat. Commun.* **2018**, *9*, 5341.

(17) Caenepeel, S.; Brown, S. P.; Belmontes, B.; Moody, G.; Keegan, K. S.; Chui, D.; Whittington, D. A.; Huang, X.; Poppe, L.; Cheng, A. C.;

- Cardozo, M.; Houze, J.; Li, Y.; Lucas, B.; Paras, N. A.; Wang, X.; Taygerly, J. P.; Vimolratana, M.; Zancanella, M.; Zhu, L.; Cajulis, E.; Osgood, T.; Sun, J.; Damon, L.; Egan, R. K.; Greninger, P.; McClanaghan, J. D.; Gong, J.; Moujalled, D.; Pomilio, G.; Beltran, P.; Benes, C. H.; Roberts, A. W.; Huang, D. C.; Wei, A.; Canon, J.; Coxon, A.; Hughes, P. E. AMG 176, a selective MCL1 inhibitor, is effective in hematologic cancer models alone and in combination with established therapies. *Cancer Discovery* **2018**, *8*, 1582–1597.
- (18) <http://clinicaltrials.gov/ct2/show/NCT02992483>.
- (19) Malumbres, M. Cyclin-dependent kinases. *Genome Biology* **2014**, *15*, 122–131.
- (20) Malumbres, M.; Barbacid, M. Cell cycle, CDKs and cancer: a changing paradigm. *Nat. Rev. Cancer* **2009**, *9*, 153–166.
- (21) Thomas, M. C.; Chiang, C. M. The general transcription machinery and general cofactors. *Crit. Rev. Biochem. Mol. Biol.* **2006**, *41*, 105–178.
- (22) Varadarajan, S.; Poornima, P.; Milani, M.; Gowda, K.; Amin, S.; Wang, H. G.; Cohen, G. M. Maritoclastin and dinaciclib inhibit MCL-1 activity and induce apoptosis in both a MCL-1-dependent and -independent manner. *Oncotarget* **2015**, *6*, 12668–12681.
- (23) Boohar, R. N.; Hatch, H.; Dolinski, B. M.; Nguyen, T.; Harmonay, L.; Al-Assaad, A.-S.; Ayers, M.; Nebozhyn, M.; Loboda, A.; Hirsch, H. A.; Zhang, T.; Shi, B.; Merkel, C. E.; Angagaw, M. H.; Wang, Y.; Long, B. J.; Lennon, X. Q.; Miselis, N.; Pucci, V.; Monahan, J. W.; Lee, J.; Kondic, A. G.; Im, E. K.; Mauro, D.; Blanchard, R.; Gilliland, G.; Fawell, S. E.; Zawel, L.; Schuller, A. G.; Strack, P. MCL1 and BCL-xL levels in solid tumors are predictive of dinaciclib-induced apoptosis. *PLoS One* **2014**, *9*, e108371.
- (24) Bywater, M. J.; Pearson, R. B.; McArthur, G.; Hannan, R. D. Dysregulation of the basal RNA polymerase transcription apparatus in cancer. *Nat. Rev. Cancer* **2013**, *13*, 299–314.
- (25) Adelman, K.; Lis, J. T. Promoter-proximal pausing of RNA polymerase II: emerging roles in metazoans. *Nat. Rev. Genet.* **2012**, *13*, 720–731.
- (26) Gilchrist, D. A.; Dos Santos, G.; Fargo, D. C.; Xie, B.; Gao, Y.; Li, L.; Adelman, K. Pausing of RNA polymerase II disrupts DNA-specified nucleosome organization to enable precise gene regulation. *Cell* **2010**, *143*, 540–551.
- (27) Sansó, M.; Fisher, R. P. Pause, play, repeat: CDKs push RNAP II's buttons. *Transcription* **2013**, *4*, 146–152.
- (28) Sonawane, Y. A.; Taylor, M. A.; Napoleon, J. V.; Rana, S.; Contreras, J. I.; Natarajan, A. Cyclin dependent kinase 9 inhibitors for cancer therapy. *J. Med. Chem.* **2016**, *59*, 8667–8684.
- (29) Wang, S.; Griffiths, G.; Midgley, C. A.; Barnett, A. L.; Cooper, M.; Grabarek, J.; Ingram, L.; Jackson, W.; Kontopidis, G.; McClue, S. J.; McInnes, C.; McLachlan, J.; Meades, C.; Mezna, M.; Stuart, I.; Thomas, M. P.; Zheleva, D. I.; Lane, D. P.; Jackson, R. C.; Glover, D. M.; Blake, D. G.; Fischer, P. M. Discovery and characterization of 2-anilino-4-(thiazol-5-yl)pyrimidine transcriptional CDK inhibitors as anticancer agents. *Chem. Biol.* **2010**, *17*, 1111–1121.
- (30) Anderson, M.; Andrews, D. M.; Barker, A. J.; Brassington, C. A.; Breed, J.; Byth, K. F.; Culshaw, J. D.; Finlay, M. R. V.; Fisher, E.; McMiken, H. H. J.; Green, C. P.; Heaton, D. W.; Nash, I. A.; Newcombe, N. J.; Oakes, S. E.; Paupit, R. A.; Roberts, A.; Stanway, J. J.; Thomas, A. P.; Tucker, J. A.; Walker, M.; Weir, H. M. Imidazoles: SAR and development of a potent class of cyclin-dependent kinase inhibitors. *Bioorg. Med. Chem. Lett.* **2008**, *18*, 5487–5492.
- (31) Lapenna, S.; Giordano, A. Cell cycle kinases as therapeutic targets for cancer. *Nat. Rev. Drug Discovery* **2009**, *8*, 547–566.
- (32) Cidado, J.; Shen, M.; Grondine, M.; Boiko, S.; Wang, H.; Borodovsky, A.; Mazzola, A. M.; Wu, A.; Lawson, D.; Ferguson, F.; Gao, B.; Cui, A.; D'Cruz, C.; Drew, L. AZ5576, a novel potent and selective CDK9 inhibitor, induces rapid cell death and achieves efficacy in multiple preclinical hematological models. Proceedings of the 107th Annual Meeting of the American Association for Cancer Research (AACR), New Orleans, April 16–20, 2016. *Cancer Res.* **2016**, *76* (14 Suppl.), Abstract 3572.
- (33) AZ5576 is also known as PC585: Garcia-Cuellar, M. P.; Füller, E.; Mäthner, E.; Breitingner, C.; Hetzner, K.; Zeitlmann, L.; Borkhardt, A.; Slany, R. K. Efficacy of cyclin-dependent-kinase 9 inhibitors in a murine model of mixed-lineage leukemia. *Leukemia* **2014**, *28*, 1427–1435.
- (34) AZ5576 was described in patent literature: Heiser, U.; Niestroj, A. J.; Zeitlmann, L. Inhibitors of Protein Kinases. PCT Int. Appl., WO 2011110612, 2011.
- (35) Albert, T. K.; Rigault, C.; Eickhoff, J.; Baumgart, K.; Antrecht, C.; Klebl, B.; Mittler, G.; Meisterernst, M. Characterization of molecular and cellular functions of the cyclin-dependent kinase CDK9 using a novel specific inhibitor. *Br. J. Pharmacol.* **2014**, *171*, 55–68.
- (36) Yin, T.; Lallena, M. J.; Kreklau, E. L.; Fales, K. R.; Carballares, S.; Torres, R.; Wishart, G. N.; Ajamie, R. T.; Cronier, D. M.; Iversen, P. W.; Meier, T. I.; Foreman, R. T.; Zeckner, D.; Sissons, S. E.; Halstead, B. W.; Lin, A. B.; Donoho, G. P.; Qian, Y.; Li, S.; Wu, S.; Aggarwal, A.; Ye, X. S.; Starling, J. J.; Gaynor, R. B.; de Dios, A.; Du, J. A novel CDK9 inhibitor shows potent antitumor efficacy in preclinical hematologic tumor models. *Mol. Cancer Ther.* **2014**, *13*, 1442–1456.
- (37) Scholz, A.; Luecking, U.; Siemeister, G.; Lienau, P.; Boemer, U.; Ellinghaus, P.; Walter, A. O.; Valencia, R.; Ince, S.; von Nussbaum, F.; Mumberg, D.; Brands, M.; Karl Ziegelbauer, K. BAY 1143572: A first-in-class, highly selective, potent and orally available inhibitor of PTEFb/CDK9 currently in phase I, inhibits MYC and shows convincing anti-tumor activity in multiple xenograft models by the induction of apoptosis. Proceedings of the 106th Annual Meeting of the American Association for Cancer Research (AACR), Philadelphia, April 18–22, 2015. *Cancer Res.* **2015**, *75* (15 Suppl.), Abstract DDT02–02.
- (38) Luecking, U.; Scholz, A.; Lienau, P.; Siemeister, G.; Kosemund, D.; Bohlmann, R.; Briem, H.; Terebesi, I.; Meyer, K.; Prella, K.; Denner, K.; Boemer, U.; Schaefer, M.; Eis, K.; Valencia, R.; Ince, S.; von Nussbaum, F.; Mumberg, D.; Ziegelbauer, K.; Klebl, B.; Choidas, A.; Nussbaumer, P.; Baumann, M.; Schultz-Fademrecht, C.; Ruehter, G.; Eickhoff, J.; Brands, M. Identification of atueveciclib (BAY 1143572), the first highly selective, clinical PTEFb/CDK9 inhibitor for the treatment of cancer. *ChemMedChem* **2017**, *12*, 1776–1793.
- (39) Luecking, U. T. R.; Scholz, A.; Kosemund, D.; Bohlmann, R.; Briem, H.; Lienau, P.; Siemeister, G.; Terebesi, I.; Meyer, K.; Prella, K.; Valencia, R.; Ince, S.; von Nussbaum, F.; Mumberg, D.; Ziegelbauer, K.; Brands, M. Identification of potent and highly selective PTEFb inhibitor BAY 1251152 for the treatment of cancer: from p.o. to i.v. application via scaffold hops. Proceedings of the 2017 Annual Meeting of the American Association for Cancer Research (AACR), Washington D.C., April 1–5, 2017. *Cancer Res.* **2017**, *77* (13 Suppl.), Abstract 984.
- (40) Larsen, S. D. Novel Parham-type cycloacylations of 1H-pyrazole-1-alkanoic acids. *Synlett* **1997**, 1997, 1013–1014.
- (41) Galeta, J.; Tenora, L.; Man, S.; Potacek, M. Dihydropyrrolo[1,2-b]pyrazoles: withasomnine and related compounds. *Tetrahedron* **2013**, *69*, 7139–7146.
- (42) Hole, A. J.; Baumli, S.; Shao, H.; Shi, S.; Huang, S.; Pepper, C.; Fischer, P. M.; Wang, S.; Endicott, J. A.; Noble, M. E. Comparative structural and functional studies of 4-(thiazol-5-yl)-2-(phenylamino)-pyrimidine-5-carbonitrile CDK9 inhibitors suggest the basis for isotype selectivity. *J. Med. Chem.* **2013**, *56*, 660–670.
- (43) Jones, C. D.; Andrews, D. M.; Barker, A. J.; Blades, K.; Daunt, P.; East, S.; Geh, C.; Graham, M. A.; Johnson, K. M.; Loddick, S. A.; McFarland, H. M.; McGregor, A.; Moss, L.; Rudge, D. A.; Simpson, P. B.; Swain, M. L.; Tam, K. Y.; Tucker, J. A.; Walker, M. The discovery of AZD5597, a potent imidazole pyrimidine amide CDK inhibitor suitable for intravenous dosing. *Bioorg. Med. Chem. Lett.* **2008**, *18*, 6369–6373.
- (44) Compounds **6**, **23**, and **24** have been disclosed in Pike, K. G.; Barlaam, B. C.; Hawkins, J.; De Savi, C.; Vasbinder, M. M.; Hird, A.; Lamb, M. Polycyclic Amide Derivatives as CDK9 Inhibitors. PCT Int. Appl., WO2017001354, 2017. Preparation and characterization of crystalline forms (e.g. Form B of **6**, Form B of **23** and Form A of **24**) are described herein.
- (45) Smith, D. A.; Beaumont, K.; Maurer, T. S.; Di, L. Volume of distribution in drug design. *J. Med. Chem.* **2015**, *58*, 5691–5698.
- (46) Cidado, J.; Boiko, S.; Proia, T.; Ferguson, D.; Criscione, S. W.; San Martin, M.; Pop-Damkov, P.; Su, N.; Roamio Franklin, V. N.;

Sekhar Reddy Chilamakuri, C.; D'Santos, C. S.; Shao, W.; Saeh, J. C.; Koch, R.; Weinstock, D. M.; Zinda, M.; Fawell, S. E.; Drew, L. AZD4573 is a highly selective CDK9 inhibitor that suppresses Mcl-1 and induces apoptosis in hematological cancer cells. *Clin. Cancer Res.* **2020**, *26*, 922–934.